Investigating the role of AtVAMP714 in Arabidopsis root development

HAMILTON, KATHERINE,ANNE

Investigating the role of AtVAMP714 in Arabidopsis root development

Katherine Anne Hamilton

Submitted for the qualification of Masters by Research

School of Biological and Biomedical Sciences

January 2016

Abstract

This thesis examines the potential of a role for AtVAMP714 (Vesicle Associated Membrane Protein 714) root development of *Arabidopsis thaliana*.

The *VAMP714* gene was identified as having a possible role in plant development by activation tagging. In this thesis is described a bioinformatics study on the gene and predicted protein, describing its expression and predicted protein localisation and structure. Evidence is presented that the *VAMP714* gene is transcriptionally expressed in the root of Arabidopsis and up-regulated by auxin. The protein, a predicted vesicle-associated R-SNARE (Soluble NSF Attachment Protein Receptor), is likely to be localised to the plasma-membrane, Golgi apparatus and vesicles. Loss-of-function tDNA insertion and dominant negative mutants were analysed for phenotypic effects, and the results presented show that VAMP714 function is required for correct root gravitropism and architecture in Arabidopsis, in particular for primary root growth and total lateral root number but not lateral root density or elongation. A novel cell staining technique was developed to improve observation of starch accumulation in cells of the root stem cell niche, and it was found that VAMP714 is required for correct maintenance of stem cell identity in the columella initials.

In light of other experimental data generated in this laboratory, these results support a model for the involvement of VAMP714 in root development through mediating PIN localisation and auxin transport in the root tip.

Contents

Figure List

Copyright Declaration

Acknowledgements

A big thank you to everyone who has supported me throughout this project. To Keith and Jen for their support, time and kindness throughout; without which I wouldn’t have enjoyed the year nearly as much as I did. I am privileged to have been able to work with two such lovely people.

Thank you also to Tim and Joanne who’s help and advice with the confocal microscope was so valuable.

Thank you to Anna, James, Flora, Amy and Sam who made working in the lab so fun and for their friendship and support throughout the year.

And finally, thank you to my parents, sister and Will for putting up with and supporting me whilst completing this thesis.

1.0 Introduction

Arabidopsis thaliana is an angiosperm in the Brassicaceae family and has developed the status of model organism in plant biology over years of research. It was the first plant genome to be sequenced, with the full genome sequence made publically available and constantly updated by The Arabidopsis Information Source (TAIR at www.arabidopsis.org). With the availability of tDNA insertional mutants from the Salk Institute Genome Analysis Library (signal.salk.edu) who work alongside TAIR and the Arabidopsis Biological Resource Centre (ABRC), a great range of research into the function of Arabidopsis genes and proteins has been made possible.

This project aims to investigate the function of a specific gene in the *Arabidopsis thaliana* genome, At5g22360, encoding the Vesicle Associated Membrane Protein 714 (VAMP714 protein). VAMP714 is thought to play a role in the regulation of growth at the root tip and have subsequent effects on development across the whole root.

Root growth and development in *Arabidopsis thaliana*, is controlled by developmental triggers in the root tip involving signalling events from the plant phytohormone auxin, the function of which depends on its concentration across the root tissue (Pan et al., 2015). Auxin localisation is dependent on PIN-FORMED (PIN) proteins, which are thought to be transported or recycled throughout the root tip via an endosomal or vesicle trafficking pathway (Baster et al., 2013).

1.1 Root Structure and Development

Angiosperm roots are made up of functionally distinct cell layers, organised during development by the differentiation of distal stem cells from the quiescent centre (QC) (Kajala et al., 2014). This specific cell organisation is maintained by auxin gradients in the root (Ganguly et al., 2010). Growth is controlled by specific localisations of auxin maxima; maintained by polar auxin transport mediated by auxin efflux proteins (which include the PIN protein family which traffic auxin out of cells (Ganguly et al., 2010)), working alongside influx carrier proteins of the AUX/LAX family (Peret et al., 2012). Together these proteins traffic auxin across entire tissues. In general, angiosperm roots contain a columella, root cap, lateral root cap, epidermis, endodermis, cortex, pericycle and stele, all produced from initials (stem cells) surrounding the quiescent centre (Kajala et al., 2014). The quiescent centre is found in the root apical meristem, and contains mitotically relatively inactive cells from which all of the cell layers are produced. The cells in the quiescent centre rarely divide and are surrounded by the undifferentiated initials (Figure 1), an auxin concentration maximum generated through PIN protein activity determines the fate of these stem cells (Lee et al., 2013; Sarkar et al., 2007).

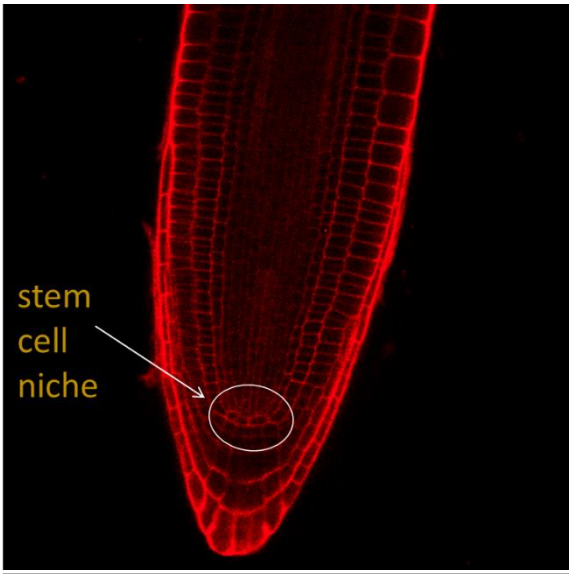

Figure 1: Taken from Fonseka et al., under development. Confocal image showing a cross section of an Arabidopsis root, with stem cell niche highlighted.

During plant development, the root develops through cell division in the meristematic region, followed by a zone of cell expansion and differentiation (Cole

et al., 2014). The differentiation of the products of the daughter cells derived from the stem cells surrounding the QC allows formation of defined tissues and columella cell layers during root growth. This involves several levels of control via hormone and protein transport to produce all cell types and ensure the correct localisation of each.

1.2 Differentiation in the Root

During root development, a fine balance is kept between stem cell maintenance and differentiation. This is in part controlled by auxin concentrations mediated by PIN proteins at specific localisations around the root tip. At high auxin concentrations, the QC and its stem cell identity is maintained, while at low auxin concentrations, differentiation is promoted and the development of columella initials from the stem cell niche is initiated (Figure 2) (Lee et al., 2013). Auxin therefore has a regulatory role in the maintenance of the QC and so the activity in the root meristem through the *PLT* (*PLETHORA*) gene family and ARFs (Auxin Response Factors). ARF10 and ARF16 promote identity control in the stem cell niche, by activating the transcriptional repressor IAA17/AXR3 which in turn restricts *WOX5* (WUSCHEL-related homeobox 5) transcription factor expression to the QC (Ding and Friml, 2010).

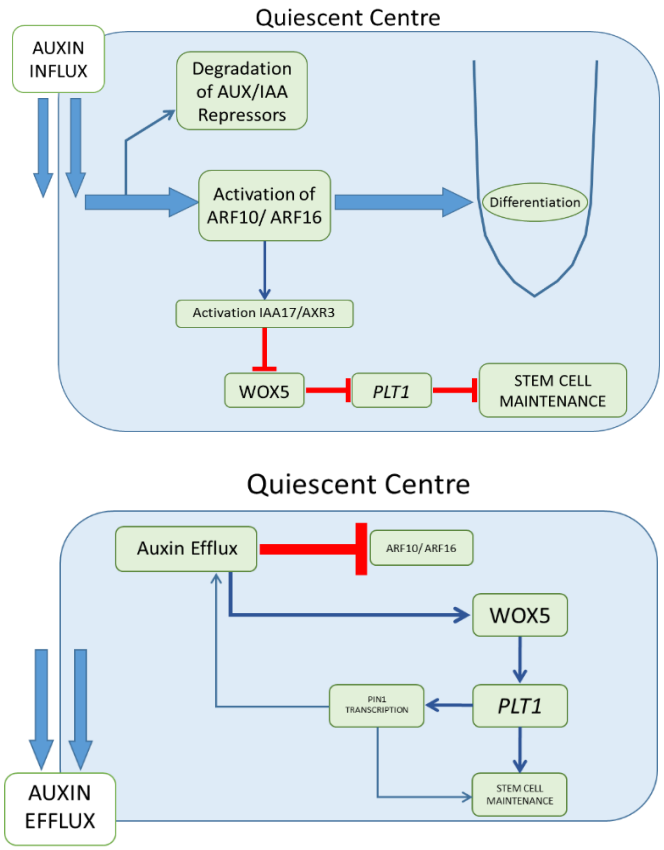

Figure 2: Model showing the effect of the presence and absence of auxin on the identity of the stem cell niche.

WOX5 is expressed in the QC and is responsible for maintaining the stem cell population (Sarkar et al., 2007; Stahl et al., 2009). *WOX5* is a homologue of *WUS*; both are homeobox genes capable of preventing the differentiation of the stem cell niche alongside the *PLT* gene family. *WOX5* and auxin have opposing effects on the fate of the stem cell niche during development where *WOX5* expression leads to maintenance of the stem cell niche, whereas auxin influx causes activation of ARFs, repression of *WOX5* and differentiation of the stem cell niche. *PLTs* are AP2-domain transcription factors, *PLT1* is the key member of the gene family involved in root development and *WOX5* is required for *PLT* activity in the maintenance of the stem cell niche (Ding and Friml., 2010). Double mutants such as *plt1 pin3* exhibit

abnormal differentiation of the stem cell niche alongside ectopic division of columella initials, and *plt1 plt2* double mutants show similar defects (Ding and Friml., 2010). Both PLT1 and WOX5 act downstream of auxin, and WOX5 is required for *PLT1* expression; and so at high auxin concentrations, *WOX5* activity is repressed by IAA17/AXR3 preventing the expression of *PLT1*. During high PLT1 activity the stem cell niche is maintained, and low PLT1 activity leads to their differentiation (Ding and Friml., 2010).

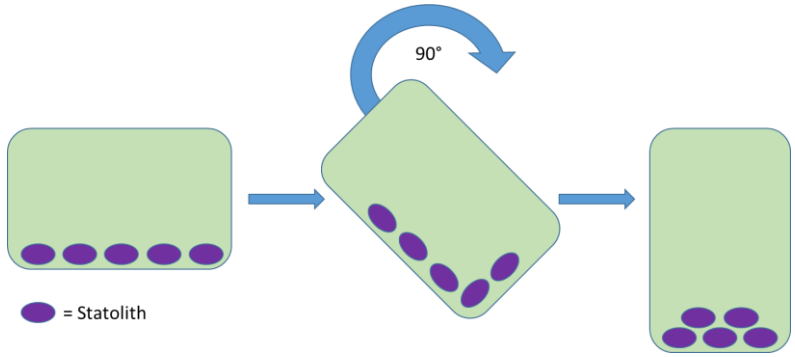

Figure 3: Diagram illustrating the displacement of statoliths in columella cells during a gravitational stimulus.

Starch production in the root cap is used as a marker for differentiation in the root tip (Barany et al., 2010). Starch accumulates in granules called statoliths within the cytoplasm of columella cells or statocytes. The statoliths play a major role in gravity perception in the root. The granules are free-moving in the cytoplasm, they are not anchored down at any point, and so as the root moves, so does the starch (Figure 3). Starch is denser than the intercellular fluid and so sinks; as a gravity stimulus is applied to a starch containing columella cell, the statoliths sink to the lowest point in the cell.

The cell senses the presence of statoliths at this membrane and converts the gravitational potential energy into a biochemical signal to move growth in the direction of gravity (Leitz et al., 2009). The main theory for the method by which cells sense gravity involves the cortical endoplasmic reticulum. It is suggested that direct interactions between statoliths and the ER induces an increase in intracellular Ca^{2+} which then acts as a second messenger in sensing and response to gravity. Deformation of the ER by the force induced by displacement of statoliths could also play a role, whereby the force stimulus provides the signal for Ca^{2+} production. Statoliths turn the plant-wide gravity stimulus into an intercellular force stimulus (Leitz et al., 2009). The increase in intracellular calcium concentrations triggers an accumulation of PIN3 proteins at the basal cell membrane, causing an increase in auxin concentration inducing growth toward the auxin maxima and therefore toward gravity. This sedimentation of statoliths allows the cell to perceive gravity and in turn, differentiate and grow towards it. In this study, starch accumulation was used as a marker for differentiation of cells distal to the QC.

1.3 Auxin Signalling

Auxin is a plant phytohormone involved in a number of important developmental and stress-related processes and has a proven role in the differentiation of the quiescent centre in *Arabidopsis thaliana* (Jiang and Feldman, 2005). Root growth is controlled by direct and indirect manipulation of gene expression. Auxin is produced in the root meristem and redistributed via 2 distinct pathways, the non-polar phloem or vascular pathway, and the cell-to-cell polar transport pathway. In the root, auxin is transported via the polar pathway which involves auxin influx and efflux from cell to cell across entire tissues according to demand. Polar auxin transport occurs via a pathway characterised by the

chemiosmotic model (Loefke et al., 2013). This model introduces the presence of PIN proteins as plasma membrane localised auxin efflux carriers (Figure 4). PIN proteins are rate-limiting components in the control of auxin signalling and regulate the direction of auxin fluxes in the root via co-transport in cell membranes (Loefke et al., 2013).

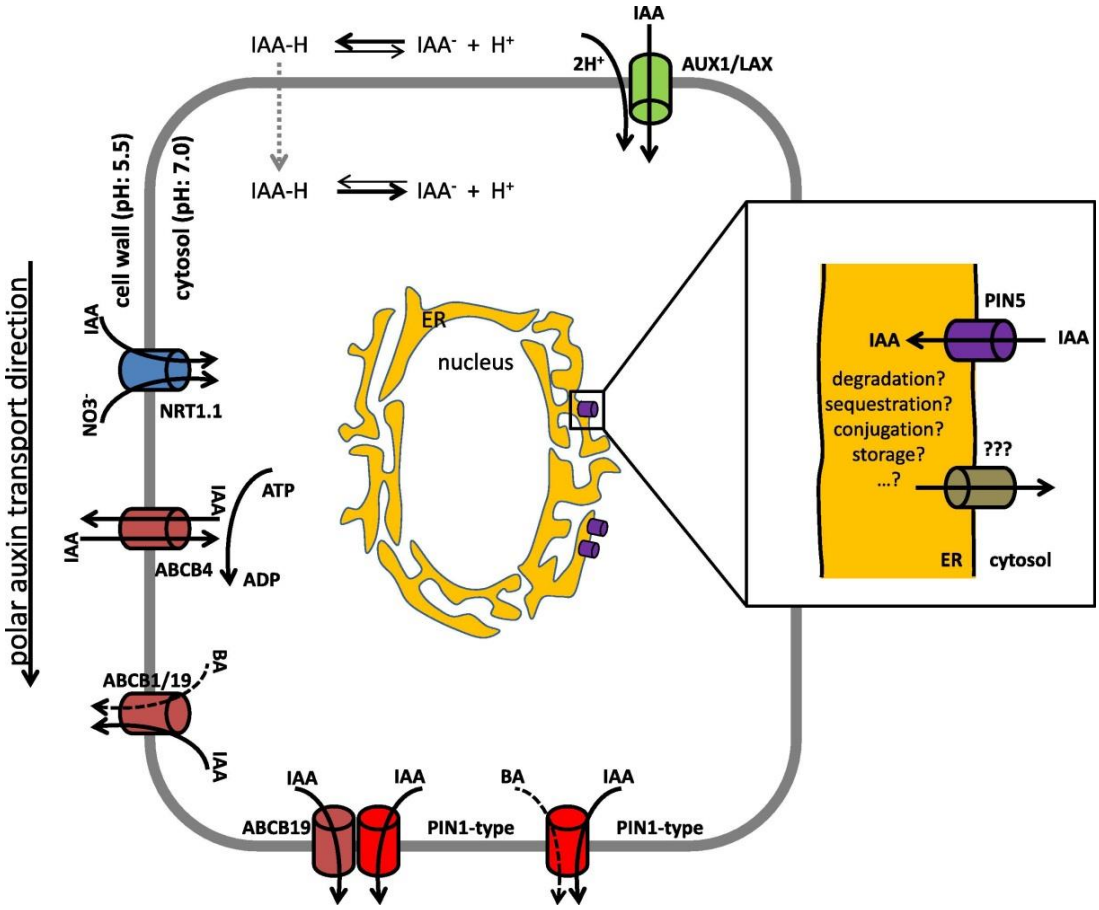

Figure 4: Taken from Loefke et al., 2013. The chemiosmotic model for polar auxin transport by PIN auxin efflux and AUX/LAX influx carriers at the plasma membrane. Model illustrates the mechanism by which auxin is transported to the endosomal membranes by PIN proteins.

The polar flow of auxin that occurs throughout the plant mainly begins at the apical tissues and moves toward the base of the plant acropetally, via vascular tissues. On reaching the root tip, auxin is redirected (basipetally) up the root epidermis, through the elongation-zone and is then recycled back into the vascular tissues (Figure 5) (Michniewicz and Friml, 2007).

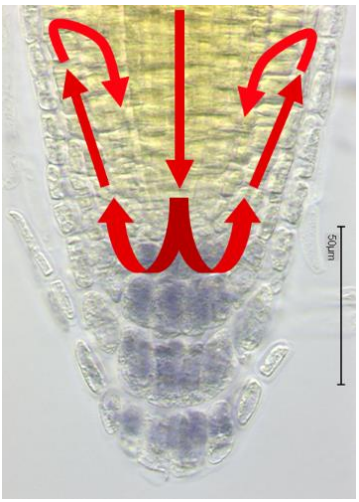

Figure 5: Image illustrating the wild-type cycling of auxin around the root cap. Fonseka et al., under development

Auxin influx carriers are members of the AUX1/LAX family, auxin efflux carriers are members of the PIN protein family (Michniewicz and Friml, 2007). This transport has a polarizing effect on tissues due to the feedback of auxin at the cellular level; auxin controls its own transport through AUX/IAA-ARF dependent regulation and polar targeting of PIN proteins (Sauer et al., 2006). By modulating PIN protein trafficking, auxin can regulate the concentration of PIN proteins at the plasma membrane (apical and basal membranes) providing a signal for the differentiation or maintenance of the stem cell niche and also acts as a feedback mechanism for auxin transport (Paciorek et al., 2005).

Auxin is a plant growth regulator; it elicits responses in the plant by causing the expression of different sets of genes in certain tissues at certain points in the cell cycle. Auxin promotes the degradation of AUX/IAA repressors, causing the release of ARF (auxin response factor) a transcriptional regulator. This allows the activation of required genes, eliciting appropriate cellular and developmental responses. PIN proteins act upstream of this process. The link between PIN protein transport and auxin signalling is key in the control of auxin maxima across the root and stem cell

differentiation in the root tip. Auxin inhibits endocytosis. By preventing the internalization of PIN proteins via endocytosis, auxin causes a significant increase of PIN protein concentration at the plasma membrane. This increases the speed and volume of auxin effluxed from that cell by increasing the number of points at which auxin can leave the cell: an increased number of PIN auxin efflux carriers on the plasma membrane. Auxin therefore facilitates its own efflux from the cell by a vesicle dependent mechanism (Pacoriek et al., 2005).

1.3.1 Chemistry of Auxin

Indole-3-acetic acid (IAAH), auxin, is made up an indole unit and an acid (see Figure 6). The indole unit is a flat hydrophobic ring system important for auxin activity, it separates the partial negative charge of the carboxylic acid group from the partial positive charge of the amine. The planar ring system is the structure that is important for the molecules function, allowing interaction with groups such as inositol, coenzyme A and glucosides. Indole-3-acetic acid is produced from tryptophan via a two-step pathway. Deactivation of either of the two enzymes involved in its synthesis causes dramatic developmental defects (Won et al., 2011). Within a cellular environment, auxin molecules can enter a cell either by slow diffusion across the membrane, or by influx via transmembrane transport proteins. Diffusion from the intercellular space into the cell is possible because the molecule is not charged. On entering the cell, via either method, the molecule is deprotonated, giving it a negative charge; this traps the molecule inside the cell. The only method of movement is either degradation within the cell or transport out of the cell via auxin efflux carriers, PIN proteins.

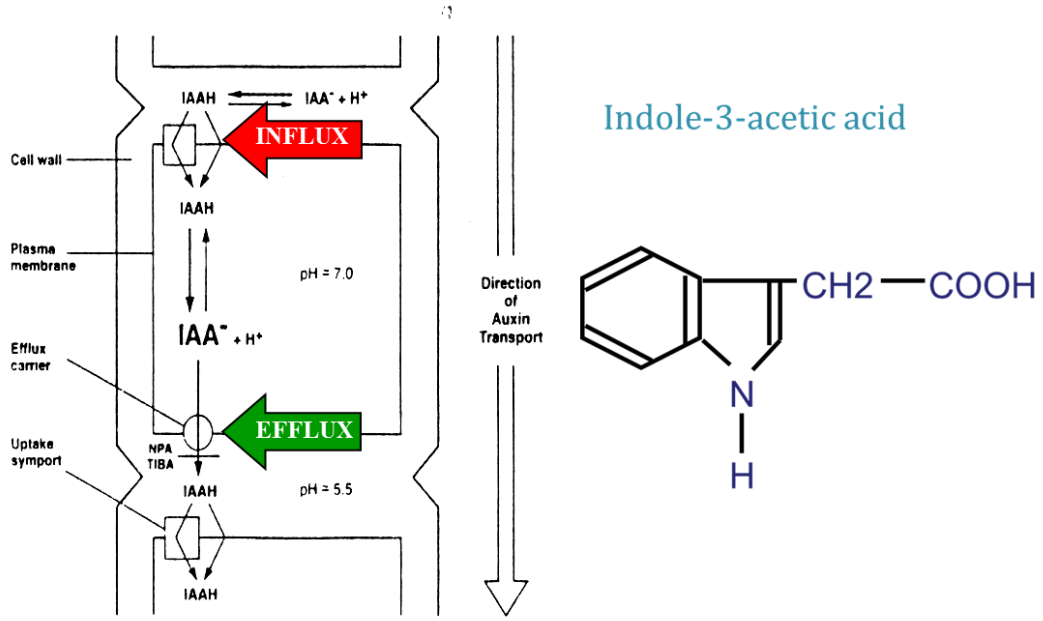

Figure 6: Left shows an illustration of a model for auxin transport through cells, highlighting the de-protonation of indole-3-acetic acid which occurs in order to trap auxin within the cell. Right shows the chemical structure or indole-3-acetic acid, auxin in its protonated form.

1.4 PIN Proteins

PIN (PIN-FORMED) proteins are a family of 8 proteins all containing a central hydrophilic loop, separating two hydrophobic regions (Figure 7) (Krecek et al., 2009). The length of the proteins hydrophilic region determines its cellular localisation. The family is split into two subgroups, type 1 (PINs 1-4 and 7) contain a long hydrophilic loop localised at the plasma membrane with type 2 (PINs 5, 6 and 8) containing a short hydrophilic loop found at the endoplasmic reticulum (Loefke et al., 2013).

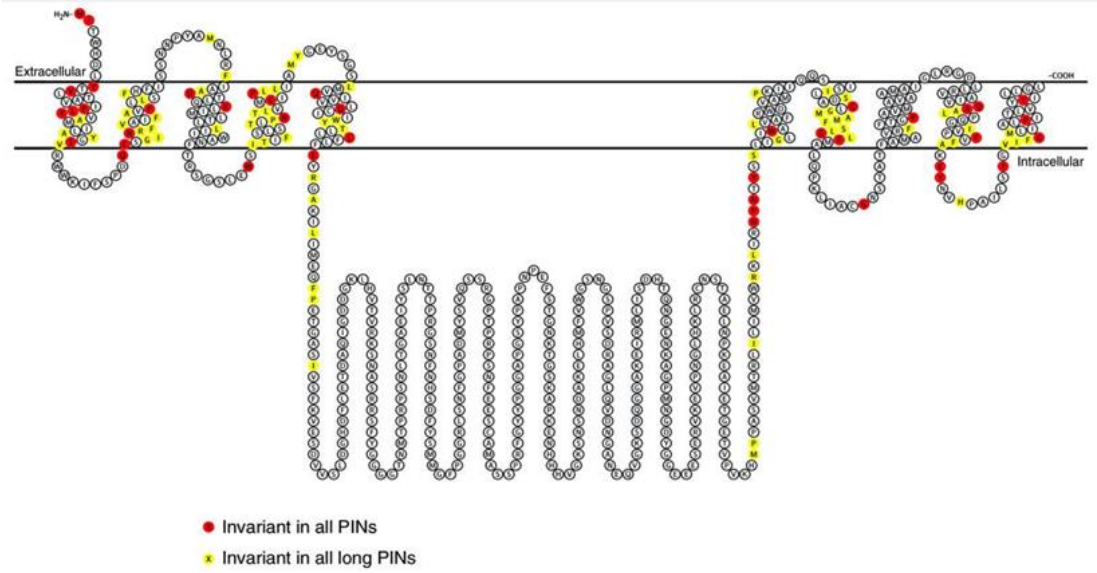

Figure 7: Taken from Krecek et al., 2009. Diagram depicting a predicted PIN protein structure, clearly showing the two hydrophobic, membrane spanning domains separated by a hydrophilic loop structure.

PIN proteins play a central role in controlling the balance kept between stem cell maintenance and differentiation. PIN protein concentration is linked to the localisation of auxin maxima in the root (Stahl et al., 2009). PIN protein transcription is mediated by *PLT* gene expression, allowing control over PIN protein concentration at the plasma membrane during specific auxin signals and maxima (Friml, 2010). *PLT* activity is linked to *WOX5* expression. During high auxin concentrations *WOX5* and *PLT* are repressed, leading to the differentiation of distal stem cells (Ding and Friml, 2010).

PIN proteins undergo constitutive recycling between the plasma membrane and endosomes in root cells; these rearrangements of PIN localisations change the direction of auxin influx (Krecek et al., 2009). This cycling dictates the polarisation of the surrounding tissue, affecting the function of that tissue through manipulation of auxin signalling. This cycling process is dependent on clathrin-mediated vesicle

trafficking (Kitakura et al., 2011). Polarity comes from the endocytic cycling which only occurs in auxin conducting cells. PIN targeting utilizes distinct ARF-GEF (ADP-ribosylation factor (ARF) - Guanine exchange factor (GEF)) dependent apical and basal pathways (Kleine-Vein et al., 2008), such that PIN1 is typically found at the basal membranes of cells in the central cylinder, whereas PIN2 is localised to the apical membrane of cells in the root cortex and epidermis.

Experimentally, auxin application leads to changes in PIN-auxin transport component localisations. Application leads to the movement of PIN1 to the inner and PIN2 to the outer cell walls. The exact mechanism by which auxin influences PIN protein localisation however, is unknown (Sauer et al., 2006). A study has shown by using *in vivo* visualisation of PIN2, that it undergoes differential degradation in response to environmental signals such as gravity (Kleine-Vehn et al., 2008). This differs to the function of PIN1 proteins in that there is no polar delivery of PIN2 proteins to the basal membrane. PIN2 trafficking does not depend on the vesicle trafficking regulator ARF-GEF GNOM (Kleine-Vehn et al., 2008). Experiments have shown that apical (PIN2) and basal (PIN1) targeting in plants are functionally distinct pathways, using different sets of ARF-GEF proteins. Brefeldin A (BFA) is a fungal toxin which induces aggregation of endosomes into 'BFA compartments' and inhibits trafficking between the endosomes and plasma membrane (Kitakura et al., 2011). Under BFA treatment, most basal cargoes including PIN1 in the stele, were completely internalised into BFA compartments, whereas apically localised cargoes were largely unaffected and remained in the plasma membrane. It is therefore proposed that apical cargoes use ARF-GEFs that are insensitive to BFA, whereas basal targeting uses BFA-sensitive ARF-GEFs, thus apical and basal pathways can

be seen to act in parallel to one another within the same cell (Kleine-Vehn et al., 2008).

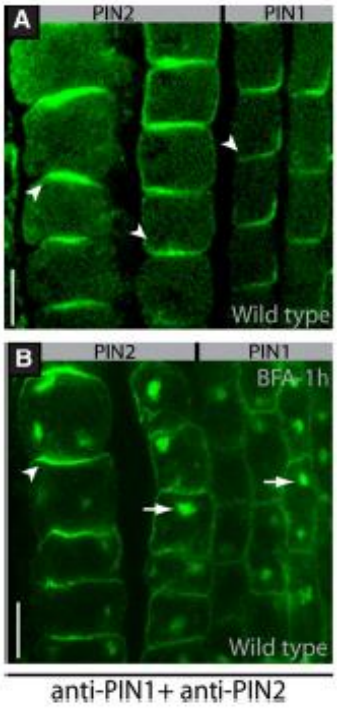

Figure 8: A: Apical PIN2 localisation in the epidermis, basal PIN2 localisation in the cortex, and PIN1 in both the stele and endodermis (WT).
B: BFA treatment (50μm) leads to strong internalisation of basal PIN1 and PIN2 into BFA compartments. Apically localised PIN2 is not affected. Taken from Kleine-Vehn et al., 2008.

Apical and basal PIN deposition pathways are distinct at the molecular level Figure 8. The recruitment of PIN proteins to these pathways depends on the phosphorylation state of the PINs: an apical/basal switch. Initial PIN protein secretion is actually non-polar; their polar distribution is established during the endocytic recycling stage (Kleine-Vehn et al., 2011). Post-translational modification of PIN proteins has been found to provide further specifity of function. Post-translational phosphorylation of PIN protein hydrophilic loops play a role in guiding

the polar cycling of the protein (Loefke et al., 2013). PIN proteins are phosphorylated by the Ser/Thr protein kinase, PINOID (PID), causing a shift in PIN1 localisation from the basal to the apical axis during auxin signalling events therefore providing control of the direction of auxin efflux (Loefke et al., 2013). PID and GNOM influence PIN membrane localisation and its polarity; PID-dependent PIN phosphorylation causes GNOM-independent polar PIN targeting (Kleine-Vehn et al., 2009).

GNOM is a key regulator of the endosomal trafficking pathway. It activates ARF-GEF which in turn activates small GTPases of the ARF class to enable vesicle budding at targeted endomembranes, therefore initiating vesicle transport of the cargo at the initial membrane. The ARF-GEF GNOM complex is a regulator of recycling, ARF-GEFs recruit coat proteins and cargos to the initial membrane to promote vesicle formation through the subsequent activation of ARF-GTPases via the exchange of bound GDP for GTP and thus providing the energy required for budding. GNOM is known to localise to the membranes of recycling endosomes and it has therefore been speculated that GNOM may be a key component of the endosomal recycling of PIN proteins during the polar transport of auxin. GNOM is often found at the cisternae of the Golgi apparatus during trafficking events and has a predicted role in maintaining the trans-Golgi network and early endosomal function during vesicle trafficking (Naramoto et al., 2014)

A two-step mechanism exists for the generation of PIN-protein polarity in plant cells involving vesicle trafficking (Dhonukshe., 2009). This mechanism involves the analysis of the recovery of photobleached YFP-tagged PIN1 at the plasma membrane and the analysis of initial targeting of PIN1 after inducing its

expression in cells that do not normally express PIN1. This method revealed that PIN proteins are initially targeted to the plasma membrane after synthesis and this is a random process. The PIN proteins then undergo lateral diffusion before being endocytosed and recycled to their target membrane (Dhonukshe., 2009). This polarized endocytic recycling toward preferred target membranes can explain PIN protein polarity. When PIN internalization is quenched by short-term auxin treatment, the PIN proteins remain largely non-polar, suggesting an important link between endocytic recycling and PIN protein polarity within the cell (Dhonukshe., 2009).

1.4.1 PIN Protein Recycling

A study investigating polar PIN distribution has used a semi-quantitative confocal microscopy technique to look at the way in which PIN proteins are recycled in plant cells (Kleine-Vehn et al., 2011). Relative fluorescence intensity of PIN2-GFP was visualised, allowing insight into the ratio of polar PIN distribution within the plasma membrane. Confocal microscopy allows 3D imaging in x, y and z planes: z-stack imaging. This study's profiling showed a majority of PIN2 proteins localized to the apical membrane, with a significant decrease in intensity at the edges of the apical domain. The paper also looks at PIN2:PIN1-GFP2 transgenic lines in order to compare the cellular localisations of the two PIN proteins. Photo bleaching of the apical membrane has been used to record the endocytic recycling based on recovery within 15-30 minutes. This method showed stronger PIN2 recovery in the apical cell side in cells showing super-polar PIN2 localization. This suggests that super-polar PIN2 localization therefore requires a polar exocytosis mechanism (Kleine-Vehn et al., 2011).

1.5 Vesicle Trafficking

Vesicle transport plays an important role in all cells, transporting newly synthesised proteins from the endoplasmic reticulum through the trans-Golgi network to other organelles (Zarsky et al., 2009). Transport can be retrograde, endoplasmic reticulum to Golgi apparatus, or anterograde which involves transport in the reverse direction. The process is adapted depending on the final required localisation and concentration of the cargo protein (Yao and Xue, 2011). The anterograde or secretory pathway begins in the endoplasmic reticulum where many newly synthesised proteins are targeted. The trafficking pathway of these new proteins involves movement through the Golgi apparatus to the plasma membrane or the extracellular matrix (via a transmembrane channel). The retrograde pathway transports endocytosed cargo from the plasma membrane in endocytic vesicles, to the vacuole. For PIN proteins, this is regulated by the ARF/GEF GNOM pathway which regulates vesicle trafficking through polarisation of PIN proteins (Geldner et

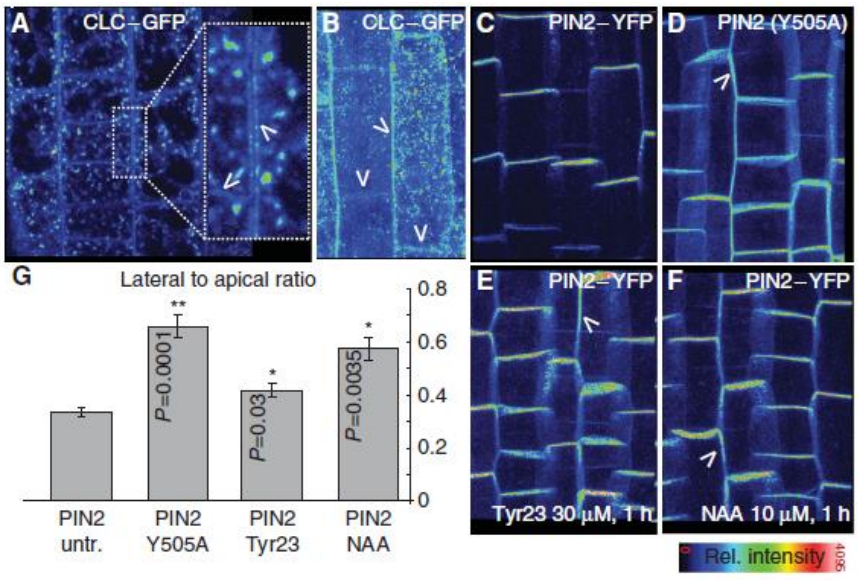

Figure 9: Taken from Kleine-Vehn et al., 2011. Confocal micrographs showing clathrin-dependent PIN internalisation at lateral cell side. A and B: lateral localisation of clathrin light chain-GFP (CLC-GFP). Arrowheads point to basal and lateral cell margins. C-F: Polar localisation of PIN2:YFP to apical cell membrane. G: Evaluation of lateral PIN2:YFP localisation, lateral:apical ratio measurements.

al., 2003)The retrograde pathways serve as a method of recycling in the cell (Bassham and Blatt, 2008).

The transport of substances along these pathways is believed to be facilitated by small membrane-enclosed transport vesicles which bud from the donor organelle via a complex system of association with coat proteins which nucleate on the membrane surface and cause deformation and eventual scission of a fragment of the membrane (Gillon et al., 2013). Once excised from the parent organelle, the vesicle moves through the cytoplasm via small and frequent interactions with cytoskeletal motors until the target membrane is reached where docking and tethering factors are utilised alongside SNARE proteins to allow membrane fusion (Bassham and Blatt, 2008). ARF-GEF regulates vesicle trafficking and is required for PIN localisation during tissue development, protein sorting and facilitation of degradation by the Golgi network allows for efficient control of PIN protein temporal and spatial localisation (Yao and Xue, 2011). Formation and trafficking of vesicles is a controlled event. Cargo selection is an important aspect of initiating the pathway along with a signal indicating the initiation site (Bassam and Blatt., 2008; Groen et al., 2014). There is also a large family of coat proteins involved in orchestrating the production of a complete vesicle, these coat proteins are specific to specific organelles (Bassam and Blatt., 2008). GTPases are recruited to the initiation site to coordinate the coating of the membrane and some of these GTPases are members of the ARF family of regulators (Naramoto et al., 2014). The ARF family are required for clathrin-type coat formation (Figure 9) (Bassham and Blatt, 2008).

1.5.1 SNARE Proteins

SNARE proteins (soluble N-ethylmaleimide-sensitive factor attachment protein receptors) are essential for the targeting and fusion of cargo proteins during endo- and exocytosis. They are localised to the plasma and Golgi membranes and facilitate the fusion of transport vesicles to specific organelles within the cell (Ohya et al., 2009). Each protein contains a conserved coiled coil domain consisting of a series of hydrophobic heptad repeats (Uemura et al., 2005). These proteins overcome huge dehydration forces to enable the fusion of two membranes, two immensely hydrophobic lipid bilayers, in an aqueous environment (Bassham and Blatt, 2008). An important relationship in this process is that of SNARE proteins and Rab GTPases. Rab GTPases regulate the binding and tethering of membrane proteins during vesicle fusion. This fusion involves interaction between v-SNARE and t-SNARE proteins and is a controlled process, the 2 proteins must be energetically compatible, this enables opposed membranes to overcome the energy barrier and bind (Ohya et al., 2009). The pairing of complementary SNARE protein partners forms a tetrameric bundle between the target and vesicular membranes enabling the two bilayers to be drawn close enough for fusion. The SNARE core complex is made up of bundled α-helices of which at least one is derived from a membrane anchored protein derived from the target membrane allowing specificity of binding. The complex includes elements from each of four subdomains, Qa, Qb, Qc and R, making the complex amphipathic meaning it contains regions of hydrophilic amino acids and hydrophobic amino acids, thus promoting their assembly (Figure 10) (Bassham and Blatt, 2008).

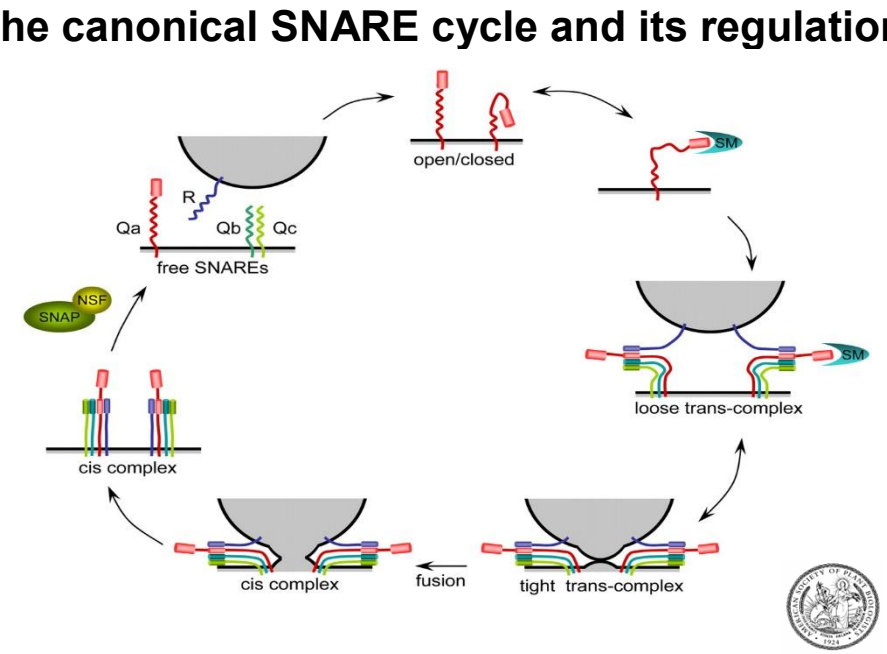

Figure 10: Taken from Bassham and Blatt, 2008, the illustration depicts the canonical SNARE cycle and the mechanism of tethering to a target membrane.

Truncating SNARE proteins enhance their binding efficiency and the speed of the reaction; this could indicate that naturally, SNARE proteins contain regulatory domains which slow the rate of binding but increases specificity allowing higher levels of control of trafficking. Particularly on endosomal membranes, Rab5 assembly is a tightly controlled event, involving complex pathways of regulators and effectors (Ohya et al., 2009). PIN proteins are recruited to their target tissues via clathrin-dependent vesicle trafficking.

PIN proteins are initially recruited to non-mobile clusters in the plasma membrane, these clusters are then internalised by SNARE proteins, producing vesicles for endocytosis. This process allows control of polarity across tissues (Groen et al., 2013). During endocytosis in plants, all proteins must pass through the trans-Golgi network before being cycled to the plasma membrane or being delivered

to the lytic vacuole for degradation. Many plant proteins including PIN proteins undergo constitutive endocytic recycling, rather than only being internalised upon ligand binding as other plant proteins are. This constitutive recycling of PIN proteins is what allows control of cell-to-cell polarity and auxin transport and function (Groen et al., 2013).

1.5.2 Endosomal Recycling

Clathrin-mediated endocytosis, an evolutionarily conserved endocytic pathway, is an important process which regulates protein abundance at the plasma membrane and the Golgi apparatus. It is thought that this may be the mechanism by which PIN proteins are transported between membranes. Clathrin is a triskelion protein complex made up of 3 heavy protein chains and 3 light chains these complexes form a cage around vesicles formed from the plasma or Golgi membrane. The complexes associate with cargo proteins within the vesicle allowing pinching as the vesicle leaves the plasma membrane. In plants, this process is critical for a number of developmental processes, in this case the process of interest is the determination of cell polarity and hormone signalling (Wang et al., 2013).

1.6 VAMP714

When looking for potential regulators of embryo and meristematic patterning in *Arabidopsis thaliana*, activation tagging was used to identify new genes of interest by inducing gain of function mutations and observing the resulting phenotypes. The *conjoined* mutant was discovered with stunted root growth and abnormal root architecture. The activation tagging event used in the synthesis of this mutant occurred at a locus between two genes: At5g22360 and At5g22370.

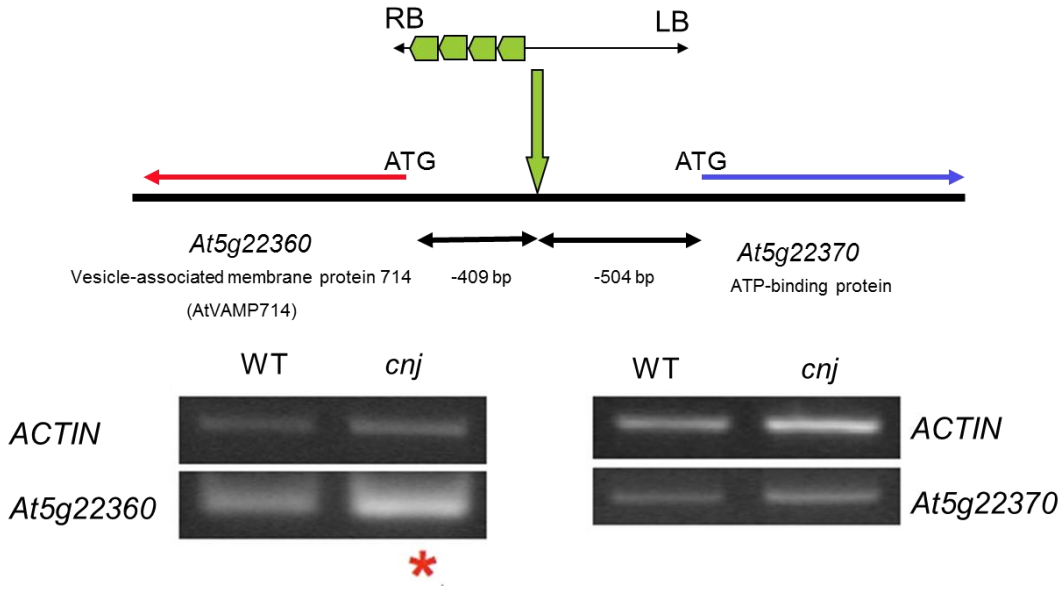

Figure 11: Figure shows illustration of activation tagging locus between the two genes, At5g22360 and At5g22370 (top). PCR gel photographs from the genotyping experiment undertaken with WT DNA and *conjoined* DNA, showing that the activation tag induced increased expression of VAMP714.

In order to determine which gene was over expressed, a genotyping PCR experiment was done using actin primers and DNA extracted from the *conjoined* mutant and from wild-type plants. The results showed increased expression in At5g22360, a gene which encodes Vesicle-Associated Membrane Protein 714 (VAMP714). This experiment highlighted VAMP714 as having a possible key role in vesicle transport in the root tip, linked to root growth and development.

VAMP714 is a Vesicle Associated Membrane Protein. It is a SNARE protein involved in vesicle trafficking in plant cells. VAMP7-like proteins are a type of R-SNARE containing a longin domain (profilin-like fold) (Rossi et al., 2004) found in *Arabidopsis* including AtVAMP714 which is located on the Golgi apparatus (Uemura et al., 2005).

A study looking into the function of AtVAMP727, an R-SNARE related to VAMP714, has found that it co-localises with SYP22/VAM3 which is a Q-SNARE (Figure 12) (Ebine et al., 2008). This co-localisation occurs when there is a subpopulation of endosomes in close proximity to the vacuolar membrane. A functioning SNARE complex consists of four coiled-coil helical bundles, usually 3 Q-SNARE bundles and 1 R-SNARE bundle, so this experiment provided evidence for the role of proteins in the VAMP family in SNARE complexing and subsequent vesicle transport. The authors suggest that the role of VAMP727 is to mediate fusion of the prevacuolar compartment and vacuolar membranes during seed development. This VAMP protein, like VAMP714, is a seed plant specific SNARE, suggesting that they function in physiological events unique to seed plants (Ebine et al., 2008).

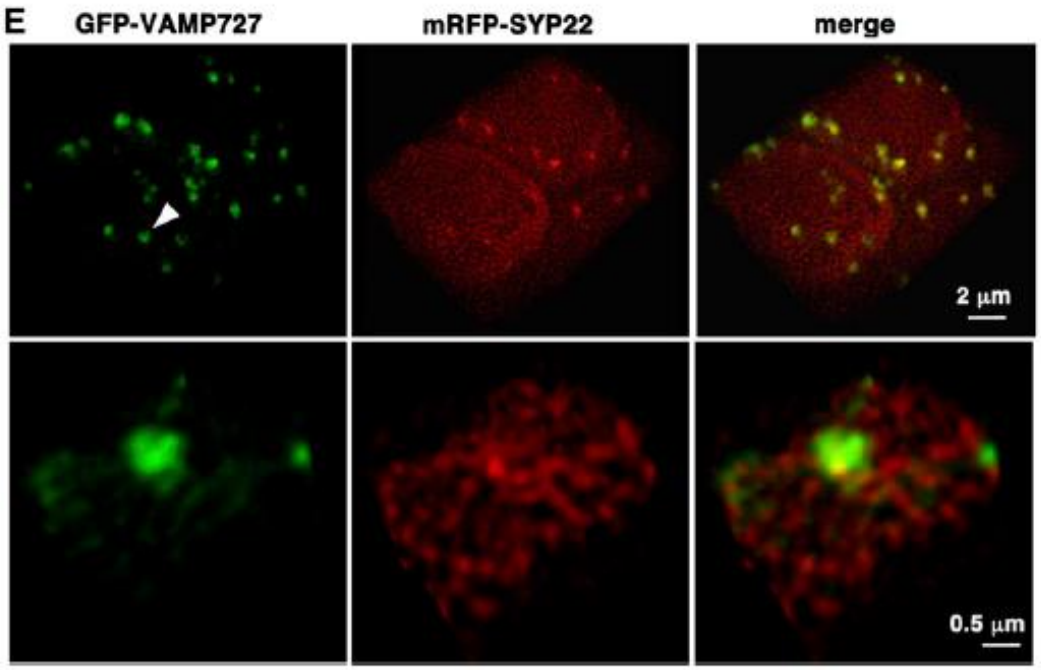

Figure 12: E: 3D confocal imaging showing co-localisation of VAMP727 and SYP22 at subdomains between endosomal compartments and the vacuole. VAMP727:GFP and SYP22:RFP were co-expressed in *Arabidopsis* seedlings. Separate images have been merged in order to display the interaction between the two proteins. Taken from Ebine et al., 2008.

From the findings presented in this chapter, it is possible to hypothesise that VAMP714 may have a functional role in the transport of PIN proteins from the endosomal compartments to the plasma membrane during endosomal cycling. As a vesicle associated membrane protein it may have a role in the identification of target membranes or docking and delivery of cargo to the target membrane during vesicle trafficking. The phenotype exhibited in the *conjoined* mutant suggests that when a mutation occurs in the At5g22360 gene, root development is disrupted. It is possible that this is because VAMP714 in a WT root, is involved in the polar transport of PIN proteins to facilitate correct auxin distribution across the tissue during growth.

1.7 VAMP:CFP PIN1:GFP

Previous work was able to show that the subcellular localisation of VAMP714 is at the Golgi apparatus. This was done using the onion epidermal cells transient expression system, allowing identification of the localisation of AtVAMP714:GFP fusion proteins alongside the localisation of a Golgi:RFP marker (Kumari PhD thesis, 2011).

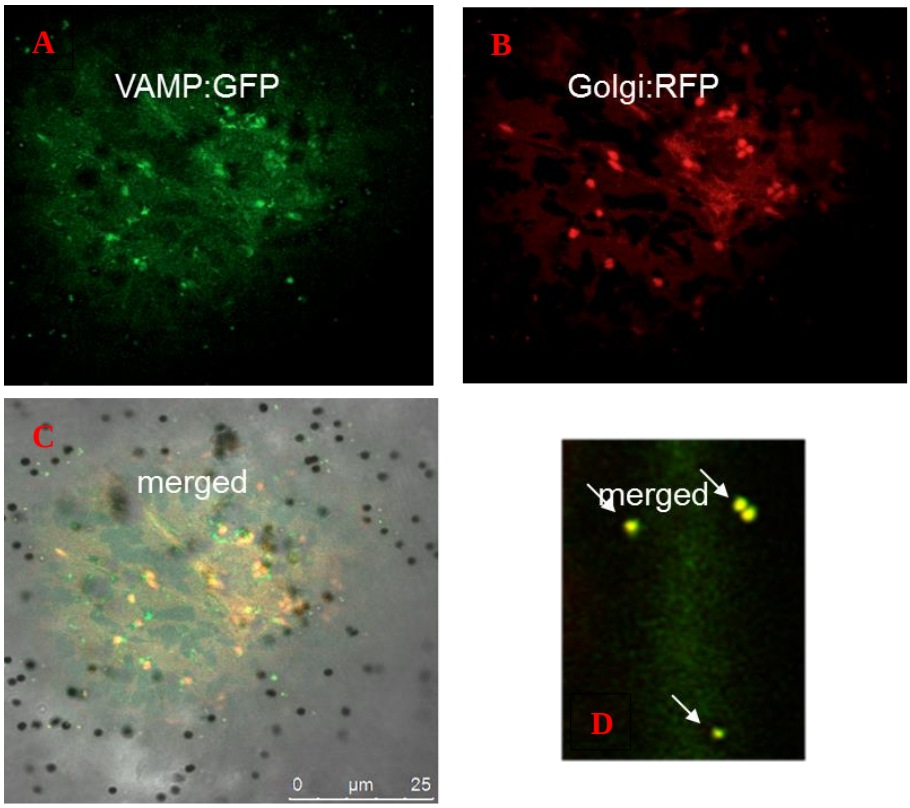

Figure 49: Taken from Kumari PhD Thesis, 2011. Microscopy images showing the co-localisation of AtVAMP714::GFP with golgi vesicles.

A: Expression pattern of AtVAMP714::GFP on onion epidermal cell

B: Expression pattern of Golgi::RFP on onion epidermal cell

C: Merge of AtVAMP14::GFP and Golgi::RFP (A and B respectively)

D: AtVAMP714 co-localisation to golgi vesicles- arrows indicate the co-localisation with vesicles.

The results showed VAMP714 proteins localising to golgi vesicles and support the theory that VAMP714 is involved in the golgi vesicle trafficking pathway. Following this experiment, the use of fusion-tagged proteins enabled the investigation of the potential co-localisation of VAMP714 and PIN1 proteins.

VAMP714:CFP and PIN1:GFP fusions were used to look for co-localisation of these proteins during vesicle trafficking and PIN1 delivery to the plasma membrane during auxin transport. An *AtVAMP714* gene construct was introduced into PIN1:GFP plants. From the primary transformants that were produced from this crossing event, one seedlings was found containing both fusion tags, shown in Figure 50.

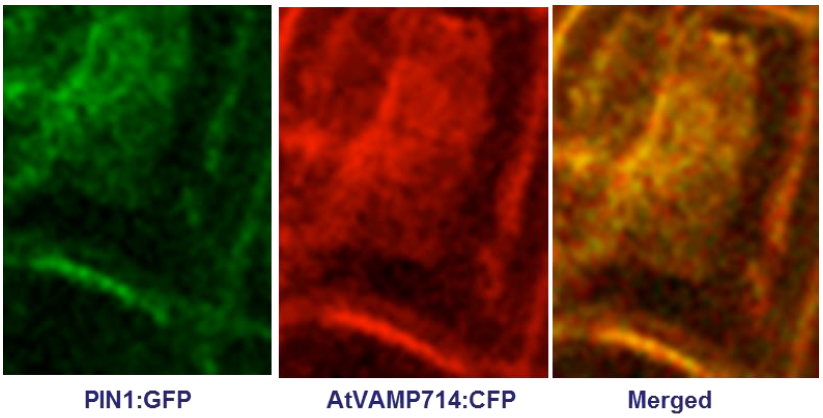

Figure 50: Taken from Kumari PhD Thesis 2011. Image taken under confocal microscope showing the co-localisation of AtVAMP714::CFP and AtPIN1::GFP at the plasma membrane.

During the course of this study the image could not be duplicated, another mutant containing both fusion tags was not found and so further evidence to show the co-localisation of VAMP714 and PIN was not achieved.

1.8 Project Aim

The aim of this project is to further investigate the role of VAMP714 in root development. In order to achieve this, several mutant seed lines were grown up in order to observe possible mutant phenotypes. Aniline blue staining was used alongside confocal microscopy in order to observe the differentiation of the quiescent centre and the stem cell niche in the root tips. Various other staining methods were tested in order to reveal any starch production in the stem cell niche, indicating cellular differentiation. Transgenic seeds containing fluorescent proteins tagged to PIN1 and VAMP714 were grown up in an attempt to observe the co-localisation of PIN proteins and VAMP714 in order to deduce their functional relationship.

2.0 Materials and Methods

All plant material used were from *Arabidopsis thaliana.* Wild-type seeds were of the Columbia-0 (Col-0) ecotype, originally obtained from Lehle Seeds (Texas, USA). Dominant Negative and VAMP:CFP PIN1:GFP seeds were produced by and obtained from Kumari, Durham University. SALK_5917 seeds were purchased from the SALK institute via NASC, the European Arabidopsis Stock Centre (http://arabidopsis.info/).

2.1 Growth on Media

The media used to create standard growth conditions in all experiments was ½ MS10 (half strength Murashige and Skoog medium, Sigma containing 10g/l sucrose). This was made up in a 2L stock solution and stored in 400ml aliquots.

10g sucrose was added to 1.5l dH_2O (water) and dissolved using a magnetic stirrer. 4.4g MS salts were added and mixed until fully dissolved. The media was adjusted to a pH of 5.7 by the addition of either KOH (Potassium Hydroxide) or HCl (Hydrochloric acid) and tested with a pH probe. The solution was made up to 2l using deionised H_2O and separated into 400ml aliquots. Agar was then added in a 2g/400ml ratio to the medium. The stock was then autoclaved (120°C, 20 min) to ensure sterility. These 400ml aliquots were then stored at room temperature, in an air tight container, and melted down as required.

2.1.1 Sterilising Seeds

Seeds were sterilised to prevent fungal or bacterial growth before applying to media. Seed sterilisation was done under sterile conditions in a sterile flow hood.

Seeds were washed in 70% v/v EtOH (Ethanol), inverting several times in an Eppendorf tube. The EtOH was then removed using a sterile transfer pipette, being

careful not to remove any seeds. 20% v/v bleach was then added, inverted several times and left for 15 minutes. The bleach was removed in the same way as described above. Finally, seeds were washed 4-5 times with sterile milliQ H_2O, inverting the tube with each wash.

Seeds were stored in sterile milliQ H_2O for up to 2 weeks at 4^oC. Once seeds were sterilised they were ready to be plated out (under sterile conditions) on media for tissue culture.

2.1.2 Plating seeds

Plating seeds onto sterile media for tissue culture was done under sterile conditions, in a sterile laminar flow hood.

Sterile ½ MS10 was melted down slowly in a microwave at around 30% power, taken to a sterile flow hood and poured into each sterile plate (approx. 30ml for circular and 50ml for square plates). 20mins was allowed for the medium to fully set.

The seeds were always previously sterilised. Using a new sterile transfer pipette for every seed line being plated, an aliquot of seeds was taken up in dH_2O and spread gently and evenly across the medium taking care to separate each individual seed from any that might be attached without disturbing the surface of the media.

Plates were sealed with Micropore tape and stored at 4^oC for 3-4 days for stratification.

2.1.3 Vertical Plates

The same medium was used in vertical plates as in horizontal in this study, and all plates were prepared under the same sterile conditions in a sterile flow hood.

Approx. 50ml of melted ½ MS10 was poured into each sterile square plate. 20mins was left for the media to set.

A horizontal line was marked an inch from the top, on the outside of each plate. Using a sterile transfer pipette, 10 seeds were placed carefully on the surface of the media and spread at even intervals along the drawn line using either the transfer pipette or sterile wooden cocktail sticks.

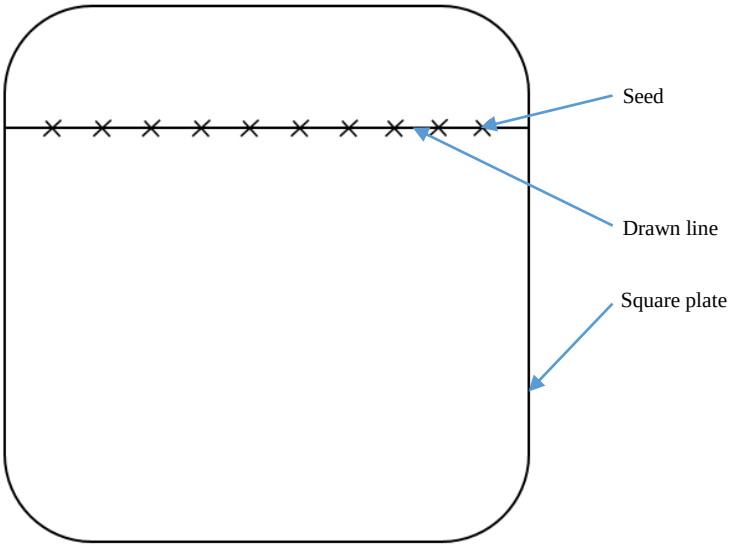

Figure 13: Illustration demonstrating the typical layout of a vertical plate.

Plates were stored at 4°C for 3-4 days for stratification and transferred into the growth cabinet at 22°C, stored vertically in a stand or box so that only the green aerial parts of the plant were receiving direct light. The roots were grown below the cardboard of the box.

Another method for preparing vertical plates was to plate and germinate seedlings on circular, horizontal plates until 1-2 d.a.g. (days after germination). They were then transferred as seedlings to vertical plates. This was done using flame sterilised fine forceps under a sterile flow hood.

Flame sterilisation involved dipping fine forceps in 98% EtOH, shaking off any excess, and placing the tip of the forceps into a Bunsen flame. The EtOH was burned off, the forceps were then left a few seconds to cool without touching the tip on any surface. They were then sterile enough to lift and transfer sterile seedlings. This whole procedure was carried out in a sterile flow hood.

2.1.4 Selection Plates

Selection plates involved the addition of antibiotics to media as a screening technique for mutants which contained a transgene construct containing an antibiotic resistance gene.

Hygromycin stocks were made up and stored at -20^{o}C until required. Stocks were made up using 15mg Hygromycin in 1ml dH_2O, and 200mg Augmentin in 1ml dH_2O.

The mutants in this experiment were Hygromycin resistant. Augmentin was used to prevent any bacterial contamination in the media.

The stocks were diluted 1000x in the media by using 50µl Hygromycin stock and 50µl Augmentin stock in 50ml molten ½ MS10 (in a 50ml falcon tube), this was mixed thoroughly by inversion. 1x 50ml was poured into 2 standard sterile circular plates.

Medium was allowed to set before plating seeds in the same way as previously described (section 2.1.2).

When using selection plates, particularly with primary transformants, a far larger number of seeds was plated out than would be seen on a standard plate. It was important to ensure that all individual seeds were separated so that every seed germinated and grew directly into the selection media.

2.1.5 Pearlite

Pearlite, a chalky substrate made up of ferrite and cementite (Lindsey Lab, Durham University) was used as an alternative to agar media in cases where seeds had a low germination frequency. Seedlings were able to be moved directly onto soil once germinated and grown to a few days old.

Pearlite was used to line the base of a sterile plate in a sterile flow hood. Liquid MS media was poured on top until enough was absorbed by the pearlite such that it was immobile. The seeds were then sprinkled over the plate- they did not need to be sterile. Plates were sealed with Micropore tape, stored at 4^{o}C for stratification and then moved into a growth cabinet for germination.

<u>MS Solution:</u>

To make a 500ml stock, 1.1g of MS salts (Sigma) was dissolved in 400ml of sterile dH_2O and mixed using a magnetic stirrer. The pH of the solution was adjusted to 5.7 by addition of either KOH or HCl. The solution was then topped up to 500ml with dH_2O and aliquoted into glass flasks. The media was then autoclaved for sterility and stored at room temperature until required.

2.2 Soil Based

Plants were grown on soil for bulking up and for growing tissue for gDNA extraction. Seeds did not need to be sterile.

Soil was mixed in a 4:1 ratio with silver sand and packed into 5x5cm plastic pots. The soil was soaked with Intercept insecticide at a 60mg/400ml concentration with tap water. Seeds were then sown onto the soil (approx. 15 seeds per pot), wrapped in tinfoil and placed at 4°C for 3-4 days to allow stratification. Pots were then transferred to a growth cabinet at 22°C under long day conditions (16h light, 8h dark). Once seedlings reached 5-6 d.a.g., they were transferred to separate pots containing the same soil mixture and Intercept treatment, using fine forceps and gently ensuring that the roots were completely enclosed in their new soil. These pots were then stored in the same 22°C conditions and allowed to develop.

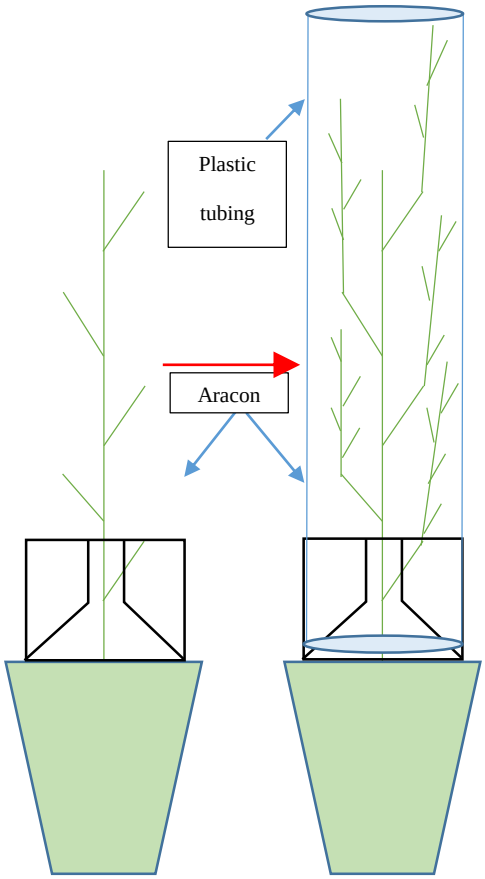

Figure 14: Illustration demonstrating the use or aracons and plastic tubing during soil based culture.

2.2.1 Bulking up

Plants were bulked up in order to replenish seed stocks and to create a more homozygous mutant stock.

Seedlings were grown, with Intercept, until they set seed. Aracons (Arasystem) were placed around the base of the plants once they reached approx. 5-7

cm tall and plastic tubing when they began to form siliques. They were left in a controlled environment growth room at 22°C under long day conditions until all siliques had formed and the plant had begun to dry out. At this point plants were moved to a seed drying room for 1 month after which the seeds were harvested.

Creating homozygous mutants by bulking involved growing up a selection of seedlings from a heterozygous line, favouring those showing the desired mutant phenotype. These plants were kept separate so that siliques were formed by selfing, and the progeny would then produce homozygous offspring.

2.3 Phenotype Screening

Vertical agar plates were used to screen seedlings for mutant phenotypes, in this case the phenotype was stunted root growth and abnormal root branching.

Vertical plates were set up as previously described. Once seedlings reached 7 d.a.g., the plates were scanned and analysed using ImageJ® software (http://imagej.nih.gov/ij/). Root length was analysed using a scaled scan of the plate and a segmented line to trace the length of the primary root. These data were compared to Col-0 WT primary root length data as a control. Any of those seedlings that showed the phenotype were either used for staining or were bulked up to produce a more homozygous seed stock.

2.3.1 Primary Root Length Assay

Dominant negative, SALK insertion line and wild-type seedlings were grown on vertical plates, set up as described above (section 2.1.3). They were grown until 7d.a.g. and then the plates were scanned. The length of each primary root was measured using ImageJ© software and compared to wild-type data.

2.3.2 Lateral Root Assay

Mutants were grown on vertical plates alongside wild-type controls. The plates were scanned at 12d.a.g. and the images analysed using the SmartRoot© plug-in for ImageJ©. Using this software, the entire root system of each seedling was traced and analysed for lateral root lengths, density and root surface area and volume, and all compared to the same data taken from Col-0 wild-type seedlings of the same age.

2.3.3 Gravitropism Assay

Mutants were grown on vertical plates, as described above, until 4d.a.g. Each plate was then scanned, turned 90° clockwise in their stands and scanned at 2hours, 4hours, 6hours, 8hours and 24hours to track the response of each root to the altered gravity stimulus. These scans were analysed using ImageJ©. The angle of root bend toward gravity was measured in each case, and the change in angle plotted for each mutant and compared to that seen in Col-0 wild-type plants.

2.4 Staining

2.4.1 Aniline Blue Staining

A stock solution of aniline blue (Bougourd et al., 2000, received from Hussey lab, Durham University) was prepared in dH_2O at a 0.5% concentration. This stock was then diluted 1:5 and 1:50 with dH_2O to produce 0.1% and 0.01% working solutions. These solutions were pipetted (approx. 20-50µl) directly onto a glass microscope slide. The root tip of the seedling to be stained was cut directly into the aniline solution using a razor blade. A glass cover slip was applied to the slide and secured with micropore tape. When mounted in aniline solution, the root tip was ready to image instantly using a confocal microscope with a 405nm diode laser.

An alternative staining protocol was developed involving dehydrating and rehydrating each seedling.

Seedlings were dehydrated in increasing concentrations of EtOH (15%, 50%, 70%, 96% and 100% v/v) and left in 100% v/v EtOH overnight. Seedlings were then rehydrated in decreasing concentrations of EtOH, 15 mins in each solution from 96% EtOH through 70%, 50% and 15%. Seedlings were then washed twice in dH_2O before submerging in 0.1% Aniline solution for 30 minutes. Seedlings were then dehydrated and rehydrated through the same concentration series before mounting the root tip in dH_2O and imaging on a confocal microscope.

2.4.2 Acridine Orange

Acridine orange (AO) was used as a selective nucleic acid dye for observation of the cellular structure of root tissues.

Initially, the seedlings were stained in a 0.1, 0.01 and 0.001% v/v AO solution in dH_2O. The seedlings were held in the stain for 20 minutes and imaged as described below. In order to improve the results, a vacuum infiltration step was added to the protocol, whereby seedlings were vacuum infiltrated for half of the staining period.

The protocol was then adapted further, using the same stock concentrations but the solution was made up using 98% v/v EtOH. A stock solution of 0.01% AO in EtOH was settled on and used in either a 10x or 100x dilution.

Seedlings were submerged in the ethanol solution for 20 minutes in total, 10 minutes in an Eppendorf vacuum infiltrator (no spin) and ten minutes on a heat block at 37°C. Seedlings were washed and mounted in dH_2O

Roots were imaged using Leica SP5 confocal microscope using a 405nm diode laser.

2.4.3 Propidium Iodide and Lugol Staining

Lugol staining Protocol:

5 d.a.g. seedlings were submerged in Lugol's staining solution (Sigma) for 5 minutes, washed and mounted in dH_2O. The solution dyed starch a blue-black colour that was observed under a light microscope.

Propidium Iodide Protocol:

300µl of a 10mg/L stock solution of propidium iodide (Sigma) was added to 500µl of dH_2O. The root tip of a 5 d.a.g. seedling was submerged in this solution for 1min 30sec. The seedling was then transferred to dH_2O for another 1min 30sec and then mounted on a glass microscope slide in water. The root was imaged under an SP5 Leica confocal microscope, using an argon laser. The dye was excited at 304nm and had an emission wavelength of 619nm. (http://www.sigmaaldrich.com/catalog/product/sigma/p4170?lang=en&region=GB).

Combining staining protocols:

A 5 minute lugol stain was reduced (to avoid the stain blocking the PI fluorescence under the confocal microscope) through 5, 3, 1.5 and 1 minutes. The staining time in PI was altered several times as well in order to find the optimum balance of the two stains and protocols. The two staining solutions were also mixed to test if using both stains simultaneously would be effective.

The protocol that was optimal was submerging the root in PI solution for 1.5 minutes, then transferring to water for a further 1.5 minutes. The root was then submerged in Lugol's solution for 1.5 minutes, and then again into water for 1.5

minutes. The root tip was then mounted in water and imaged under the confocal microscope, using the argon laser to view the propidium iodide fluorescence, and the microscopes brightfield channel to view the starch staining by the Lugol's solution.

2.5 SALK Mutant Genotyping

2.5.1 Primer Design

The SALK_5917 mutant used in this study was a t-DNA insertion mutant within the At5g22360 gene that encodes VAMP714. In order to genotype this mutant, to prove that the insertion was present, primers were designed either side of the expected insertion site. These primers were designed using ApE plasmid editor software (see appendix 2). The primers which straddled the insertion site only produced a band if the plant being screened was a wild-type. The left border primer was used with the reverse primer and was found on the inserted sequence. The insertion was read in the same direction as the gene, and so the left border primer was paired with reverse (if it had read in the opposite direction then the left border would be paired with the forward primer). This combination would produce a band if the insertion was present and the plant was therefore the SALK mutant.

Primer Pair	Wild-type	Mutant	Product length (bps)
Fwd. Rev	/		~640
Fwd. RP	/		~890
LB. Rev		/	~280
LB. RP		/	~480

2.5.2 Genomic DNA Extraction

Genomic DNA was extracted from mutant and wild-type seedlings following the Sigma gDNA miniprep kit protocol. The prep required 100mg of plant leaf tissue, plants were grown in soil until 2-3 weeks old, whole leaves were then removed by fine forceps and placed into pre-weighed Eppendorf tubes, roughly 100mg of plant tissue was weighed out and then immediately submerged in liquid nitrogen ensuring that the cap of the Eppendorf tube was securely fastened. Once frozen, the tissue was ground to a fine powder using Eppendorf grinders while keeping the base of the tube in liquid nitrogen (not allowing the tissue to thaw). The protocol was followed from this point to extract genomic DNA from the prepared tissue.

Once the prep was complete, the concentration of gDNA produced was measured using a Nanodrop ND1000 spectrophotometer (Thermo Fisher Scientific, Hemel Hempstead, UK). This tested the yield of the extraction and gave a concentration in ng/µl which was then increased if necessary using an Eppendorf Concentrator with no heat and no spin to evaporate off some of the elution solution making the concentration of DNA greater.

2.5.3 Optimising PCR

An optimising PCR was used to test both the success of the gDNA extraction and provided information on the optimal volume of DNA to use for the subsequent experiments.

Eight PCR reactions were set up, each containing a slightly different volume of gDNA extracted previously, the brightest band from this experiment gave the volume of DNA to be used in the next. Actin primers were used because both wild-

type and mutants contain actin, so it worked as a control for the presence of gDNA in the PCR product.

The PCR mix was made up as described below:

	Master Mix/µl	**X9/µl**
	4x Buffer	36x Buffer
	0.5x Act2 FWD	4.5x Act2 FWD
	0.5x Act2 REV	4.5x Act2 REV
	0.1x Taq DNA Polymerase	0.9x Taq DNA Polymerase
Total:	5.1	45.9

Vol. mMix/µl	**Vol. DNA/µl**	**Vol. dH_2O/µl**	**Total vol. /µl**
5.1	0.2	14.7	20
5.1	0.4	14.5	20
5.1	1.0	13.9	20
5.1	3.0	11.9	20
5.1	3.5	11.4	20
5.1	4.0	10.9	20
5.1	6.0	8.9	20
5.1	7.0	7.9	20

The PCR was run on an Applied G-Storm GS1 PCR machine and the programme used had an annealing temperature of 53.5°C and ran for 33 cycles.

2.5.4 Standard PCR

New primers needed to be prepped and made up to the correct dilution before use. Primers were made up to a stock concentration of 100pmol/µl and then diluted 1 in 5 in dH_2O for a working stock. The PCR was prepared using the master mix outlined below:

	Master Mix/µl	**X5/µl**
	4x Buffer	20x Buffer
	3.0x Mutant DNA (1)	15x Mutant DNA (1)
	0.1x Taq DNA Polymerase	0.5x Taq DNA Polymerase
	11.9x H_2O	59.5x H_2O
Total:	19	95

	Master Mix/µl	**X5/µl**
	4x Buffer	20x Buffer
	4.0x Mutant DNA (2)	20x Mutant DNA (2)
	0.1x Taq DNA Polymerase	0.5x Taq DNA Polymerase
	10.9x H_2O	54.5x H_2O
Total:	19	95

Vol. mMix/µl	**Vol. fwd primer/µl**	**Vol. rev primer/µl**	**Total vol. /µl**
19	0.5 Fwd	0.5 Rev	20

19	0.5 Fwd	0.5 RP	20
19	0.5 LBb1.3	0.5 Rev	20
19	0.5 LBb1.3	0.5 RP	20

Two combinations of wild-type primers were used to improve reliability of the resulting bands: primers designed specifically for this experiment (Fwd and Rev), and primers suggested by the SALK institute (Fwd and RP) (For sequences, see appendix 2).

Based on the melting temperature of each primer, the same PCR programme used for the optimising experiment was used here, with 33 cycles and an annealing temperature of 53.5°C.

2.5.5 Gel Electrophoresis

Once the PCR had run its full programme, the products were run on an agarose gel with an 80V electric current, the bands which formed gave an indication of the size of the fragment because larger fragments travel slower through the gel and therefore appear higher up on the hyperladder.

Based on the estimated band sizes, Hyperladder 100bp Plus (Bioline®) was used in both PCR experiments and was run on a 2% agarose gel.

The gel was made up as follows:

70ml of 1x TAE buffer was measured into a conical flask. 1.6g of Agarose powder was added to the buffer and heated in a microwave at full power for 1 minute. This allowed the agarose to completely dissolve into the buffer. Then, in a fume cabinet, 7.8µl of Ethidium Bromide was added to the molten gel and mixed by swirling until evenly displaced throughout the liquid. The contents of the conical flask was then poured into a secure gel mould with gel comb (with the correct

number of teeth to correspond to wells required for the experiment) in place. This was then left for approx. 20 mins to fully set.

Once set, the gel comb was carefully removed and gel was lifted (in the mould) into a gel tank filled with 1x TAE buffer, ensuring that the gel is completely covered.

Loading the wells:

Using the corresponding DNA loading buffer to Hyperladder, 2.5µl of loading buffer was aliquotted (the same number as number of PCR products) along a piece of Parafilm®. Using an Ethidium Bromide safe pipette, 5µl of the PCR product was taken up and mixed with one aliquot of loading buffer by pipetting several times. 5µl of this mix was loaded very carefully into the first well. This method was repeated for each PCR product and 5µl of Hyperladder 100bp Plus was loaded into the final well.

The gel tank was run at 80V until the bands and Hyperladder had run at least 2/3 of the way down the gel.

N.B. All work with electrophoresis gels involving Ethidium Bromide had to be undertaken with gloves on and all waste disposed of in an autoclave bin. It was very important not to come into contact with skin or to contaminate any non-EB areas of the lab.

The gel was then imaged using a BioRAD Gel-Doc 1000 under UV light and GeneSnap by Syngene imaging software.

All gels were disposed of in an Ethidium Bromide sink.

2.6 Identifying VAMP:CFP PIN1:GFP Mutants

The VAMP:CFP PIN1:GFP seeds that were used in this study were primary transformants, the stock was heterozygous. In order to screen for those seedlings containing the mutation, the insert was cloned into the plant along with resistance to a specific antibiotic, in this case Hygromycin.

Seeds were plated out on 10, 15 and 20mg/L concentrations of Hygromycin in ½ MS10 as explained in section 2.1.4. By observing the kill curve at these concentrations, a 15mg/L concentration was selected as the optimum concentration. From here thousands of primary transformant seeds were plated out on this concentration of Hygromycin and observed over the following weeks until a selection became obvious, i.e. most seedlings had died apart from a few obviously green ones.

The plate was then put under a dissecting microscope in order to observe whether or not the roots of the green seedlings were growing down into the media, and were therefore still green due to antibiotic resistance and not because they had anchored their roots onto another seedling. Once this was established the seedlings, if big enough, were mounted in dH_2O and imaged under the confocal microscope in order to screen for either CFP or GFP fluorescence.

If the seedlings had not grown big enough to easily cut the root tip, they were transferred under sterile conditions and using flame sterilised fine forceps (see section 2.1.3), onto standard ½ MS10 to grow big enough to be screened under the confocal microscope.

2.6.1 Confocal Microscopy

The confocal microscope used in this study was the Leica SP5 CLSM FLIM FCCS, primarily using the HCX PL APO Lambda Blue 63.0x1.40 Oil UV objective. Slides were prepared using dH_2O as a mounting fluid. Root tips were cut directly into dH_2O using a sharp razor blade, covered with a glass coverslip, and secured using a small strip of micropore tape on either end of the cover slip. Confocal microscopes require slides to be placed upside down on the mounting platform, so taping the coverslip prevented its movement during imaging.

Confocal settings:

	Laser	**Excitation (nm)**	**Emission (nm)**
GFP	Argon- 22%	489	508
CFP	Argon- 22%	432	474
Aniline Blue	Argon- 22%	514	550
Acridine Orange	405nm diode	502	524
Propidium Iodide	Argon- 22%	304	619

CFP and GFP imaging was done simultaneously on two separate channels with separate detectors in use allowing simultaneous scanning for two separate fluorophores.

All specimens were imaged using the Leica 63x HCX PL APO Oil UV objective.

3.0 Results

The aim of the work described in this chapter is to investigate experimentally the effect that the absence of functional VAMP714 protein has on root growth, cell structure and ability to respond to a gravitational stimulus. Two types of mutant were analysed, namely 1) a Dominant Negative loss-of-function mutant, in which a transgene comprising VAMP714 lacking its transmembrane domain (Figure 21) and so is expected not to be able to interact with vesicle or target membranes; and 2) a SALK mutant (SALK_005917) which contains an insertional mutation in the At5g22360 gene sequence which results in the plants inability to produce VAMP714 at all, hence it is a knock-out mutant. Both mutants were observed alongside Columbia-0 seedlings of the same age and grown under the same conditions. Columbia-0 (Col-0) is a wild-type ecotype of *Arabidopsis thaliana* and used in these following experiments as a control, exhibiting wild-type responses and wild-type architecture in all situations.

3.0.1 Genotyping SALK_5917

The SALK_5917 mutant used in these experiments was genotyped in the laboratory by Kumari (Kumari PhD thesis., 2011). Primers were designed specifically for this experiment, in order to allow clarification of the gene sequence

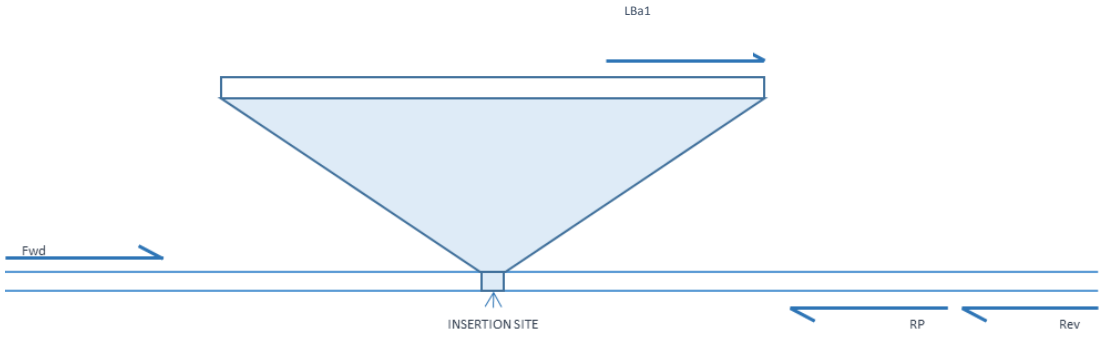

Figure 48: Taken from section 3.3. Illustration depicting insertion site in SALK_5917 mutant and approximate sites of each primer used in this experiment. For primer sequences and exact positions within At5g22360 gene sequence, see Appendix 2.

present in the plant. A primer pair for the wild-type gene sequence was designed to be used alongside a primer complimentary to the inserted sequence that would be present in the mutant. This would allow, via standard-PCR, classification of the plant tissue as either wild-type or the expected mutant. Successfully genotyping the mutant proved that the mutation in the seedlings was as expected. The mutation is an insertion at 259bp in the At5g22360 gene and Figure 48 shows the approximate locations of each primer used in the genotyping experiment.

3.0.1.1 Bioinformatics

At5g22360 gene encodes AtVAMP714, a 221 amino acid predicted R-SNARE protein and member of the synaptobrevin-like AtVAMP7C, v-SNARE protein family.

This chapter describes the bioinformatics of the At5g22360 gene and corresponding protein alongside that of At1g73590. At1g73590 encodes PIN-FORMED 1, a protein that is hypothesised to be functionally linked to AtVAMP714.

Software used in this chapter are cited in the text.

3.0.1.2 At5g22360

At5g22360 is the gene which encodes the VAMP714 protein. VAMP714 is a predicted Vesicle Associated Membrane Protein. The main function of this family of proteins is in the targeting of endosomal vesicles to target membranes (Uemura et al., 2005). This involves the identification of the correct target membrane, docking and binding. This process depends on the association of SNARES with both docking and tethering factors at the target membrane and requires a high level of specificity

in order to ensure correct delivery of cargo (Bassam and Blatt, 2008). Figures 15 to 18 have been produced using bioinformatics programmes to propose gene expression, and protein structural and localisation data compiled from the programmes databases.

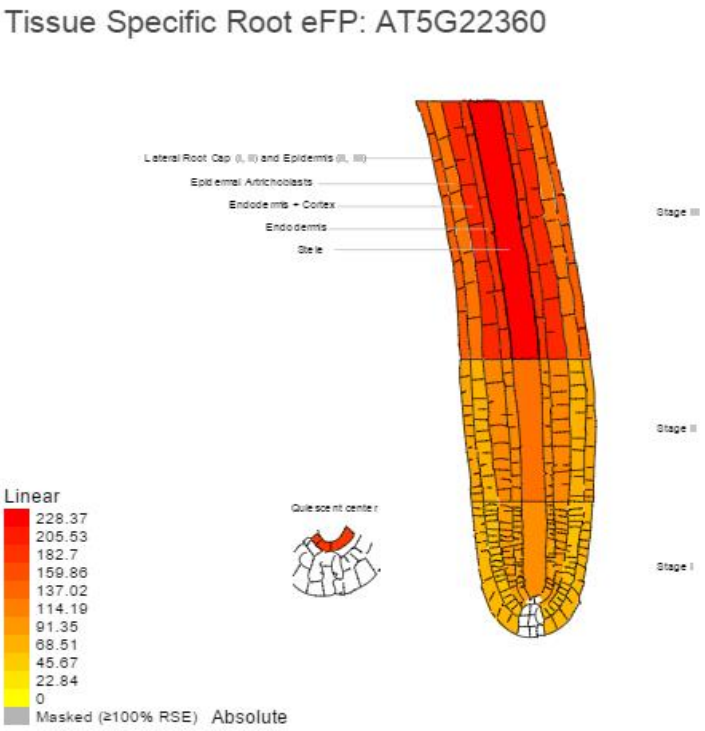

Figure 15: Expression of VAMP714 mRNA in *Arabidopsis thaliana* root tissue. The Affymetrix ATH1 array data comes from: Birnbaum et al., 2003, Science 302:1956; Nawy et al., 2005, Plant Cell 17:1908

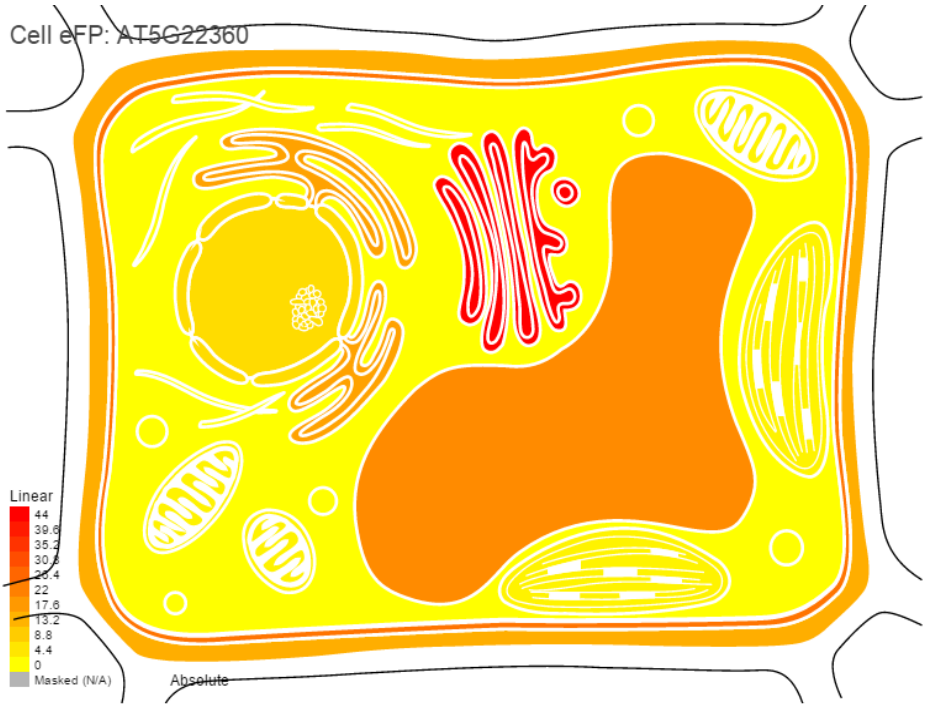

Figure 16: The Cell eFP depicts the subcellular localisation of *VAMP714* gene product, VAMP714 proteins. The data comes from Tanz SK, Castleden I, Hooper CM, Vacher M, Small I; Millar, AH (2013) SUBA3: a database for integrating experimentation and prediction to define the subcellular location of proteins in Arabidopsis. Nucleic Acids Res. 41: D1185-91

The abundance of VAMP714 mRNA across the entire root is shown in the Figure 15. It displays the results of compiled gene expression profiling experiments. The colour gradient represents the quality of information from the SUBA database and the abundance of VAMP714 mRNA in each cell type; the darker the colour, the higher the abundance of VAMP714 transcript. The illustration of the root shows the presence of VAMP714 across all cell types. Interestingly, the stele and quiescent centre (shown as an enlarged section to the left of the root) exhibits the highest concentration of VAMP714 mRNA. This supports the idea that one of the main functions of VAMP714 is in the transport of auxin through the root into the stem cell niche via PIN1 transport and therefore indirectly, is necessary for the maintenance of the quiescent centre. Relatively high levels of expression are also seen in the epidermal and cortex cells, where PIN2 is localised, for the transport of auxin from the root tip to the proximal region of the root.

Figure 16 illustrates the relative abundance of the VAMP714 protein across organelles in a standard Arabidopsis cell, depicting its predicted subcellular localisation. The colour coding works to the key found on the left hand side of the image. The darker, more red the colour, the higher the protein abundance and the higher the quality of data from the database. Here, it is clear that VAMP714 exists in far higher concentrations at the plasma membrane and in the golgi-apparatus compared to other organelles in the cell. This is consistent with the hypothesis that VAMP714 plays a role in trafficking PIN1 from the Golgi apparatus to the plasma membrane in order to control the abundance of efflux proteins at the plasma membrane, necessary for the trafficking of auxin via these proteins.

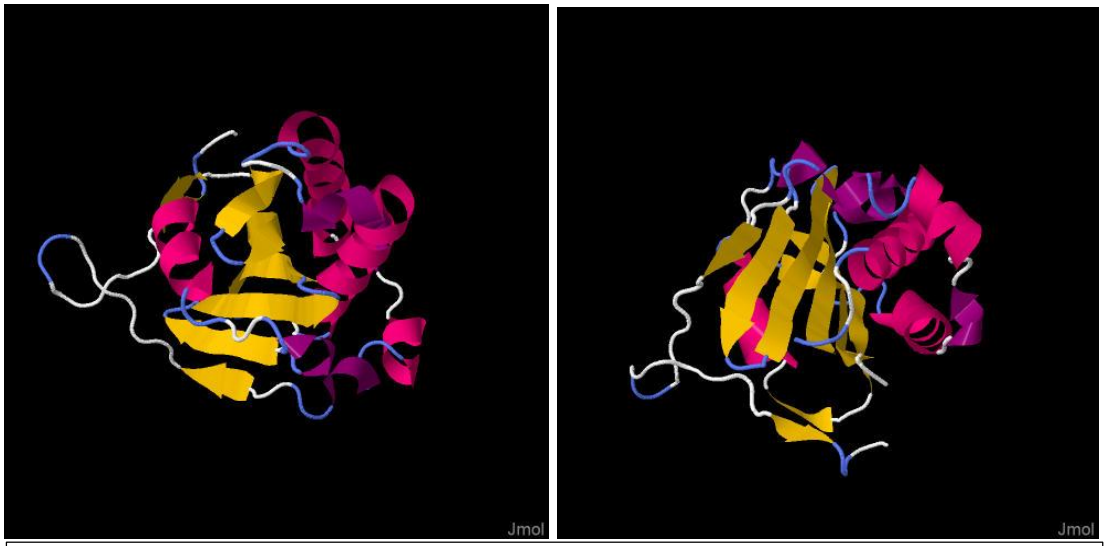

Figure 17: Predicted VAMP714 protein structure exported using Phyre[2] protein fold recognition server.

The Phyre2 web portal for protein modelling, prediction and analysis, Kelley LA et al. Nature Protocols 10, 845-858 (2015)

Model viewed using Jmol: an open-source Java viewer for chemical structures in 3D. http://www.jmol.org/

The images in Figure 17 are of the predicted structure of the VAMP714 protein produced by PHYRE2 software, a Protein Homology/Analogy Recognition Engine which predicts protein structures based on the protein sequence and known protein structure databases. The image highlights the secondary structures, highlighting β-sheet structures in yellow and α-helices in magenta. This allows visualisation of key domains that are expected to influence protein function. The synaptobrevin domain of the protein, for example, is made up of an α-helix and a long primary amino acid chain. Synaptobrevin domains are found on SNARE proteins and are involved in the tethering of vesicles to target membranes (Gracheva et al., 2010) and so, in this case, is particularly important in the functioning of the protein. This domain has been specifically highlighted in green in Figure 18.

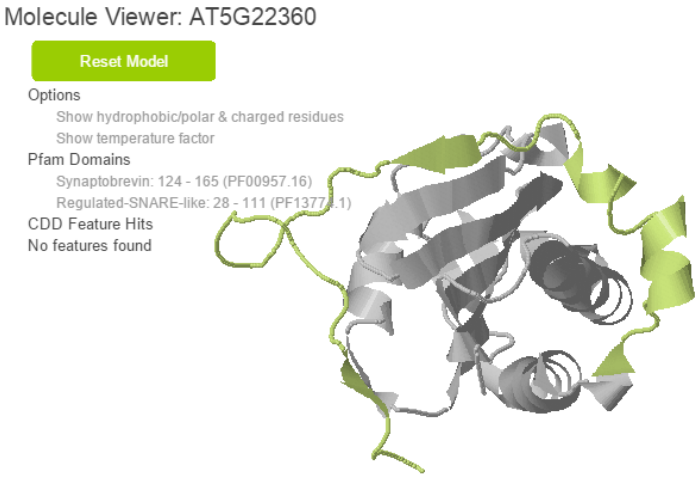

Figure 18: Data from Phyre2- Kelley LA and Sternberg MJE. Nature Protocols 4, 363-371 (2009)

SNP Data: Joshi et al., 2012

This image was generated with the ePlant Arabidopsis thaliana Tissue Specific Root eFP at bar.utoronto.ca by Waese, Fan, Yu, Pasha & Provart 2015.

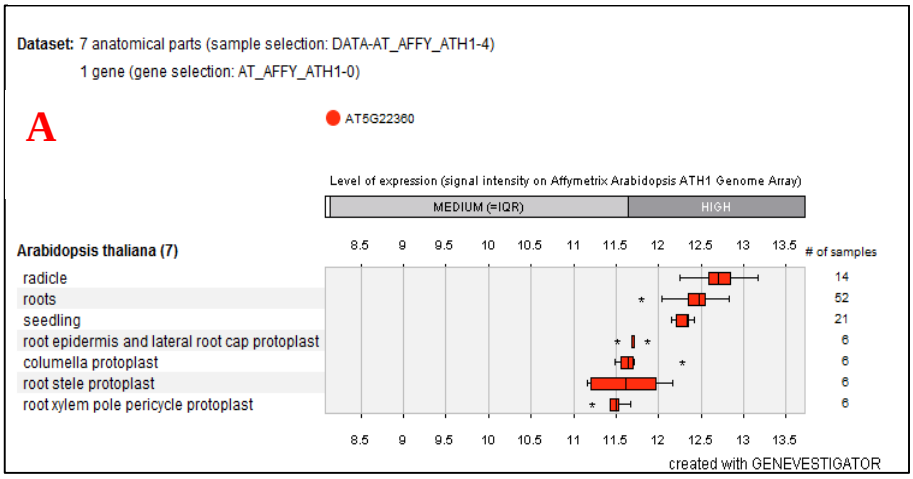

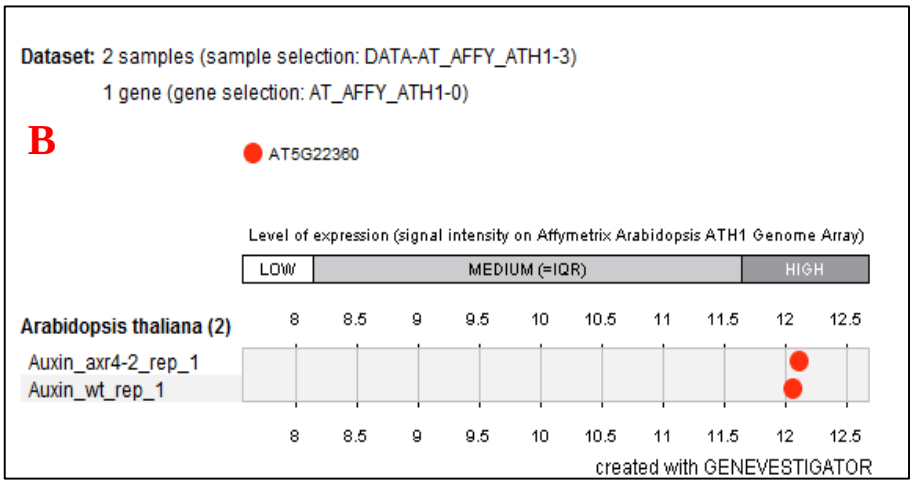

Figure 19: Data collected from Genevestigator software (Hruz et al., 2008)

A: Expression level of At5g22360 in different organs across plant

B: Expression level of At5g22360 under auxin treatment.

Genevestigator was used in order to investigate the expression levels of At5g22360 under auxin treatment. Figure 19a demonstrates the level of expression in different organs across the plant, it shows that At5g22360 is expressed at high levels in the root, as expected. Figure 19b shows high At5g22360 expression under auxin treatment on both wild-type and axr4-2 mutants, this indicates that *AtVAMP714* expression is upregulated by auxin, providing evidence for the hypothesis that VAMP714 plays a role in the auxin transport pathway. Figure 20, also produced using Genevestigator, shows a high percentage of expression potential of At5g22360 under six different auxin induced environments in six experiments. This provides further evidence that At5g22360 is upregulated by auxin and it is therefore possible that VAMP714 is involved in the polar transport of auxin during root development.

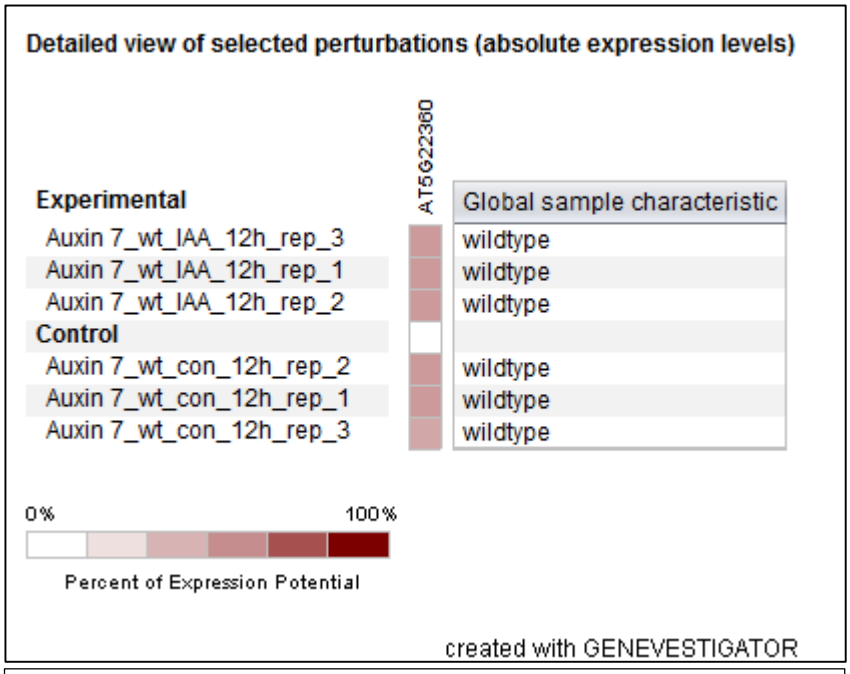

Figure 20: Data collected from Genevestigator software (Hruz et al., 2008)

Expression potential of At5g22360 during different auxin treatment experiments.

3.0.1.3 At1g73590

At1g73590 is the gene encoding the PIN1 protein. PIN1 is an auxin efflux carrier protein, it functions as a transmembrane channel protein, specifically designed to facilitate the efflux of deprotonated auxin molecules from cells during the cell-to-cell polar transport pathway. In order to allow control of the volume and direction of auxin flow from the cell, PIN1 may only be localised to the plasma membrane when delivered there by VAMP714 under the correct intracellular conditions. When auxin is not required to leave the cell, PIN1 would be internalised in endosomal vesicles; when auxin efflux is required, PIN1 would be cycled to the plasma membrane. These two localisations are similar to the predicted cellular localisation of VAMP714 as seen in Figure 16. Figures 21-23 compare the plant-wide and cellular localisation of PIN1 and the protein structures related to function.

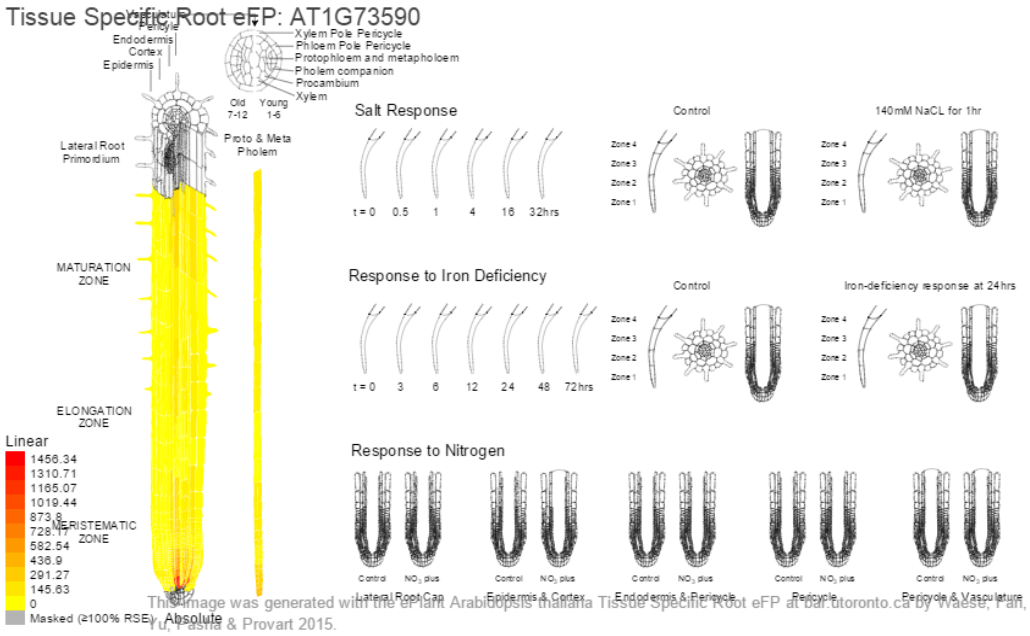

Figure 21: The Affymetrix ATH1 array data come from: Birnbaum et al., 2003, Science 302:1956; Nawy et al., 2005, Plant Cell 17:1908

This image was generated with the ePlant *Arabidopsis thaliana* Tissue Specific Root eFP at bar.utoronto.ca by Waese, Fan, Yu, Pasha & Provart 2015.

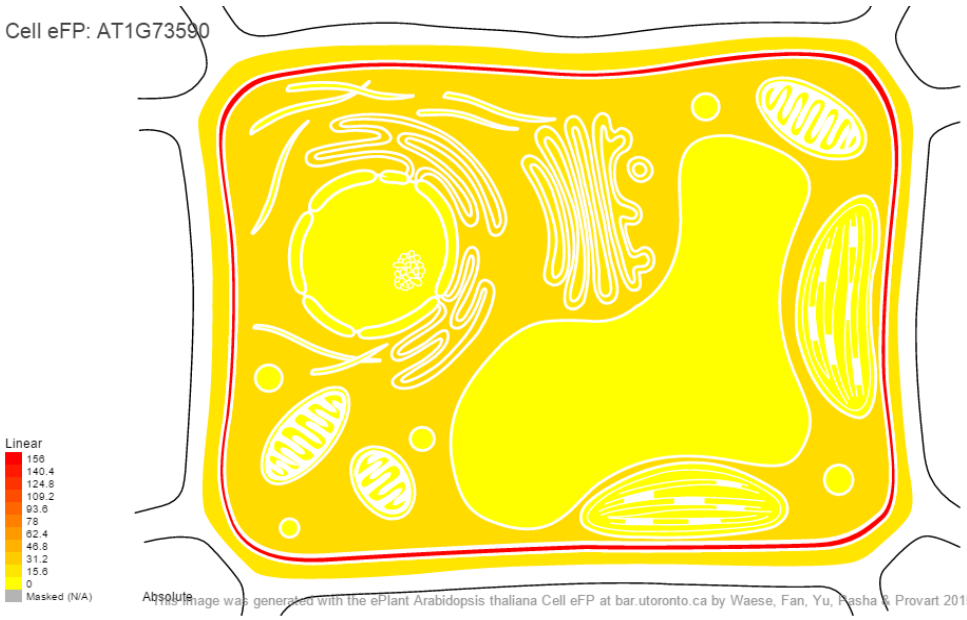

Figure 22: The data come from Tanz SK, Castleden I, Hooper CM, Vacher M, Small I; Millar, AH (2013) SUBA3: a database for integrating experimentation and prediction to define the SUBcellular location of proteins in Arabidopsis. Nucleic Acids Res. 41: D1185-91

Figure 21 illustrates the relative concentration and localisation of PIN1 mRNA in Arabidopsis roots. PIN1 proteins function in the root tip, and the mRNA is expressed in the quiescent centre, the stele and endodermis. It is expressed in similar cell-types as VAMP714.

Figure 22 illustrates the subcellular localisation of PIN1 proteins in an Arabidopsis cell. The highest protein concentration is found in the plasma membrane, consistent with the function of the protein as a transmembrane channel protein which traffics auxin from the cell during polar hormone transport.

PIN 1 is a transmembrane channel protein with two membrane-spanning domains separated by a hydrophilic domain which interacts with molecules inside the cell, and so could interact with molecules such as VAMP714 or auxin. The hydrophilic domain provides specificity to the function of the protein (Loefke et al., 2013). This specificity enables PIN1 proteins to recognise and traffic auxin molecules out of cells when localised to the plasma membrane. Their protein structure may also be involved in their recognition by VAMP714 during predicted targeting of PIN proteins by VAMP714 to target membranes.

Figure 23: Predicted PIN-FORMED 1 protein structure exported using Phyre[2] protein fold recognition server. The Phyre2 web portal for protein modelling, prediction and analysis, Kelley LA et al. Nature Protocols 10, 845-858 (2015). Model viewed using Jmol: an open-source Java viewer for chemical structures in 3D. http://www.jmol.org/

3.0.2 SALK_5917 Mutant of VAMP714

The SALK 5917 mutant used in this study contains a loss of function mutation in the At5g22360 gene of *Arabidopsis thaliana.* It is a tDNA insertional mutant overlapping exons 2 and 3 at the gene locus. This gene was identified through activation tagging of a conjoined mutant showing defective root growth. The insertional mutant was chosen because it allows observation of root growth in the absence of the protein of interest, compared to normal wild-type function.

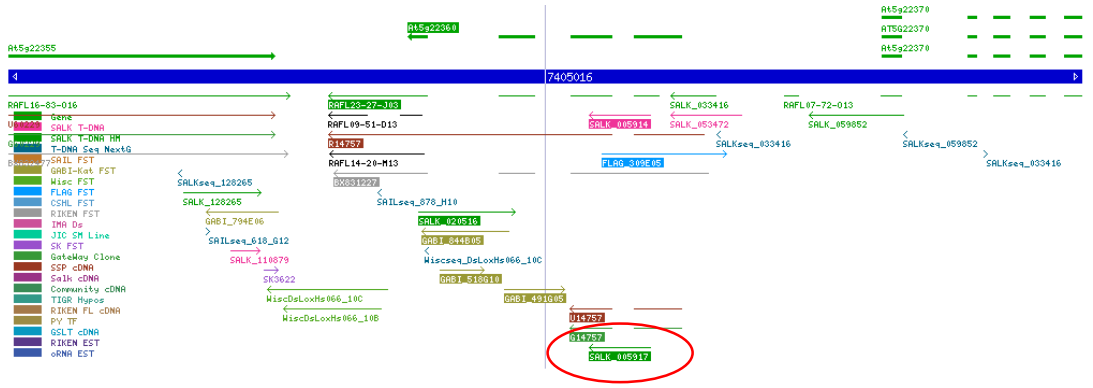

Figure 24: Taken from the Salk Institute Genomic Analysis Laboratory site: signal.salk.edu. Figure shows the positional information of the SALK_5917 insertion in the At5g22360 gene found in chromosome 5 of the *Arabidopsis* genome. This is the knock-out mutant used in the experiments in this study.

3.0.3 Dominant Negative Mutant of VAMP714

The dominant negative (Dom Neg) mutant used encodes a non-functional form of the VAMP714 protein. The mutated protein lacks its transmembrane domain (Figure 25), so the mutant protein will be synthesised and still expected to bind to a target partner protein, but would not be expected to interact with vesicle membranes, so preventing vesicle docking at the plasma membrane. As above, this will allow observation of the importance of VAMP714 in correct root development.

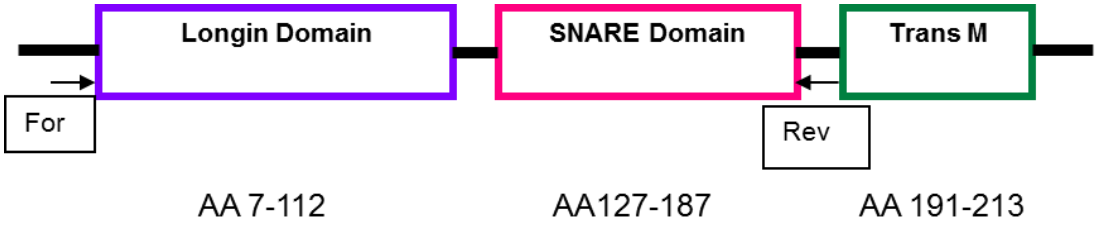

Figure 25: Shows the sites of transcription of the dominant negative mutant VAMP714 protein. The protein is transcribed without its transmembrane domain in these mutants, affecting the functioning ability of the protein product.

3.1 Genotyping SALK_5917 insertional mutant

Genotyping a SALK mutant involves designing two sets of primers. A forward and reverse pair needs to be designed to amplify the sequence either side of the insertion site, as shown in Figure 26, and so the primers need to straddle this site. These primers will only produce a product if the genomic DNA being tested is either wild-type or heterozygous. The left border primer, LBa1, was designed based on the tDNA sequence that is inserted into the wild-type. This primer is paired with the reverse or RP primer on the Arabidopsis gene and will only produce a PCR product if the inserted sequence is present, which means that the mutation has been successful and the plant being tested is a homozygous mutant.

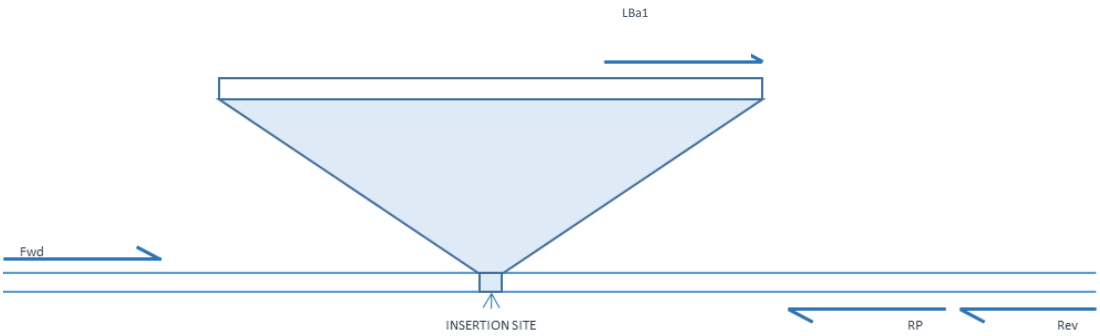

Figure 26: Illustration depicting insertion site in SALK_5917 mutant and approximate sites of each primer used in this experiment. For primer sequences and exact positions within At5g22360 gene sequence, see Appendices 1 and 2.

In this study, two reverse primers were used. ‘Rev’ is the reverse primer that was designed specifically for the experiment and was designed to pair with ‘Fwd’, a primer designed to sit before the expected insertion site and will only amplify a PCR product if the insertion is not present. RP is a reverse primer that was recommended by the SALK institute for genotyping this particular mutant, and so is designed to work well with LBa1. The genotyping experiment was undertaken by Kumari (Kumari PhD thesis., 2011). A homozygous mutant was successfully identified, proving that the insertional mutation was successful. PCR gels from this experiment can be found in Appendix 3.

3.1 Root Architecture

Seedlings were grown on ½ MS10 under sterile conditions in order to observe phenotypic differences in their root growth and structure. If VAMP714 has a role in the auxin transport system, as hypothesised, it might be predicted that mutant seedlings for this gene would exhibit altered root architecture and gravitropic responses (Michniewicz and Friml, 2007). The primary root length, lateral root initiation and growth and their gravitropic responses were recorded in order to compare the responses between wildtype and mutant seedlings.

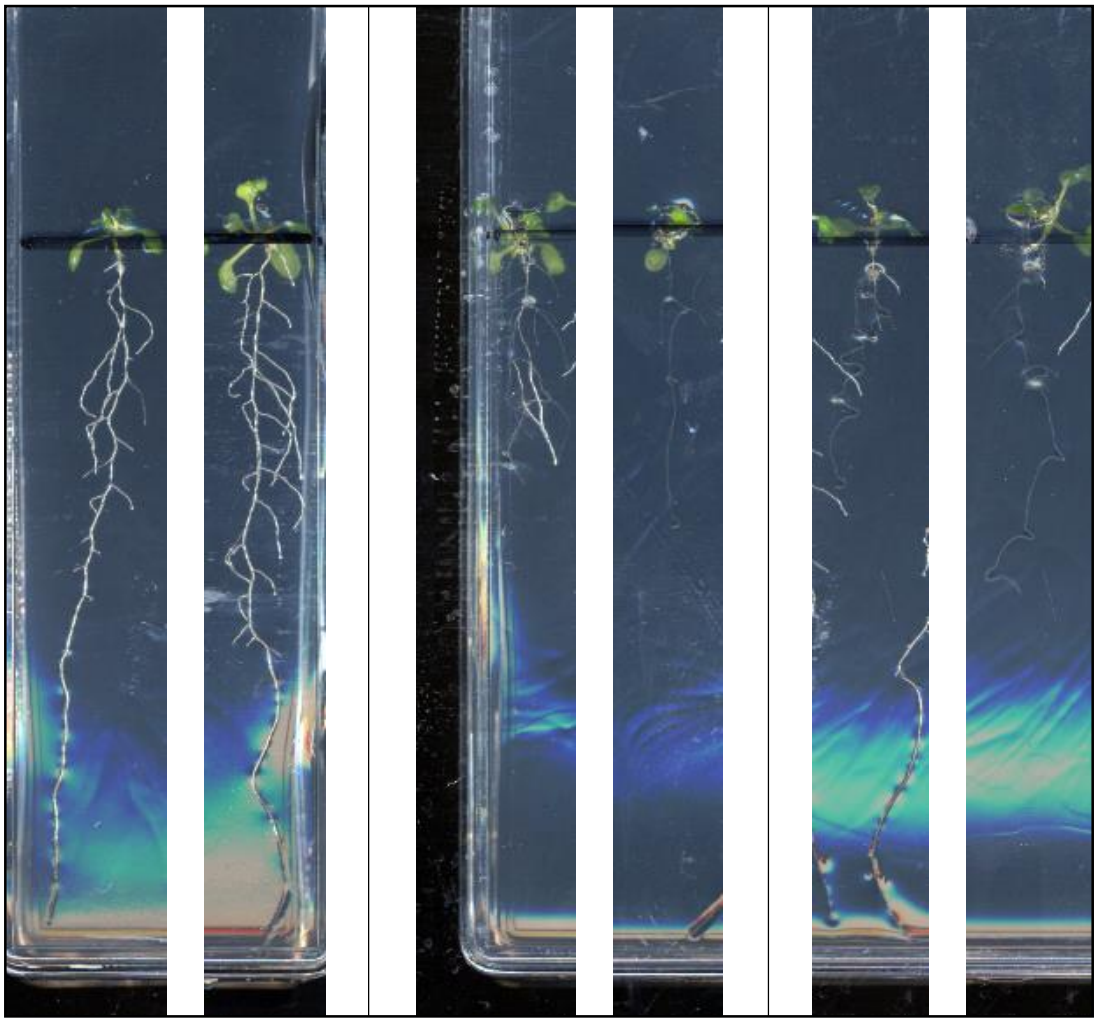

Figure 27: 12 days after germination (d.a.g.) specimens of Col-0, Dom Neg and SALK_5917 seedlings exhibiting the desired phenotype.

Figure 27 shows the mutant phenotypes of dominant negative (Dom Neg) and SALK 5917 seedlings compared to two Col-0 wild-type seedlings. The mutant seedlings have root systems that are shorter than the Col-0 seedlings.

3.1.1 Primary Root Length

Seedlings were grown on 1/2MS10 sterile medium until 7 days after germination and then scanned to allow tracing and measurement of the length of the primary root. The primary root length was measured using ImageJ image processing and analysis software using a segmented line and a 200-300% zoom to allow accurate measurement of the roots, taking account of each bend and curve developed during growth.

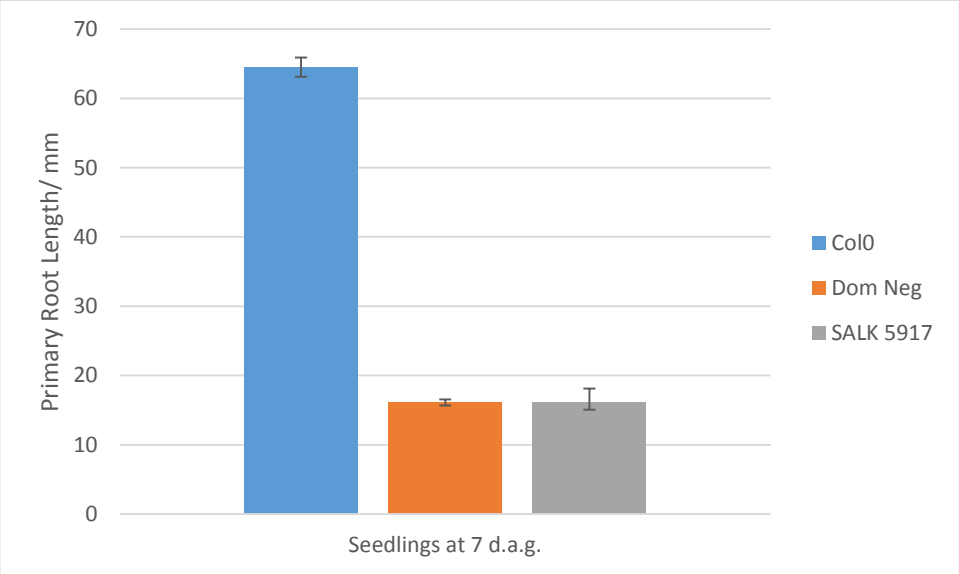

Figure 28: Average primary root lengths of Col-0, SALK 5917 and Dominant Negative seedlings at 7 days after germination (d.a.g.). Number of replicates= 18, for table of measurements, see Appendix 4.

Figure 28 shows that Col-0 wild-type roots are 2- to 3-fold longer than those of either the dominant negative mutant or the SALK 5917 mutant at day 7 post-germination. These results show that the presence of a functional VAMP714 protein is required for primary root growth in Arabidopsis.

3.1.2 Lateral Roots

The results in Figure 28 showed that a lack of wildtype VAMP714 function was detrimental to primary root growth. Lateral root growth is also regulated via auxin signalling (Fukaki et al., 2002), and so if VAMP714 is required for correct auxin responses, it might be predicted that lateral root initiation or elongation might also be affected in the mutants. Therefore the aim of the work in this section is to assess the effect of VAMP714 on lateral root development of Dom Neg and SALK 5917 seedlings in comparison to Col-0 wildtype controls. This was achieved by analysing 12 day old seedlings using Smart Root, a semi-automated image analysis software which works as a plug-in for ImageJ and allows the quantification of root architecture in complex root systems. Each seedling's entire root system was traced using this software, enabling the collection of data for lateral root length, density, mean interbranch distance, surface area and projected volume of the roots.

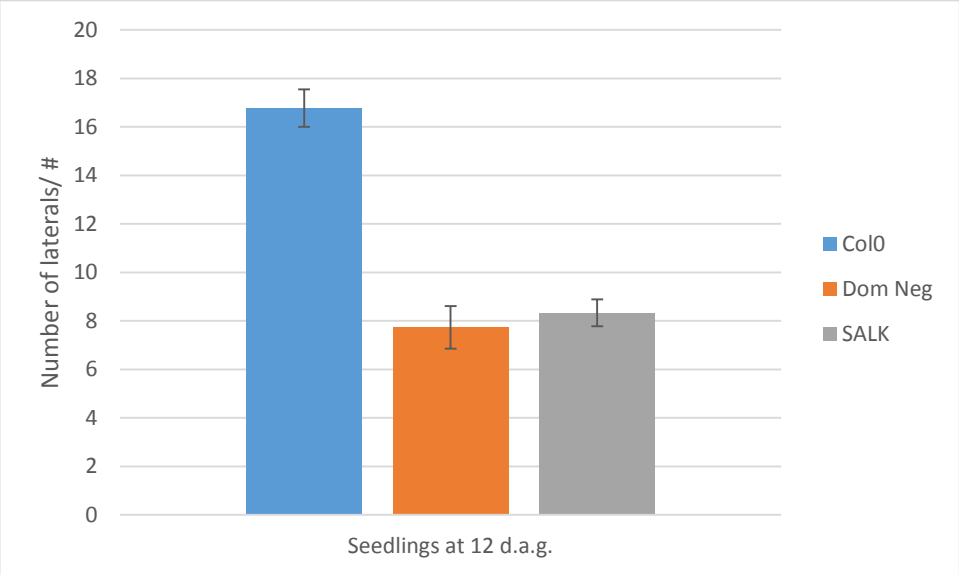

Figure 29: Average number of lateral roots seen in Col-0, SALK 5917 and Dominant Negative seedlings at 12 days after germination (d.a.g.). For table of measurements, see Appendix 5.

The results presented in Figure 29 show a significant decrease in the number of laterals in both the dominant negative and SALK 5917 mutants, with approximately 50% of the number initiated compared to Col-0 wild-type.

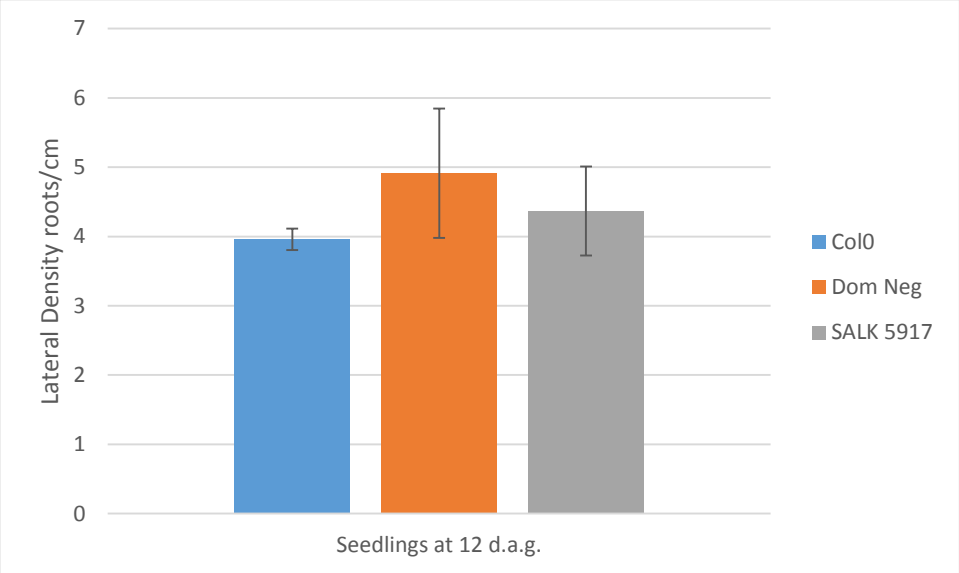

Figure 30: Average lateral density of root systems of Col-0, SALK 5917 and Dominant Negative seedlings at 12 days after germination (d.a.g.). For table of measurements, see Appendix 5.

Given that the number of lateral roots formed is expected to be linked to the length of the primary root, lateral root density (i.e. number of lateral roots per unit length of primary root) was investigated. Figure 30 shows the average lateral root density of the Dom Neg and SALK 5917 mutants is not significantly different compared to the Col-0 wild-type. This suggests the rate of lateral root initiation is unaffected by mutation of the *VAMP714* gene.

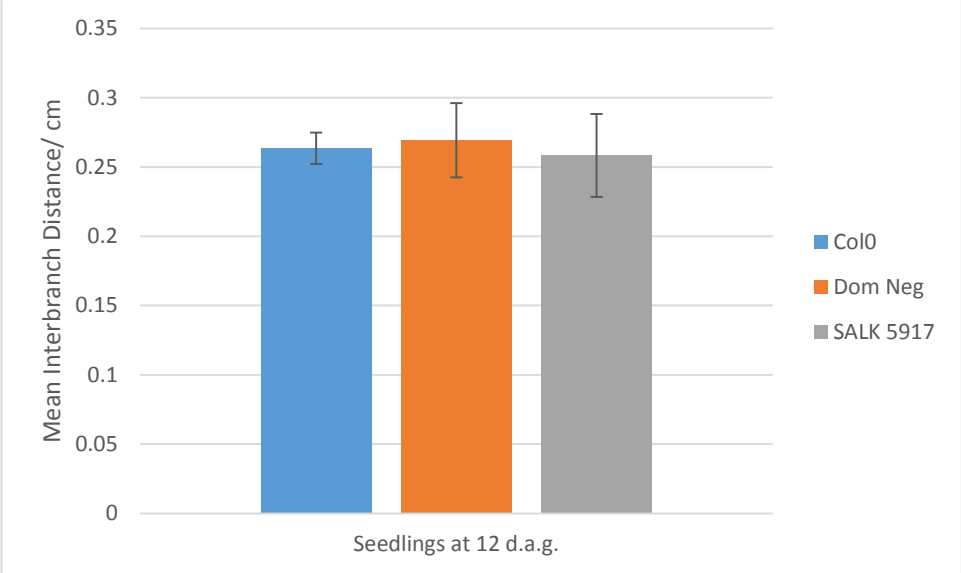

Figure 31: Mean interbranch distances of Col-0, SALK 5917 and Dominant Negative seedlings at 12 days after germination (d.a.g.). For table of measurements, see Appendix 5.

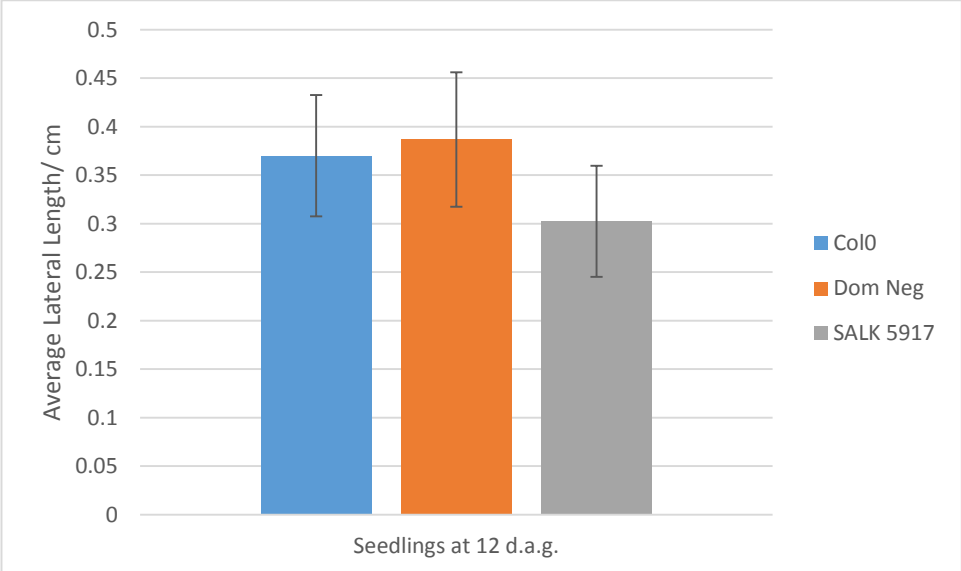

Figure 32: Average lateral root lengths of Col-0, SALK 5917 and Dominant Negative seedlings at 12 days after germination (d.a.g.). For table of measurements, see Appendix 5.

Mean interbranch distance measures the distance between each node placed at the point where a lateral is formed from the primary root, measured in cm. The results presented in Figure 31 show that there is no significant difference in the mean lateral root interbranch distance between mutant and wildtype seedlings.

Lateral root initiation and elongation are regulated by different processes (Casimiro et al., 2001). To determine whether VAMP714 plays a role in lateral root elongation, average lateral root length was also analysed. The results presented in Figure 32 show that mutant and wildtype seedlings show no significant difference in lateral root length, suggesting that VAMP714 does not play an essential role in lateral root elongation, or frequency of initiation.

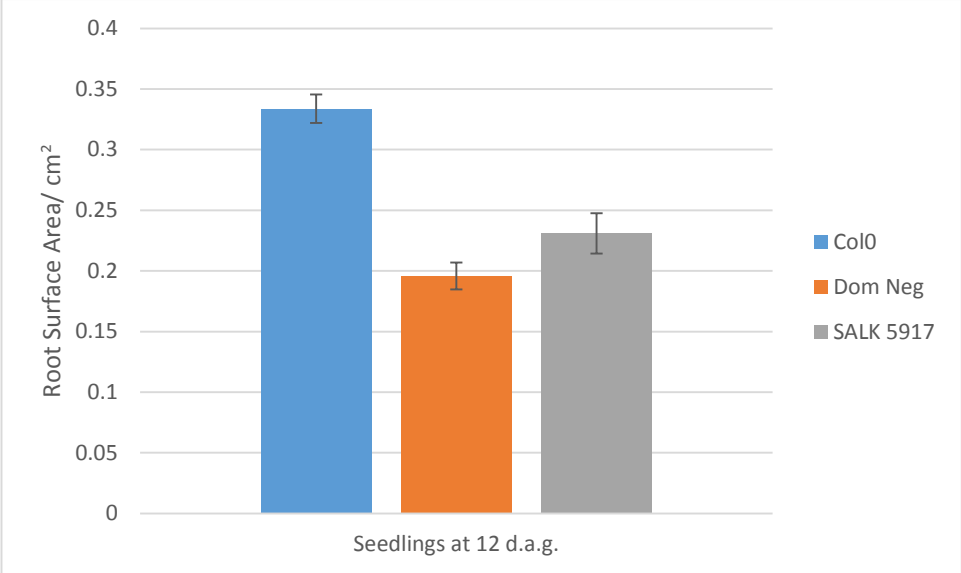

Figure 33: Average surface area of root systems of Col-0, SALK 5917 and Dominant Negative seedlings at 12 days after germination (d.a.g.). For table of measurements, see Appendix 5.

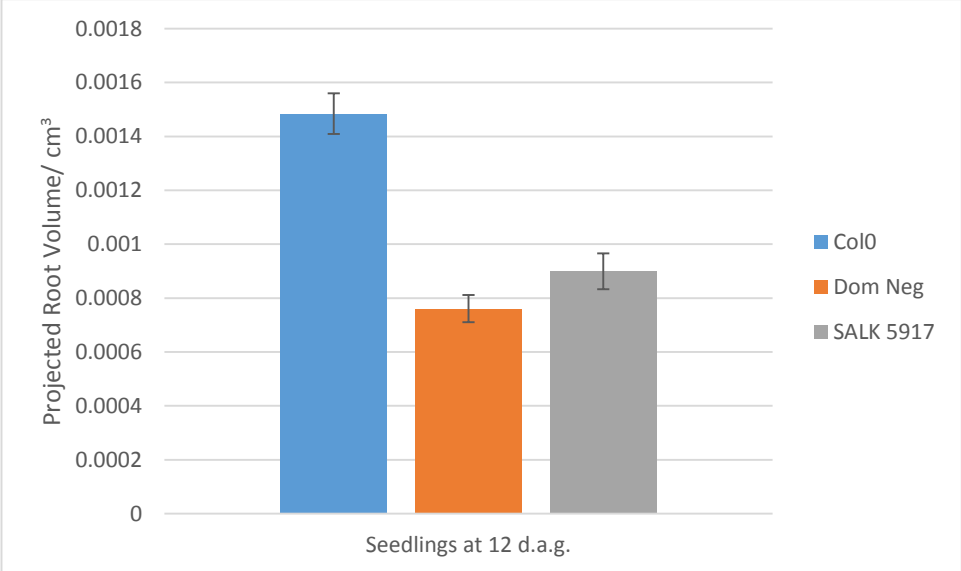

Figure 34: Projected volume of root systems of Col-0, SALK 5917 and Dominant Negative seedlings at 12 days after germination (d.a.g.). For table of measurements, see Appendix 5.

Data collected from root tracings using the Smart Root plug-in for ImageJ provided proposed surface area and volume data for each traced root. These data were plotted on bar graphs to see if the proposed measurements matched the trend already appearing with lateral root development in VAMP714 mutants. Figures 33 and 34 show the average surface area and projected volume of each complete root system traced. The resulting graphs show a major decrease in root surface area in both mutants compared to Col-0 wild-type. It can be presumed that a reduced proposed surface area and reduced proposed volume of root tissue is linked to the significant drop seen in primary root lengths and number of lateral roots in VAMP714 mutants.

3.1.3 Gravitropism Assay

The results described in the previous section showed that the absence of functional VAMP714 coincided with a detrimental effect on the development of roots, and in particular on the length of the primary roots, with associated reductions in the numbers of lateral root systems. The aim of the work in this section is to determine whether VAMP714 has a role in the plant's perception of and reaction to gravity stimuli, an auxin-dependent process (Rahman et al., 2010). The response of dominant negative, SALK 5917 and Col-0 roots to a gravity stimulus was analysed by recording the angle that each root bends towards gravity at 2, 4, 6, 8 and 24 hours after turning each plate 90° clockwise. The angle was measured using ImageJ, and was measured as illustrated in Figure 35.

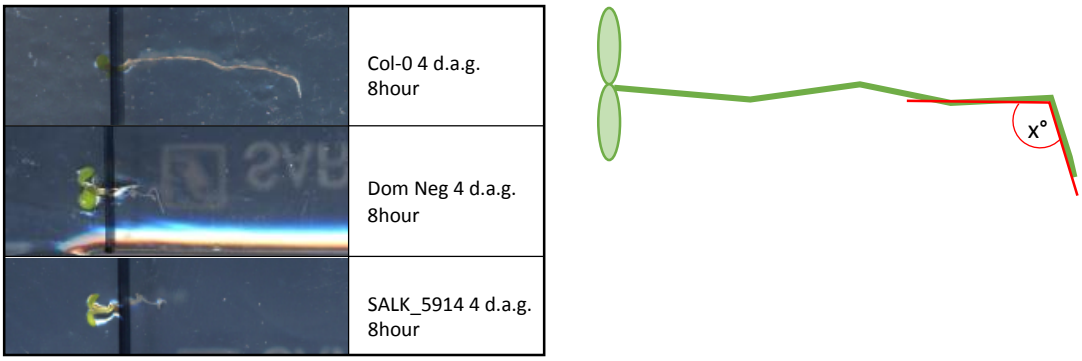

Figure 35: (Left) gravitropic phenotype of Dom Neg, SALK_5917 and Col-0 seedlings. (Right) illustration depicting method used in this experiment to measure the angle of bend towards gravity.

Figure 36 displays the gravitropic responses of dominant negative, SALK 5917 mutant and Col-0 wildtype seedlings (4 days after germination) after an 8 hour period of reorientation.

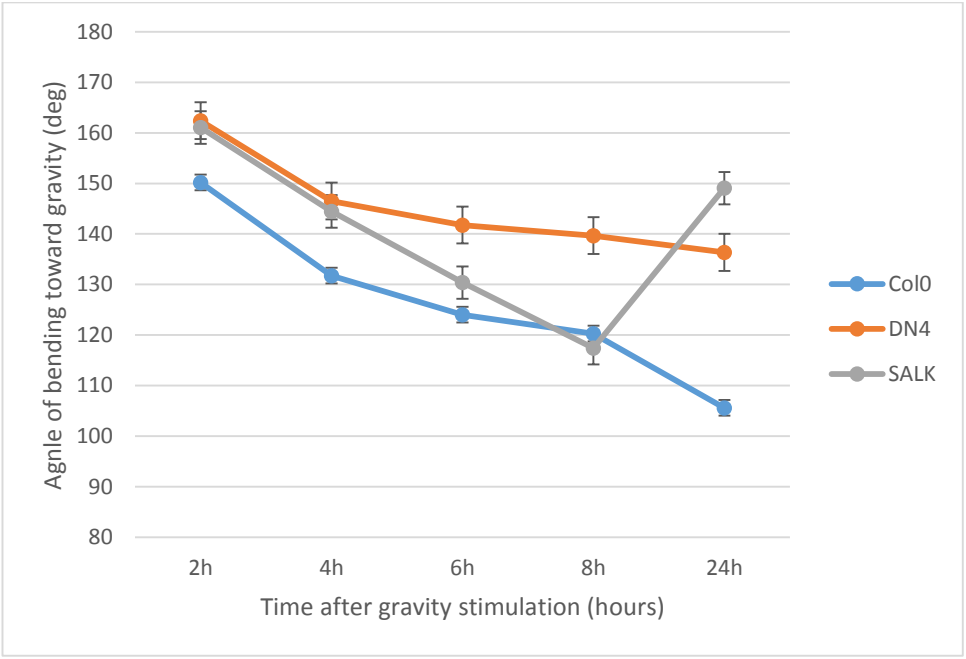

Figure 36: Average angle of bending towards gravity at 2h, 4h, 6h, 8h and 24h of Col-0, SALK 5917 and Dominant Negative seedlings at 4 days after germination (d.a.g.). For table of measurements, see Appendix 6.

The results in Figure 36 quantify the gravitropic responses of mutant and wildtype seedlings. Col-0 seedlings show bending close to 10° from vertical by 24h after plate reorientation. The dominant negative mutants showed a reduced response, with a mean angle of bending ca. 50° from vertical by 24h. The SALK 5917 mutant did not appear to perceive gravity at all, whereby at 24h, the root showed no reorientation. Between 2h and 8h after the plate reorientation, the SALK 5917 mutants had a tendency to 'corkscrew', meaning that, at points in the growth period the roots transiently grew towards gravity but then rotated to grow back against it. These results show that VAMP714 function is required for the wildtype growth response to gravitational forces.

Summary

This section has provided insight into the role of VAMP714 in the growth, architecture and response to gravitational stimulus of Arabidopsis roots. In the absence of normally functioning VAMP714, primary roots are shorter than wildtype, though lateral root density and elongation is similar to wildtype. Seedlings mutant for VAMP714 also show an incapability to react correctly to a gravity stimulus. These results are consistent with a possible role for VAMP714 in the auxin signalling pathway.

3.2 Role for VAMP714 in stem cell maintenance in the root

The short root phenotype presented in Figure 28 is believed to be related to a prevention of auxin-efflux from the stem cell niche due to a breakdown of possible VAMP714-facilitated targeting of PIN proteins. This breakdown of auxin transport is expected to have an effect on the maintenance of stem cell identity in the QC. An indicator therefore, of breakdown of auxin trafficking is abnormal differentiation of stem cells surrounding the QC and the synthesis of starch granules in the newly differentiated cells. Where normal differentiation is prevented by the expression of *WOX5* and *PLT* genes, in the absence of correctly targeted PIN proteins, these genes are repressed causing stem cell niche to differentiate. The development of staining methods that can highlight this process may provide a biological link between the short root phenotype and the possible role of VAMP714 in PIN-targeting.

After establishing in the previous section, that the mutants in VAMP714 grew stunted and abnormal root development, the next step was to look at root development on a cellular level. The aim of this section is to provide links between the abnormal growth phenotype seen in the last section, and the changes that are happening in the absence of VAMP714 on a cellular level in order to prove whether this absence is having an effect on the maintenance of the stem cell niche due to a breakdown of auxin-transport. This was done using a series of staining methods to enable observation of both the cellular structure and differentiation of the cells around the root cap.

3.2.1 Aniline Blue

The aniline blue staining protocol from Sue Bougourd et al., 2000 (see section 2.4.1) was adapted as follows. Seedlings were dehydrated and rehydrated though a series of EtOH concentrations before being stained in a 0.1% Aniline solution for 30 minutes.

The root tip was then cut and mounted in a glass microscope slide in dH_2O and imaged under a confocal microscope using the settings stated in section 2.6.1.

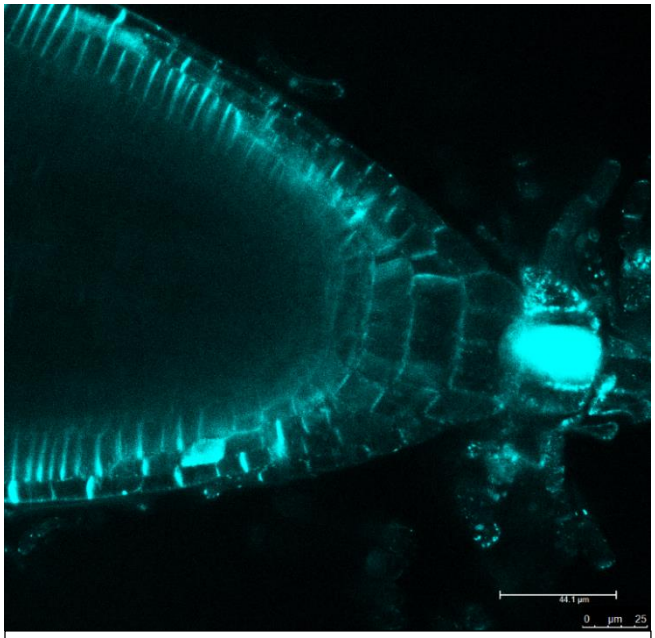

Figure 37: Col-0 seedling at 7 days after germination, stained with 0.1% aniline blue solution for 30 min. Imaged under Leica SP5 CLSM FLIM FCCS confocal microscope using HCX PL APO Lambda Blue 63.0x1.40 Oil UV objective. For full microscope settings see section 2.6.1.

The images gained were typically very blurry and the fluorescence often very weak. The cell walls of peripheral cells of the root cap were visible, as seen in Figure 37, however penetrance was poor and the QC was therefore difficult to identify. This therefore led to trying an acridine orange staining method as an alternative approach.

3.2.2 Acridine Orange

The acridine orange (AO) dye produced far clearer images of the cellular structure of the root tip. The protocol was adapted and improved, producing clearer images with better contrast between cells. Initially, the protocol stated to produce a 0.1% staining solution of AO in H_2O, to submerge the root tip for 20 minutes, wash with water and then mount in water. This produced images typical of that seen in Figure 38 a-c. In order to improve the penetrance of the stain, vacuum infiltration was introduced into the protocol. The root was vacuum infiltrated for 10 minutes whilst submerged in the staining solution. This allowed the stain to be carried further into the centre of the tissue and to be taken up into a higher proportion of cells. The concentration of the staining solution was also reduced from 0.1% to 0.01% in order to reduce the exposure of the staining images. A 0.01% staining solution was then produced using 98% EtOH instead of H_2O and using a 10x dilution as a working solution. This drastically improved the clarity of the images and reliability of the staining process in producing clear images as seen in Figure 38 d-f. A 100x dilution was tested but the resulting image became very blurred and it was concluded that the stain was far too dilute in this solution.

The images produced through acridine orange staining provided information on the differences in cell structure around the quiescent centre between the dominant negative and SALK mutants as compared to the wild-type structure. The mutants showed abnormal cell layers around the QC and the production of starch grains in the cells immediately south of the stem cell niche (circled in Figure 38 e and f), where in Col-0 wild-type these cells remained clear of starch showing only 3 distinct layers of starch containing cells. The cell pattern was disorganised in the mutants compared to the wildtypes, which had neat uniform cell layers.

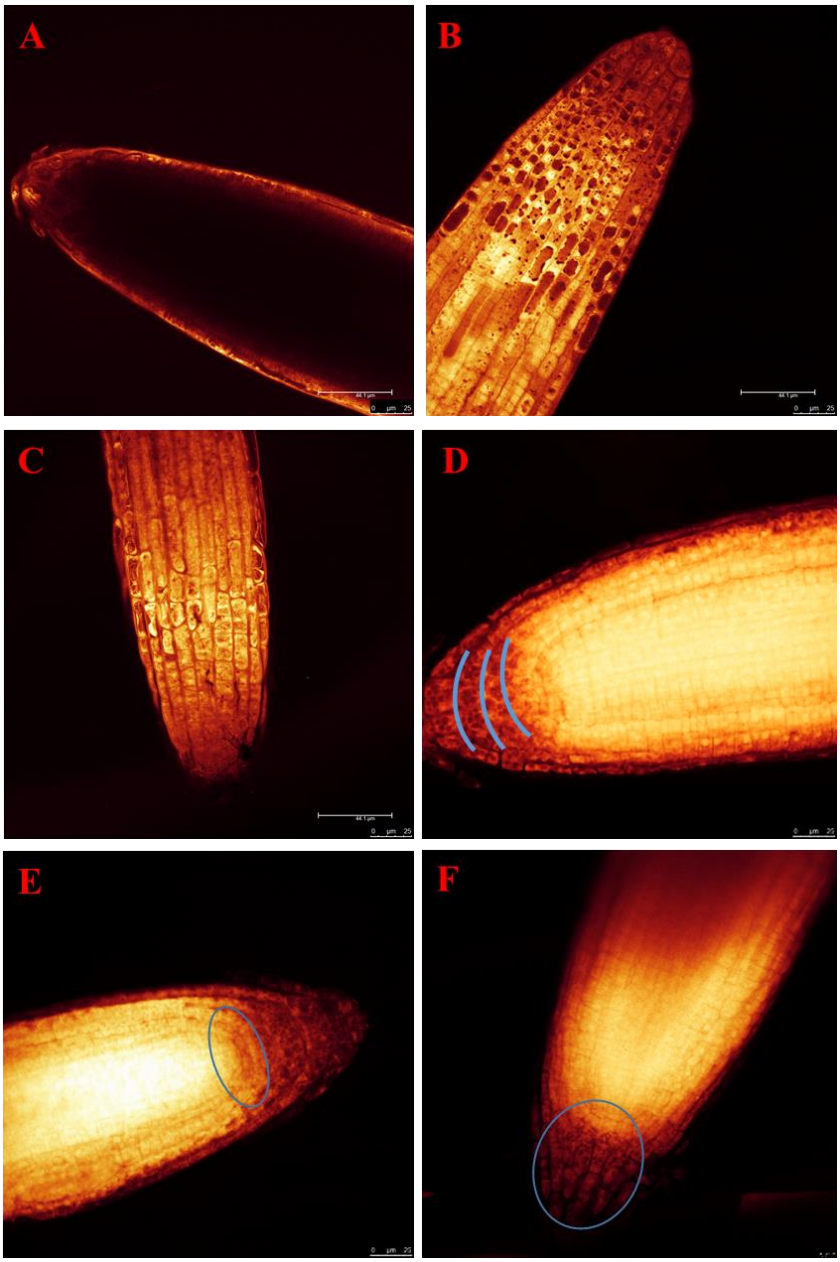

Figure 38: Imaged under Leica SP5 CLSM FLIM FCCS confocal microscope using HCX PL APO Lambda Blue 63.0x1.40 Oil UV objective. For full microscope settings see section 2.6.1.

A: 7 day old Col-0 seedling stained 10 min w. 0.1% AO in H_2O.

B: 7 day old Col-0 seedling stained 20 min w. 0.1% AO in H_2O.

C: 7 day old SALK 5917 seedling stained 20 min w. 0.1% AO in H_2O.

D: 7 day old Col-0 seedling stained 20 min w. 10x dilution 0.01% AO in EtOH w. 10 min vacuum infiltration. Uniform cell layers marked in blue.

E: 7 day old SALK 5917 seedling stained 20 min w. 10x dilution 0.01% AO in EtOH w. 10 min vacuum infiltration. Starch granules in QC circled in blue.

F: 7 day old dominant negative seedling stained 20 min w. 10x dilution 0.01% AO in EtOH w. 10 min vacuum infiltration. Disorganised cell layers circled in blue.

3.2.3 Propidium Iodide and Lugol's Solution

The appearance of starch granules in the acridine orange images led to the use of Lugol's solution as a starch-specific stain. This allowed clear visualisation of an extra layer of statocytes in the root cap of mutant seedlings. In Col-0 wild-type plants, 3 distinct layers of starch containing cells were observed at the root cap (Figure 39, A), but the mutants displayed an extra row (Figure 39, B-C). This showed evidence supporting the hypothesis that starch production in the stem cell niche can be used as an indicator of incorrect auxin-transport, and that VAMP714 has a possible role in the correct transport of the hormone.

3.2.4 Lugol Staining

Staining with Lugol's solution was a fast and effective way of showing the phenotypic difference between the two loss-of-function mutants (Dom Neg and SALK) and Col-0 wild-type with regards to starch production in the root cap.

It showed that when VAMP714 is absent, an extra set of starch containing cells is visible in the stem cell niche, indicative of differentiation of the columella stem cells (Figure 39).

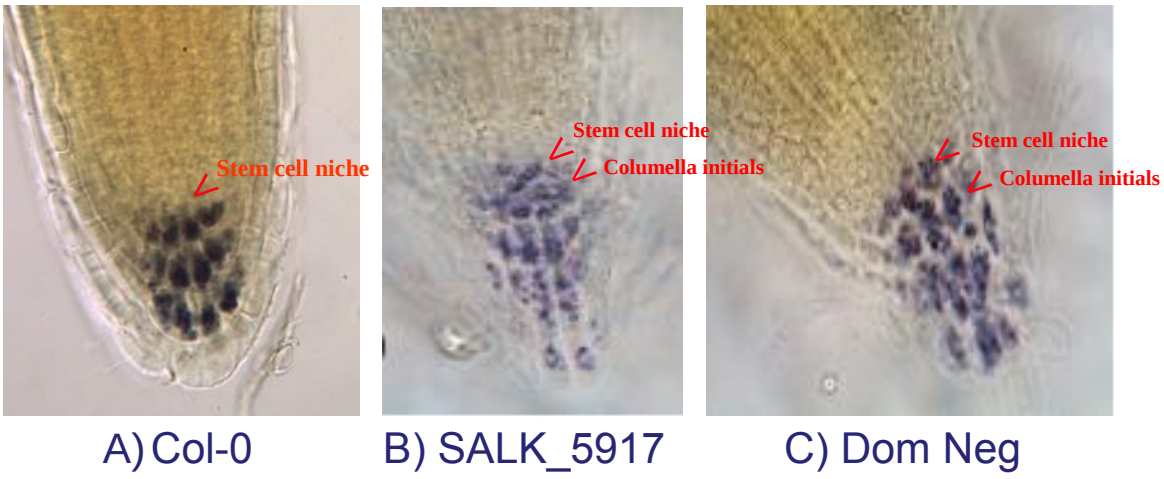

Figure 39: Col-0, SALK_5917 and dominant negative seedling at 7 days after germination stained with Lugol's solution and imaged under a light microscope in order to view blue/black staining of starch grains. For full microscope settings see section 2.6.1.

3.2.5 Propidium Iodide Staining

Propidium Iodide (PI) was then used alongside Lugol's solution in developing a novel staining technique that would clearly show both starch granule formation and cell structure. PI is a well-established cell wall stain, which is expelled by cells due to its polar nature, allowing it to accumulate in the extracellular space. The stain is unable to diffuse into the cells and so fluoresces in the exracellular space, effectively outlining each cell.

3.2.6 Combining two staining protocols

When developing a method for using both stains together, the first step is to identify the key components of the separate protocols. In this case the protocols were very similar, and so mixing the two staining solutions was the first obvious approach. This resulted in blurred images, no cell structure could be identified and it appeared that the Lugol's stain was too concentrate. Trial and error then came into the process to strike a balance between the effects of both stains. The decision was made to use the stains in succession in order to allow each stain to work alone at each stage. Trial and error was used to test different concentrations and staining periods with each stain. It became apparent that the Lugol's solution was affecting the propidium iodide staining. Normal propidium iodide function relies on it being membrane impermeant, which means that it contains a charge and therefore cannot pass through cell membranes. This is why in PI images, the fluorescence is seen around the borders of cells, effectively highlighting the cellular structure of tissues. When mixed with Lugol's solution, it appears to lose its charge by reacting with the Lugol's solution, which is made up of potassium iodide ions, producing a neutral compound that can diffuse through cell membranes. So the PI fluorescence in these

images highlight the cells cytoplasm rather than membranes (Figure 40), and so was found to still allow clear visualisation of the cell structure.

The Brightfield channel on the confocal microscope proved effective at imaging the starch staining by the Lugol's solution (Figure 40, C). The PI fluorescence and Lugol's staining were imaged simultaneously but on separate channels, so the output was two images, one showing the PI fluorescence, and one showing the Lugol's-stained starch. These two images were overlaid in order to visualise the position of starch granules clearly over the cellular structure of the tissue.

As before, the images clearly show an extra layer of starch containing cells in the mutants when compared to the wild-type roots.

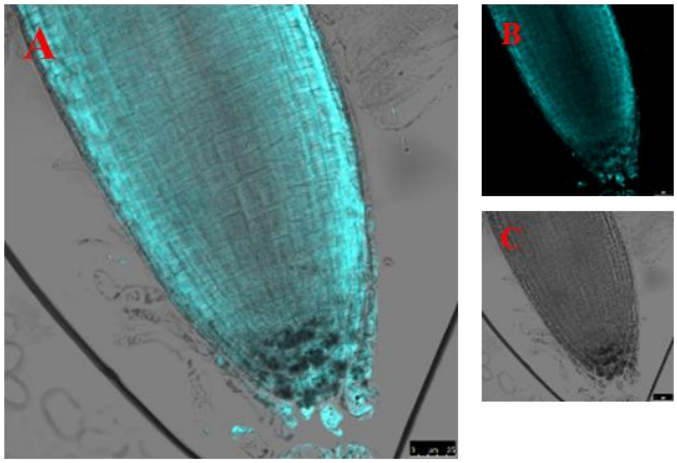

Col-0 WT

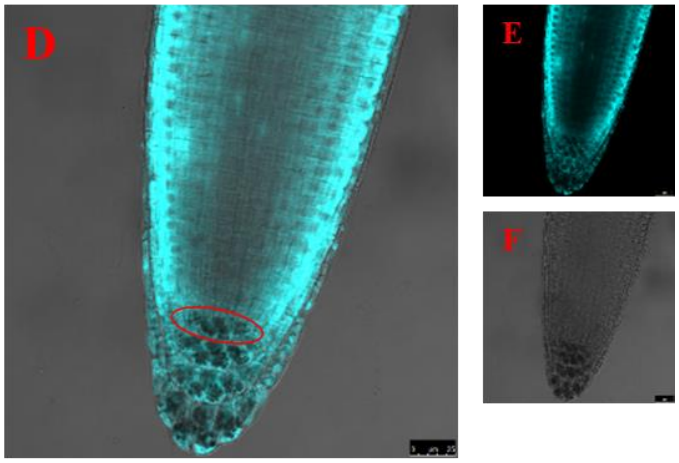

Dom Neg

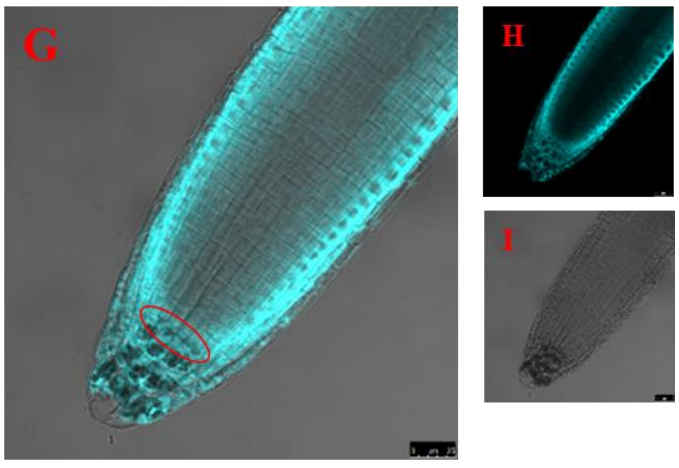

SALK_5917

Figure 40: **A, D and G:** Col-0, Dom Neg and SALK respectively. 7 day old seedlings,. PI and Lugol stained. Merged channels. **B, E and H:** Col-0, Dom Neg and SALK respectively. 7 day old seedlings, PI and Lugol stained. Fluorescence channel. **C, F and I:** Col-0, Dom Neg and SALK respectively. 7 day old seedlings, PI and Lugol stained. Brightfield channel. Imaged under Leica SP5 CLSM FLIM FCCS confocal microscope. For full microscope settings see section 2.6.1.

Summary

The work in this section has provided an improved method for the visualisation of cell patterning in the root tip of Arabidopsis. It has shown that mutation of VAMP714 leads to defective maintenance of the stem cell niche, resulting in differentiation of the columella initials.

3.4 Identifying the VAMP:CFP PIN1:GFP double transgenic

Previous work into the function of VAMP714 led to the production of a transgenic line containing fusion tagged VAMP714 and PIN1 proteins. The aim of this line was to allow imaging of the possible co-localisation of these two proteins in cells at the root tip by scanning for the fluorescence of CFP and GFP proteins that were fused to each protein. A PIN1:GFP line that transformed with a VAMP:CFP transgene. Once a doubly transgenic seedling (containing both fluorescently tagged proteins) is found, it would allow imaging of both proteins together in the root using a confocal microscope with two channels, one tuned to each fluorophore.

The seeds that were available during this study were VAMP:CFP in a wild-type background and VAMP:CFP in a PIN1:GFP background, both of which were primary transformants i.e. they were the first generation seed produced following the dipping event (also known as F0 seedlings). The low frequency of transformation events means that selection and screening systems are used to identify those seedlings which contain the construct(s), such as resistance to a particular antibiotic (Kumari PhD thesis., 2011).

In this case unfortunately, double transgenics containing both VAMP714:CFP and PIN1:GFP proteins were not found. Thousands of seeds were tested but none showed any level of fluorescence above a level that was deemed

auto-fluorescence. This may have been due to the possibility that the double transgenic seed is present in such a small quantity.

Summary

The results presented in this chapter provide new information on the role of the VAMP714 protein in root growth and development in *Arabidopsis thaliana* seedlings. Bioinformatic analysis provided information on the subcellular localisations of AtVAMP714 and AtPIN1 proteins. Both proteins are found at the plasma membrane, providing evidence for a potential role in transport across the membrane. VAMP714 proteins were also found at the Golgi apparatus, suggesting that the protein is capable of moving between the two organelles. Predicted protein structures highlighted protein domains that could be involved in the hypothesised function of the VAMP714 protein. tDNA-insertion and dominant negative mutants showed similar defective phenotypes, including a reduced primary root length and gravitropic response compared to wild-type Col-0 seedlings. The surface area and volume of the entire root system of the mutants was also significantly reduced. To investigate defects in cellular pattern or differentiation in the stem cell niche, a novel staining procedure was developed, involving using Lugol's solution as a counterstain alongside propidium iodide; the propidium iodide allows clear observation of each cell and the overall cell structure, while Lugol's solution clearly highlights the starch granules, statoliths, which are present within each cell. It was found that in both insertional and dominant negative mutants, an extra layer of statocytes (starch containing cells) were present in the region of the stem cell niche, due to differentiation of the columella initials. These results suggest a role for VAMP714 in the control of meristem function, necessary for primary root growth, possibly through effects on the auxin signalling pathway.

4.0 Discussion

In this study, the role of VAMP714 in root development was investigated. This was achieved by studying the phenotypes of tDNA insertion and dominant negative mutants of the *VAMP714* gene *in vitro* and quantifying different aspects of root architecture and stem cell maintenance in the root tip.

VAMPs are a protein family in Arabidopsis which aid the targeting of vesicles to the plasma membrane during vesicle trafficking in a range of tissues, despite high similarities in protein structure across the group of proteins, they show a range of different localisations (Uemura et al., 2005). VAMP721 and VAMP722 are known to assemble with SYP121 and SYP122 in K^+ ion channel control, affecting the gating of these channels (Zhang et al., 2015). The same two VAMP proteins have been found to interact with SYP121 and SNAP33 to produce a SNARE complex involved in the plant's fungal pathogen response (El Kasmi et al., 2013). Systematic SNARE analysis in Arabidopsis through fusion tagging with GFP (Green fluorescent protein) and YFP (yellow fluorescent protein) provided information of subcellular localisations of 54 SNARE genes, providing information on the plant's complex post-Golgi membrane trafficking system (Uemura et al., 2004). This study provided expression analysis of the VAMP714 protein and found its subcellular localisation to be at the Golgi apparatus (Uemura et al., 2004). AtVAMP7C is a subfamily of the VAMP proteins comprising 4 members with extended homology: AtVAMP711, AtVAMP712, AtVAMP713 and AtVAMP714. This group of proteins is believed to form tonoplast specific SNARE complexes in order to direct vacuolar membrane fusion at the tonoplast (Leshem et al., 2006). Selective binding of the different members of the VAMP protein family is thought to be linked to the longin domain, which varies in each member of the family (Zhang et al., 2015).

Previous work in this project provided an expression pattern of the *AtVAMP714* gene and the subcellular localisation of its protein. Expression analysis by RT-PCR (real time PCR) provided transcript abundances of the gene in different organs throughout the root (Kumari PhD thesis., 2011). VAMP714:CFP protein fusion expression found the VAMP714 protein most abundant in the Golgi apparatus. Reporter gene fusion analysis tracked the activity of the gene promotor and localisation of the AtVAMP714 protein. Three fusion tagged proteins were produced; proAtVAMP714::GUS, pro*AtVAMP714*::AtVAMP714::CFP and AtVAMP714:GFP. Experiments using proAtVAMP714::GUS fusion tagged proteins looking at histochemical localisation of GUS activity showed the protein localised to vascular tissues in both primary and lateral roots, suggesting that the protein functions in both types of root in both development and growth. Investigation of tissue specificity and promotor activity using pro*AtVAMP714*::AtVAMP714::CFP and AtVAMP714:GFP showed the co-localisation of AtVAMP714:GFP with a golgi marker, Golgi:RFP as seen in Figure 45 (Kumari PhD thesis., 2011).

The existing research in VAMP protein function and specifically VAMP714 localisation and hypothesised link to auxin transport led to looking into the effect of mutations in the *AtVAMP714* gene on root development, many aspects of which are regulated by auxin.

Auxin is a plant phytohormone involved in a wide range of signalling processes in order to orchestrate successful development and adaptation to the plants immediate environment, and including root development (Jiang and Feldman, 2005). Plants are sessile organisms and as such, cannot move away from danger or from insufficient growth conditions, it must adapt where it stands and a complex hormone signalling system is how this is achieved (Jaillais and Chory, 2011). The directional

intercellular transport of auxin is key to many aspects of plant growth and development, such as embryogenesis, flower development and root development (Zhao, Y., 2010). PIN-FORMED proteins determine directional flow, controlling when and where auxin is able to leave the cell (Kleine-Vehn et al., 2011).

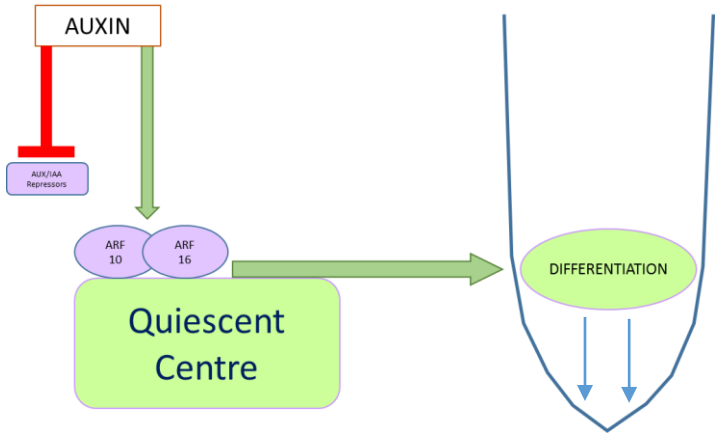

Figure 41: Flow chart illustrating the role of Auxin Response Factors (ARFs) in the quiescent centre.

Previous studies have established that auxin signalling is dependent on its polar transport, facilitated by PIN protein cycling between the golgi apparatus and the plasma membrane. Auxin signalling affects root growth and development and is a positive regulator of the gravitropic response in roots; correct auxin localisation is required for the appropriate response. Growth of the root involves promoting the differentiation of the columella stem cells by auxin which, when in the region of the quiescent centre, switches off AUX/IAA (Auxin/ Indole-Acetic Acid) repressors, allowing activation of ARF (Auxin Response Factors) and therefore differentiation of stem cells causing elongation of the root (Figure 41) (Yan et al., 2013).

In the experiments presented here, seedlings with a mutation in the At5g22360 gene cannot coordinate correct auxin transport and signalling due to the

absence of VAMP714. This is apparent in the results where the primary roots of these mutants are severely stunted, they show abnormal lateral root formation and a poor response to gravity stimuli. This is indicative of disrupted auxin signalling.

4.1 Root Architecture

During primary root growth, local auxin concentration gradients allow control of transcription around the quiescent centre. This allows control of the growth of the root. During high concentrations, auxin triggers the degradation of AUX/IAA repressors, stimulating ARFs and promoting stem cell differentiation and root growth. This occurs during low PIN concentrations, auxin then prevents the endocytosis of PIN proteins, promoting its own efflux from cells, halting the stem cell differentiation process when it is necessary to instead maintain the stem cell niche. Stem cell maintenance is dependent on the expression of *WOX5*, a gene which promotes maintenance of the stem cell identity of cells surrounding the quiescent centre (Forzani et al., 2014). ARFs repress *WOX5*, causing the restriction of both *PLT1* activation and subsequent PIN1 transcription. This traps auxin in the QC as there is no efflux route available, this auxin build-up causes over-development of the stem cell niche. During normal growth, differentiation is only promoted around the stem cell niche in order to replace a layer of columella cells that have been sheared from the root tip during movement through the soil (Petricka et al., 2013). The root maintains three layers of starch containing cells at the root tip for gravity sensing and to protect the quiescent centre. During the absence of VAMP714, PIN protein transport is disrupted, allowing a build-up of auxin in the quiescent centre which continuously activates ARFs, represses *WOX5* and promotes premature differentiation of cells surrounding the quiescent centre. Figure 42 shows the results of a quantitative RT-PCR depicting that during the absence of VAMP714 in

Dominant Negative, SALK_5917 and an overexpressing mutant, the transcript abundances of *WOX5, PLT1 and PLT2* drop severely.

This means that where VAMP714 is unable to deliver PIN1 to its target membrane via endosomal cycling, *WOX5, PLT1 and PLT2* genes remain repressed by auxin in the QC; WOX5 is produced in far fewer quantities in the mutants compared to the wild-type, this greatly reduces the transcription of *PLTs*, and so the stem cell niche cannot be maintained. The results presented in this study show a fourth layer of starch containing cells at the root cap in VAMP714 loss-of-function mutants, indicative of over-development of the stem cell niche by a built up sink of auxin.

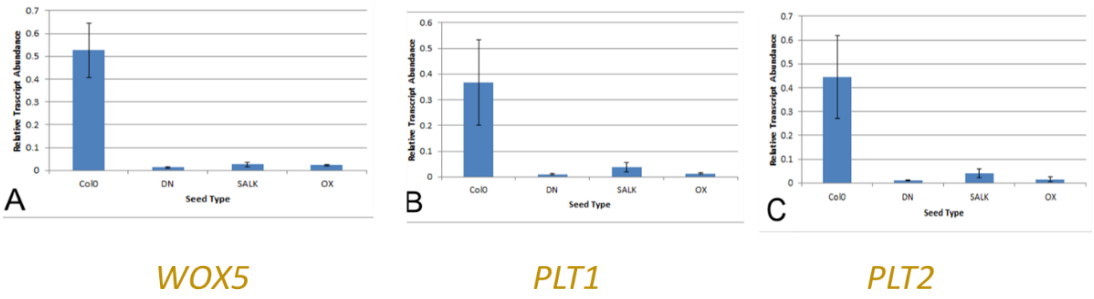

Figure 42: Taken from Katherine Hamilton Research Project 2013. Graphs produced from quantitative RT-PCR depicting a significant decrease in the transcript abundance of WOX5, *PLT1* and *PLT2* genes in Dom Neg, SALK_5917 and ox mutants when compared to Col-0 (Reference gene: Actin2).

Primary root growth is stunted in the absence of properly functioning VAMP714. In its absence, VAMP714 appears to no longer associate with Golgi vesicles and if there is a link between VAMP714 and PIN1, it would not be able to transport PIN1 proteins to their target membranes. This causes misread auxin signals due to incorrect localisation of auxin maxima, the root does not receive the correct signals in the elongation zone of the root because auxin is trapped in the quiescent centre. Under normal growth situations, PIN1 transports auxin out of the QC by

facilitating it's efflux from cells to then be trafficked acropetally through root tissue to the elongation zone in order to initiate cell elongation. This is apparent in this set of results: primary root length is significantly shorter in loss of function mutants alongside over-development of the quiescent centre. This implies that while auxin is able to repress WOX5 and promote differentiation at the root cap, an absence of PIN protein transport to the plasma membrane prevents auxin from being transported back up the root to allow cell elongation for primary root growth in the elongation zone. Auxin is trapped in the meristematic zone. See Figures 40 and 41 for an illustration of this model.

4.2 Local Auxin Synthesis

There are multiple auxin synthesis pathways utilised across a whole plant system. Auxin sinks are available in the shoot from which basipetal polar auxin transport begins. This auxin can be transported to the root as required however there are also auxin biosynthesis pathways local to the root. Root generated auxin contributes to maintenance of auxin gradients and maxima required for cellular development, but cannot perform auxin function alone, it is there to bulk up the concentration of auxin that is present from polar transport (Overvoorde et al., 2010). It is possible that the weak responses in gravitropism, lateral development and general root growth is because the locally synthesised pools of auxin have not been affected by the disruption of PIN-facilitated transport. This may explain why root growth isn't completely halted, only stunted, and also why some mutants bend slightly toward gravity but not to the same extent that Col-0 wild-type seedlings of the same age can. A study characterised two mutants, impairing the local synthesis of auxin in roots, WEAK ETHYLENE INSENSITIVE (*wei2* and *7*) and TRANSPORT INHIBITOR RESPONSE (*tir7-1*). These mutants exhibited supressed

auxin phenotypes due to a disrupted subunit of ANTHRANILATE SYNTHASE, an enzyme vital for the catalysis of the rate limiting step in tryptophan synthesis. Failure of cells to produce tryptophan reduces the ability of that cell to subsequently produce IAA. Root growth was impaired (Overvoorde et al., 2010). The study suggests that without local auxin synthesis, a similar phenotype is seen as in the results discussed here. Perhaps it is the combination of both local auxin biosynthesis and polar auxin transport from pools elsewhere in the plant is the key to correct root development and successful growth.

4.3 Auxin and Root Branching

Lateral root growth is a major developmental step in establishing a root system. Laterals allow the root to cover a larger area of soil, and vastly increase the surface area of root capable of absorbing both water and nutrients to sustain growth. Lateral root formation occurs when cells in the pericycle of the primary root begin to divide, the cells protrude from the pericycle and develop a lateral root meristem from which a root system is produced. Auxin promotes this initial division by inducing the transcription of members of the *AUX/IAA* gene family. *AUX/IAA* genes have been shown to mediate auxin-regulated developmental processes, allowing lateral root initiation amongst other aspects of root growth. Auxin plays a key role therefore in the initiation of lateral root growth (Fukaki et al., 2002). Previous studies have shown that inhibitors of auxin transport prevent lateral root formation, providing further evidence to suggest that correct auxin transport is vital for lateral root development (Casimiro et al., 2001). The observation of growth of auxin deficient mutants suggest that auxin signalling is required at several stages of lateral root development. A study has looked into three distinct mutations involved in IAAs control of lateral root growth; *alf1-1* causes hyperproliferation of laterals, *alf4-1*

prevents initiation and *alf3-1* causes defective maturation of lateral roots. This implys that auxin is involved in several stages along the lateral initiation and development pathway (Celenza Jr et al., 1995). It has been suggested that acropetal (root to shoot) auxin transport is required for lateral root initiation, where basipetal (shoot to root) auxin transport is reserved for growth responses such as gravitropism (Casimiro et al., 2001).

In the results presented here, abnormal lateral root formation is exhibited in mutants lacking the VAMP714 protein. When VAMP714 is unable to deliver PIN1 proteins to their target membrane, polar auxin transport throughout the root is prevented. In the context of lateral root formation, this means that acropetal auxin transport to the pericycle from the base of the root is slowed because PIN1 is not present in the right concentration at the plasma membrane to allow enough auxin to be effluxed from cells to move up toward the pericycle for promotion of cell division. This is backed up by the primary root length results discussed above where it was speculated that in the absence of VAMP714 vesicle-associated transport of PIN proteins, auxin is trapped in the meristematic zone, is not transported in high enough concentrations to the elongation zone or in this case, to the pericycle to allow lateral formation, auxin cannot be transported far enough along the acropetal pathway shown in Figure 43. The results found adrop in the number of laterals present in mutated seedlings and a reduced surface area and volume of entire root systems. Large amounts

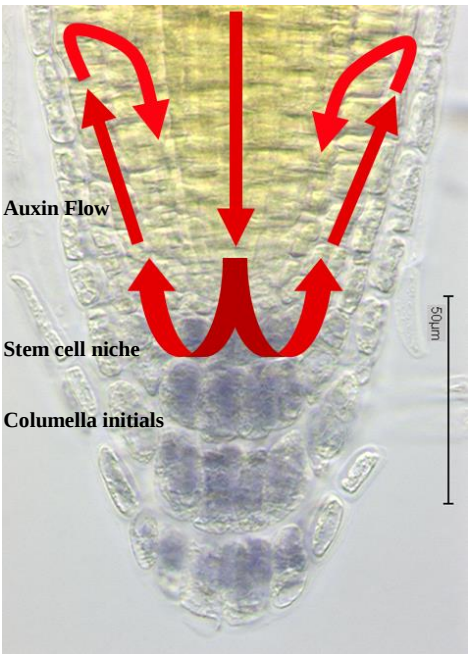

Figure 43: Image illustrating the wild-type cycling of auxin around the root cap.

of progress have been made in the characterisation of auxin signalling cascades and transport processes in recent years (Retzer et al., 2014), crosstalk between auxin signalling and cytoskeletal organisation is still unclear but may provide an explanation as to why an absence of correct polar auxin transport toward the elongation zone produces thin and weak roots, this may provide a link between auxin signalling and tissue strengthening. These findings are significant because they provide evidence for the theory that VAMP714 is an important component in the auxin trafficking pathway, the results imply that in its absence, auxin cannot reach the pericycle at a high enough concentration to promote normal lateral root formation resulting in abnormal growth.

4.4 Root Gravitropic Response

Auxin also has a key role in the initiation of bending in the root tip during a gravitropic response. Gravitropism is a very important response in plants, perception of gravity ensures that the aerial parts of the plant grow upwards (negatively gravitropic) and that the root system grows down (positively gravitropic). The root system must be able to sense gravity in order to grow deeper into dry soil to find water, for example. The sensing of a change in gravity occurs in the root tip; the response occurs in the elongation zone. This means that transport of a signal from the root tip to the elongation zone is required to coordinate the correct growth response; this signal is auxin. Once auxin reaches the elongation zone, it stimulates asymmetric growth of individual cells, allowing the bending of the entire root tissue. PIN2 is the key efflux carrier protein involved in transporting auxin to the elongation zone, a study has found that any alteration of this flow of auxin causes defects in the root's ability to bend due to a breakdown of formation of auxin asymmetry across the root. During the gravitropic response, polar auxin transport in the elongation

zone, facilitated by AUX1 influx carrier and PIN2 efflux carrier, creates an asymmetric distribution of auxin across the tissue, causing increased cell elongation on one side of the root, allowing it to bend (Rahman et al., 2010). Starch accumulation provides the cell with information on the change of orientation of the root. The root senses these changes via statolith displacement in amyloplast cells (gravity sensing cells). As the orientation of the root changes, starch granules in the amyloplasts move in a positively gravitropic manner. This movement is sensed in the cell triggering a growth response (Toyota et al., 2013). The resulting shift of growth in the new direction of gravity is due to a translocation of auxin, causing the cells to grow asymmetrically. One side of the root elongates to a greater extent than the other, causing a bending towards the stimulus (Yan et al., 2013). In the experiments presented here, the gravitropic response broke down in seedlings containing no functioning VAMP714. The results imply that without normal VAMP714 function, PIN proteins are permanently internalised, preventing the movement of auxin from the root tip to the elongation zone and therefore preventing response to a change in direction of gravity. The stimulus is sensed but the plant cannot respond due to the cycling of auxin efflux protein, PIN1 being halted.

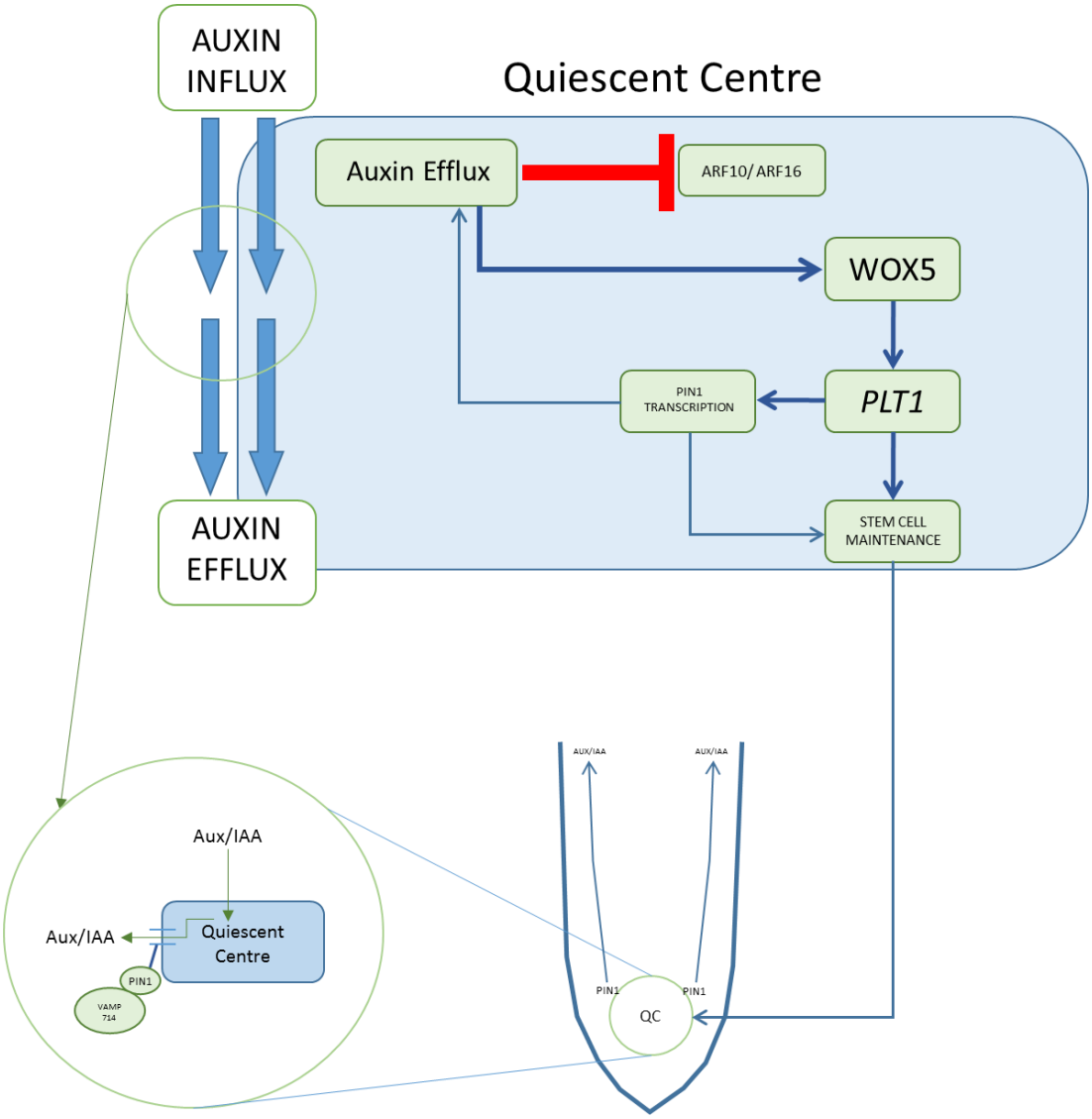

Figure 44: Model produced to illustrate the results and ideas gained through the experiments in a wild-type environment, showing how normal PIN delivery and auxin transport leads to stem cell maintenance, correct efflux of auxin from the quiescent centre (QC) and subsequent trafficking of auxin toward the elongation zone for cell elongation and lateral formation.

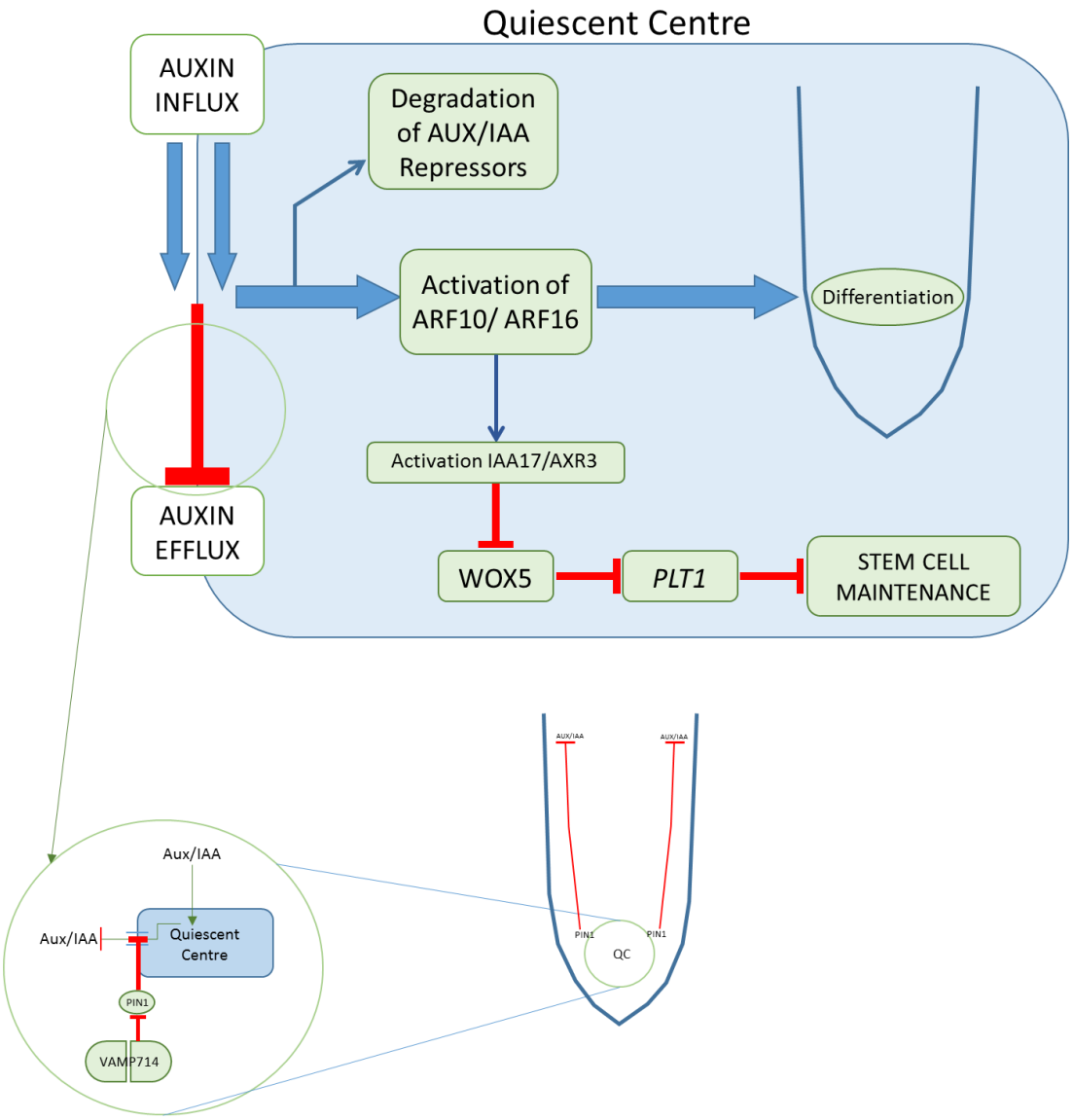

Figure 45: Model produced to illustrate the results and ideas gained through the experiments in mutants where VAMP714 function is knocked-out, showing how a breakdown of PIN delivery and auxin transport leads to differentiation of the stem cell niche, inability to efflux auxin from the quiescent centre (QC) and subsequent break-down of trafficking of auxin toward the elongation zone for cell elongation and lateral formation.

Summary

A key factor in explaining the abnormal root development exhibited in VAMP714 loss-of-function mutants is the idea that auxin may be trapped in the meristematic zone by a loss of PIN protein transport resulting in a low concentration of PIN proteins at the plasma membrane because VAMP714 is incapable of correct delivery. VAMP14 appears to be key in the placement of PIN1 on the plasma membrane. This prevents polar transport of auxin acropetally toward the elongation zone and pericycle, causing abnormal development of lateral roots in the pericycle due to arrested initiation of cell division. Stunted primary root growth and a lack of gravitropic response may be functionally linked phenotypes due to their reliance on cell elongation in the elongation zone. If auxin cannot be transported acropetally from the meristematic zone at the correct concentrations, this would stunt cell elongation both symmetrically (for primary root growth) and asymmetrically (for root bending in response to gravity) and both may be affected by a potential breakdown in cross-talk between auxin signalling and cytoskeletal organization. The root still grows to a certain extent and is able to bend due to low levels of locally synthesised auxin; but an absence of polar auxin transport will severely reduce the concentration of auxin at this point, the cells will therefore not be able to exhibit as strong a response as in wild-type roots. Figures 40 and 41 show a model produced to illustrate the results found in this study in the context of known auxin distributions and transport pathways. It depicts the cause of the phenotypes observed.

Future Work

The next logical steps with this set of results would be to do further repeats of those charts whose error bars are overlapping: lateral density, mean interbranch distance and average lateral length. The reason that the error bars are bigger in these

cases, particularly in the mutant data, is that the seed stocks that were being used were heterozygous, so a smaller proportion of those seedlings that were grown up, showed the phenotype and were able to be traced. To further the results gained from the gravitropism assay, smaller time intervals from 0 hour could be looked at. This would give information about the initiation time of the response, to investigate whether the mutant response, if seen at all, is delayed. This would be achieved by setting up the same experiment as described in Section 2.3.3 and then scanning the progress of the response at 0 hours, 30 minutes, 1 hour, 1 hour 30 minutes and 2 hours to more closely track the initiation of bending in the Dom Neg and SALK mutants compared to the wild-type. The corkscrew phenotype seen in a small number of the mutants during the gravitropism assay could also be investigated further. This would be achieved by using tighter time intervals around the time at which this phenomenon occurs, which appears to be between 6 and 8 hours. The potential crosstalk between auxin transport and signalling, and cytoskeletal development and organisation is a really interesting prospect here. Experiments into auxins effect on the cytoskeleton could provide an important insight into this link; auxin deficient mutants could be used to observe the cytoskeletal organisation of auxin-deprived cells through use of an actin filament stain.

4.5 Differentiation at the root cap

Starch has been used as a marker for differentiation in several studies, many using Lugol's solution to do so. The development of a novel staining method during the course of this study has allowed clearer visualisation of both the cell structure and the accumulation of starch granules in the same image as demonstrated in Figure 46.

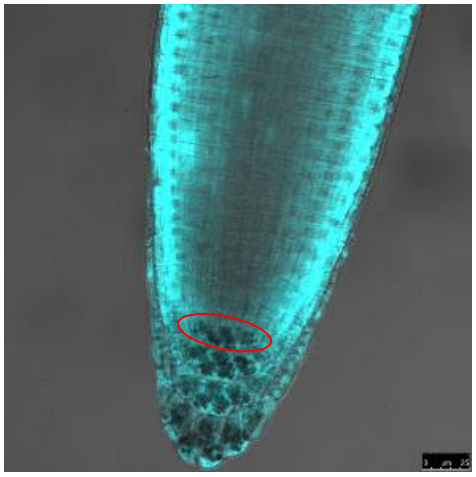

Figure 46: Taken from results section 2.3.5 showing the successful development of a new staining technique to observe both starch development and cellular organisation in the root cap.

Through many stages of development and refining, this new staining technique was achieved through the combination of the separate staining techniques and perfection of the imaging process. After the counterstaining process is complete (see section 2.4.3) imaging is achieved using a Leica SP5 CLSM FLIM FCCS confocal microscope and HCX PL APO Lambda Blue 63.0x1.40 Oil UV objective. Each stain is imaged under a separate channel and the two images overlaid to form the image seen above, allowing visualisation of both cellular organisation and starch granule production.

During root growth the stem cells surrounding the quiescent centre are constantly replaced, maintaining a stem cell niche. Stem cells that differentiate into columella cells develop starch granules called statocytes in the cytoplasm. As root cap cells are sheared off at the end of the root, the layer of columella cells behind take their place, this is how the root cap moves through the soil (Petricka et al., 2013). In the quiescent centre, it is WOX5 and PLT1 that predominantly serve to maintain the stem cell identity of the stem cell niche. During high auxin concentrations, auxin is able to send AUX/IAA repressors for degradation and to activate ARFs 10 and 16. These Auxin Response Factors are responsible for the differentiation of the stem cell niche through the activation of IAA17/AXR3 which switches off WOX5 (Ding and Friml, 2010) see model presented in Figure 41. In a wild-type plant under normal conditions, there are 3 layers of these starch containing cells at the root cap, however experiments in this study revealed that when the gene encoding VAMP714 is mutated, a 4th layer of starch containing cells develops in the root tip of mutant seedlings. This 4th row is indicative of premature differentiation of the stem cell niche, i.e. the stem cells surrounding the quiescent centre are differentiating sooner than is appropriate for normal development of the root cap. This provides additional evidence that during the absence of VAMP714 function, PIN proteins are unable to correctly transport auxin away from the root tip, causing over development of the root cap through a lack of correct hormone signals. Incorrect PIN

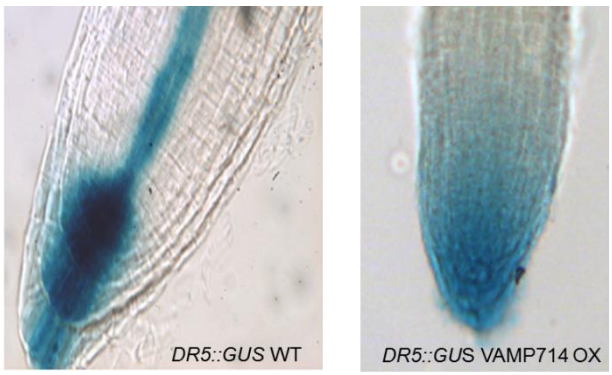

Figure 47: Taken from Fonseka et al., under development. GUS staining image depicting the localisation of auxin when VAMP714 is mutated. There is no clear transport of auxin away from the QC, localisation appears uncontrolled.

cycling here causes over development of stem cells, the transcription factors ARF10 and ARF 16 are permanently repressing WOX5 and so the columella stem cells lose their stem cell identity (Forzani et al., 2014). This backs up the theory that VAMP714 plays a key role in the transport and cycling of PIN1 proteins during this process. When VAMP714 is unable to traffic PIN1-containing endomembrane vesicles to the plasma membrane, auxin is unable to be effluxed away from the quiescent centre. Formation of a pool of auxin around the QC causes constant repression of *WOX5* and *PLT1*, the stem cells undergo a cycling of differentiation as auxin levels increase. Repression of *PLT1* expression also prevents the transcription of PIN1 proteins, worsening the situation. Ultimately, these cellular conditions lead to overdevelopment in the stem cell niche and a breakdown of development elsewhere in the root.

Future Work

To develop this work further, looking into time-lapse microscopy may be of value. If it is possible to film the growth of these roots over maybe 1 hour it may provide interesting data on the production of the starch found in the stem cell niche of the mutant roots. Development of this novel staining technique has already vastly improved the ability to observe the phenotypes of VAMP714 mutants on a cellular level and so further imaging techniques may be the way to improve visualisation further. Another area of research that may improve knowledge gained in this experiment is to look into the effect of these mutations on the AUX1 importer. AUX1 is another transmembrane channel protein which is responsible for auxin influx into the cell. If this process breaks down as a result of mutating VAMP714 then could provide a mechanism for the delivery of both auxin influx and efflux proteins to the plasma membrane for polar auxin transport. This experiment may also

provide further evidence for the theory that auxin gets trapped in the meristematic zone in the absence of VAMP714, causing growth defects in the auxin-starved elongation zone. To back up this experiment, mutants in the AUX1 gene could also be looked at to see if observation of a similar phenotype is possible.

Further work looking in to producing a new VAMP:CFP construct may also be a valuable addition to the work done here. To clone the new construct into a fresh line of seeds creating new VAMP:CFP mutants, then cross into plants that have been tested as homozygotes of the PIN1:GFP mutation. It may also prove a good idea to use a different combination of fluorescent proteins in the constructs. Both CFP and GFP have overlapping fluorophores, their emission wavelengths are almost too similar to be deciphered using a confocal microscope. Had one been found in this study, lambda scanning and linear un-mixing techniques would have been used to successfully separate the emissions, however to avoid having to do this a combination of GFP and RFP or YFP would be a better pair of emission spectra to work with. The use of brefeldin A (BFA) could provide an alternative experiment to allow the observation of co-localisation of VAMP714 and PIN1 proteins. In wild-type plants, the treatment of cells with BFA leads to an aggregation of PIN-containing endosomal compartments. If VAMP714, when mutated, cannot carry out normal endosomal recycling, then BFA treatment on mutant cells would show no effect- PIN1 would still be trapped in endosomal vesicles, unable to get to the plasma membrane. I.e. if VAMP714 is not involved in PIN1 delivery to the plasma membrane, then an increase in intracellular accumulation of PIN1 under BFA treatment would be observed. If VAMP714 is involved in PIN1 delivery, then BFA treatment would have no effect on the internalisation of PIN1 proteins. This experiment would add to the evidence presented here to prove that VAMP714 is

directly involved in the delivery of PIN1 proteins to the plasma membrane during the polar transport of auxin in the root cap.

5.0 References

1. Aida, M., Beis, D., Heidstra, R., Willemsen, V., Blilou, I., Galinha, C., Nussaume, L., Noh, Y.-S., Amasino, R., Scheres, B. (2004). The PLETHORA Genes Mediate Patterning of the Arabidopsis Root Stem Cell Niche. *Cell*, v.119, i. 1, p. 109-120, ISSN 0092-8674.
2. Bassham, D. C., & Blatt, M. R. (2008). SNAREs: Cogs and Coordinators in Signaling and Development. *Plant Physiology*, *147*(4), 1504–1515.
3. Baster, P., Robert, S., Kleine-Vehn, J., Vanneste, S., Kania, U., Grunewald, W., Friml, J. (2013). $SCF^{TIR1/AFB}$-auxin signalling regulates PIN vacuolar trafficking and auxin fluxes during root gravitropism. *The EMBO Journal*, *32*(2), 260–274.
4. Bougourd, S., Marrison, J. and Haseloff, J. (2000). An aniline blue staining procedure for confocal microscopy and 3D imaging of normal and perturbed cellular phenotypes in mature *Arabidopsis* embryos. *The Plant Journal, 24*: 543–550.
5. Casimiro, I., Marchant, A., Bhalerao, R. P., Beeckman, T., Dhooge, S., Swarup, R., Bennett, M. (2001). Auxin Transport Promotes Arabidopsis Lateral Root Initiation. *The Plant Cell, 13(4),* 843–852.
6. Celenza Jr., Grisafi, P. L. and Fink, G. R. (1995), A pathway for lateral root formation in Arabidopsis thaliana. *Genes & Development, 9*: 2131-2142.
7. Cole, R. A., McInally, S. A., Fowler, J. E. (2014). Developmentally distinct activities of the exocyst enable rapid cell elongation and determine meristem size during primary root growth in Arabidopsis. *BMC Plant Biology*, *14*, 386.

8. Dhonukshe, P. (2009). Cell polarity in plants: Linking PIN polarity generation mechanisms to morphogenic auxin gradients. *Communicative & Integrative Biology*, *2*(2), 184–190.
9. Ding, Z., Friml, J. (2010). Auxin regulates distal stem cell differentiation in *Arabidopsis* roots. *Proceedings of the National Academy of Sciences of the United States of America*, *107*(26), 12046–12051.
10. Ebine, K., Okatani, Y., Uemura, T., Goh, T., Shoda, K., Niihama, M., Ueda, T. (2008). A SNARE Complex Unique to Seed Plants Is Required for Protein Storage Vacuole Biogenesis and Seed Development of *Arabidopsis thaliana*. *The Plant Cell*, *20*(11), 3006–3021.
11. El Kasmi, F., Krause, C., Hiller, U., Stierhof, Y.-D., Mayer, U., Conner, L., Jürgens, G. (2013). SNARE complexes of different composition jointly mediate membrane fusion in *Arabidopsis* cytokinesis. *Molecular Biology of the Cell*, *24*(10), 1593–1601.
12. Fonseka et al., under development. (2016). *School of Biological and Biomedical Sciences, Durham University.*
13. Forzani, C., Aichinger, E., Sornay, E., Willemsen, V., Laux, T., Dewitte, W., & Murray, J. A. H. (2014). WOX5 Suppresses CYCLIN D Activity to Establish Quiescence at the Center of the Root Stem Cell Niche. *Current Biology, 24(16),* 1939–1944.
14. Friml, J. (2010). Subcellular trafficking of PIN auxin efflux carriers in auxin transport. *European Journal of Cell Biology*, v. 89, i. 2–3, p. 231-235, ISSN 0171-9335.

15. Fukaki, H., Tameda, S., Masuda, H. and Tasaka, M. (2002). Lateral root formation is blocked by a gain-of-function mutation in the SOLITARY-ROOT/IAA14 gene of Arabidopsis. *The Plant Journal, 29*: 153–168.
16. Ganguly, A., Lee, S. H., Cho, M., Lee, O. R., Yoo, H., Cho, H.-T. (2010). Differential Auxin-Transporting Activities of PIN-FORMED Proteins in Arabidopsis Root Hair Cells. *Plant Physiology, 153*(3), 1046–1061.
17. Geldner, N., Anders, N., Wolters, H., Keicher, J., Kornberger, W., Muller, P., Delbarre, A., Ueda, T., Nakano, A., Jurgens, G. (2008). The *Arabidopsis* GNOM ARF-GEF mediates endosomal recycling, auxin transport, and auxin-dependent plant growth. *Cell*. 112(2):219-30.
18. Gillon, A. D., Latham, C. F., Miller, E. A. (2012). Vesicle-mediated ER export of proteins and lipids. *Biochimica et Biophysica Acta, 1821*(8), 1040–1049.
19. Gracheva, E. O., Maryon, E. B., Berthelot-Grosjean, M., Richmond, J. E. (2010). Differential Regulation of Synaptic Vesicle Tethering and Docking by UNC-18 and TOM-1. *Frontiers in Synaptic Neuroscience, 2*, 141.
20. Groen, A. J., Sancho-Andrés, G., Breckels, L. M., Gatto, L., Aniento, F., & Lilley, K. S. (2014). Identification of Trans-Golgi Network Proteins in *Arabidopsis thaliana* Root Tissue. *Journal of Proteome Research, 13*(2), 763–776. 21.
21. Hamilton, K. (2013). Analysis of *AtVAMP714* gene function during the development of the root tip in Arabidopsis thaliana. Dissertation, *Durham University, School of Biological and Biomedical Sciences*.
22. Hruz, T., Laule, O., Szabo, G., Wessendorp, F., Bleuler, S., Oertle, L., Widmayer, P., Gruissem, W., Zimmermann, P. (2008) Genevestigator V3: a

reference expression database for the meta-analysis of transcriptomes. *Advances in Bioinformatics* , 420747

23. Jaillais, Y., Chory, J. (2010). Unraveling the paradoxes of plant hormone signaling integration. *Nature Structural & Molecular Biology, 17(6)*, 642–645.
24. Jiang, K., Feldman, L. J. (2005), Regulation of root apical meristem development. *Annual Review of Cell and Development Biology, v. 21*, p. 485-509.
25. Joshi, H. J., Christiansen, K. M., Fitz, J., Cao, J., Lipzen, A., Martin, J., Smith-Moritz, A. M., Pennacchio, L., Schnackwitz, W. S., Weigel, D., Heazlewood, J. L. (2012) 1001. Proteomes: A functional proteomics portal for the analysis of Arabidopsis thaliana accessions. *Bioinformatics* 28: 1303-1306.
26. Kajala, K., Ramakrishna, P., Fisher, A., C. Bergmann, D., De Smet, I., Sozzani, R., Brady, S. M. (2014). Omics and modelling approaches for understanding regulation of asymmetric cell divisions in arabidopsis and other angiosperm plants. *Annals of Botany*, *113*(7), 1083–1105.
27. Kitakura, S., Vanneste, S., Robert, S., Löfke, C., Teichmann, T., Tanaka, H., & Friml, J. (2011). Clathrin Mediates Endocytosis and Polar Distribution of PIN Auxin Transporters in *Arabidopsis*. *The Plant Cell*, *23*(5), 1920–1931.
28. Kleine-Vehn, J., Donukshe, P., Sauer, M., Brewer, P, B., Wisniewska, J., Paciorek, T., Benkova, E., Friml, J. (2008). ARF GEF-dependent transcytosis and polar delivery of PIN auxin carriers in *Arabidopsis*. *Current Biology*.

29. Kleine-Vehn, J., Huang, F., Naramoto, S., Zhang, J., Michniewicz, M., Offringa, R., Friml, J. (2009). PIN Auxin Efflux Carrier Polarity Is Regulated by PINOID Kinase-Mediated Recruitment into GNOM-Independent Trafficking in *Arabidopsis*. *The Plant Cell*, *21*(12), 3839–3849.
30. Kleine-Vehn, J., Leitner, J., Zwiewka, M., Sauer, M., Abas, L., Luschnig, C., Friml, J. (2008). Differential degradation of PIN2 auxin efflux carrier by retromer-dependent vacuolar targeting. *Proceedings of the National Academy of Sciences of the United States of America*, *105*(46), 17812–17817.
31. Kleine-Vehn, J., Wabnik, K., Martinière, A., Łangowski, Ł., Willig, K., Naramoto, S., Friml, J. (2011). Recycling, clustering, and endocytosis jointly maintain PIN auxin carrier polarity at the plasma membrane. *Molecular Systems Biology*, *7*, 540.
32. Křeček, P., Skůpa, P., Libus, J., Naramoto, S., Tejos, R., Friml, J., Zažímalová, E. (2009). The PIN-FORMED (PIN) protein family of auxin transporters. *Genome Biology*, *10* (12), 249.
33. Kumari, D. L. C., (2011). Functional Analysis of AtVAMP714 gene in Arabidopsis. PhD Thesis. *School of Biological and Biomedical Sciences, Durham University*.
34. Lee, Y., W. S. Lee, and S. –H. Kim. (2013). Hormonal Regulation of Stem Cell Maintenance in Roots. *Journal of Experimental Botany, v.64*, p.1153-65.
35. Leshem, Y., Melamed-Book, N., Cagnac, O., Ronen, G., Nishri, Y., Solomon, M., Levine, A. (2006). Suppression of *Arabidopsis* vesicle-SNARE expression inhibited fusion of H_2O_2-containing vesicles with tonoplast and increased salt tolerance. *Proceedings of the National Academy of Sciences of the United States of America*, *103*(47), 18008–18013.

36. Loefke, C., Luschnig, C., Kleine-Vehn, J. (2013). Posttranslational modification and trafficking of PIN auxin efflux carriers: *Mechanisms of Development*, v.130, p. 82-94.

37. Michniewicz, M., Brewer, P. B., Friml, J. (2007). Polar auxin transport and asymmetric auxin distribution. *Arabidopsis Book*.

38. Naramoto, S., Otegui, M. S., Kutsuna, N., de Rycke, R., Dainobu, T., Karampelias, M., Friml, J. (2014). Insights into the Localization and Function of the Membrane Trafficking Regulator GNOM ARF-GEF at the Golgi Apparatus in *Arabidopsis*. *The Plant Cell*, *26*(7), 3062–3076.

39. Ohya, T., Miaczynska, M., Coskun, U., Lommer, B., Runge, A., Drechsel, D., Kalaidzidis, Y., Zerial, M. (2009), Reconstitution of Rab- and SNARE-dependent membrane fusion by synthetic endosomes. *Nature*, v. 459.

40. Overvoorde, P., Fukaki, H., Beeckman, T. (2010). Auxin Control of Root Development. *Cold Spring Harbor Perspectives in Biology*, 2(6), a001537.

41. Paciorek, T., Zazimalova, E., Ruthardt, N., Petrasek, J., Stierhof, Y. D., Kleine-Vehn, J., Morris, D. A., Emans, N., Jurgens, G., Geldner, N., Friml, J. (2005), Auxin inhibits endocytosis and promotes its own efflux from cells. *Nature*, 435(7046): 1251-6.

42. Pan, X., Chen, J., Yang, Z. (2015). Auxin regulation of cell polarity in plants. *Current Opinion in Plant Biology*, v. 28, p.ages 144-153, ISSN 1369-5266,

43. Péret, B., Swarup, K., Ferguson, A., Seth, M., Yang, Y., Dhondt, S., Swarup, R. (2012). *AUX/LAX* Genes Encode a Family of Auxin Influx Transporters That Perform Distinct Functions during *Arabidopsis* Development. *The Plant Cell*, *24*(7), 2874–2885.

44. Petricka, J. J., Winter, C. M., Benfey, P. N. (2012). Control of Arabidopsis Root Development. *Annual Review of Plant Biology*, 63, 563–590.

45. Rahman, A., Takahashi, M., Shibasaki, K., Wu, S., Inaba, T., Tsurumi, S., Baskin, T. I. (2010). Gravitropism of Arabidopsis thaliana Roots Requires the Polarization of PIN2 toward the Root Tip in Meristematic Cortical Cells. *The Plant Cell*, *22(6)*, 1762–1776.

46. Retzer, K., Butt, H., Korbei, B., Luschnig, C. (2014). The far side of auxin signaling: fundamental cellular activities and their contribution to a defined growth response in plants. *Protoplasma*, *251(4)*, 731–746.

47. Rossi, V., Banfield, D. K., Vacca, M., Dietrich, L. E., Ungermann, C., D'Esposito, M., Galli, T., Filippini, F. (2004). Longins and their longin domains: regulated SNAREs and multifunctional SNARE regulators. *Trends Biochem Sci.* 29(12): 682-8.

48. Sarkar, A. K., M. Luijten, S. Miyashima, M. Lenhard, T. Hashimoto, K. Nakajima, B. Scheres, R. Heidstra, T. Laux. (2007). Conserved factors regulate signalling in Arabidopsis thaliana shoot and root stem cell organisers *Nature*, v. 466, p. 811-814.

49. Sauer, M., Balla, J., Luschnig, C., Wisniewska, J., Reinohl, V., Friml, J., Benkova, E. (2007). Canalization of auxin flow by Aux/IAA-ARF-dependent feedback regulation of PIN polarity. *Genes and Development*, 20(20), 2902-2911, doi: 10.1101/gad.390806.

50. Stahl, Y., Wink, R. H., Ingram, G. C., R. Simon. (2009), A Signaling Module Controlling the Stem Cell Niche in Arabidopsis Root Meristems. *Current Biology*, v. 19, p. 909-914.

51. Toyota, M., Ikeda, N., Toyota, S. S-., Kati, T., Gilroy, S., Tasaka, M., Morita, M. T. (2013). Amyloplast displacement is necessary for gravisensing in *Arabidopsis* shoots as revealed by a centrifuge microscope. *The Plant Journal*. 76, 648-660.

52. Uemura, T., Sato, M. H., Takeyaso, K. (2005). The longin domain regulates subcellular targeting of VAMP7 in Arabidopsis thaliana. *Febs Letters,* v.579, p. 2842-2846.

53. Uemura, T., Ueda, T., Ohniwa, R.L., Nakano, A., Takeyasu, K. Sato, M.H. (2004) Systematic analysis of SNARE molecules in Arabidopsis: dissection of the Post-Golgi Network in plant cells. *Cell Struct. Funct*. 29(2), 49–65.

54. Wang, C., Yan, X., Chen, Q., Jiang, N., Fu, W., Ma, B., Pan, J. (2013). Clathrin Light Chains Regulate Clathrin-Mediated Trafficking, Auxin Signaling, and Development in *Arabidopsis*. *The Plant Cell*, *25*(2), 499–516.

55. Won, C., Shen, X., Mashiguchi, K., Zheng, Z., Dai, X., Cheng, Y., Kasahara, H., Kamiya, Y., Chory, J., Zhao, Y. (2011). Conversion of tryptophan to indole-3-acetic acid by TRYPTOPHAN AMINOTRANSFERASES of *Arabidopsis* and YUCCAs in *Arabidopsis*. *PNAS 108* (45) 18518-18523.

56. Yan, D.-W., Wang, J., Yuan, T.-T., Hong, L.-W., Gao, X., Lu, Y.-T. (2013). Perturbation of Auxin Homeostasis by Overexpression of Wild-Type IAA15 Results in Impaired Stem Cell Differentiation and Gravitropism in Roots. *PLoS ONE*, 8(3), e58103.

57. Yao, H. –Y., Xue, H.-W. (2011). Signals and mechanisms affecting vesicular trafficking during root growth. *Current Opinion in Plant Biology*, v.14, p. 571-579.

58. Žárský, V., Cvrčková, F., Potocký, M. and Hála, M. (2009). Exocytosis and cell polarity in plants – exocyst and recycling domains. *New Phytologist*, 183: 255–272.

59. Zhang, B., Karnik, R., Wang, Y., Wallmeroth, N., Blatt, M. R., Grefen, C. (2015). The Arabidopsis R-SNARE VAMP721 Interacts with KAT1 and KC1 K^+ Channels to Moderate K^+ Current at the Plasma Membrane. *The Plant Cell*, *27*(6), 1697–1717.

60. Zhao, Y. (2010). Auxin biosynthesis and its role in plant development. *Annual Review of Plant Biology*, *61*, 49–64.

6.0 Appendices

6.1 Appendix 1

Primer Sequences:

Act2 Fwd: GGATCGGTGGTTCCATTCTTGC

Act2 Rev: AGAGTTTGTCACACACAAGTGCA

SALK_5917 Fwd: GTATCCGAACCCAAACCGAAAAGT

SALK_5917 Rev: CCTGAAAATCCAATCACCAACACATC

SALK_LBa1: TGGTTCACGTAGTGGGCCATCG

SALK RP: TTAAAGAAGCCTGTGTGAGCC

6.2 Appendix 2

At5g22360 Gene sequence:

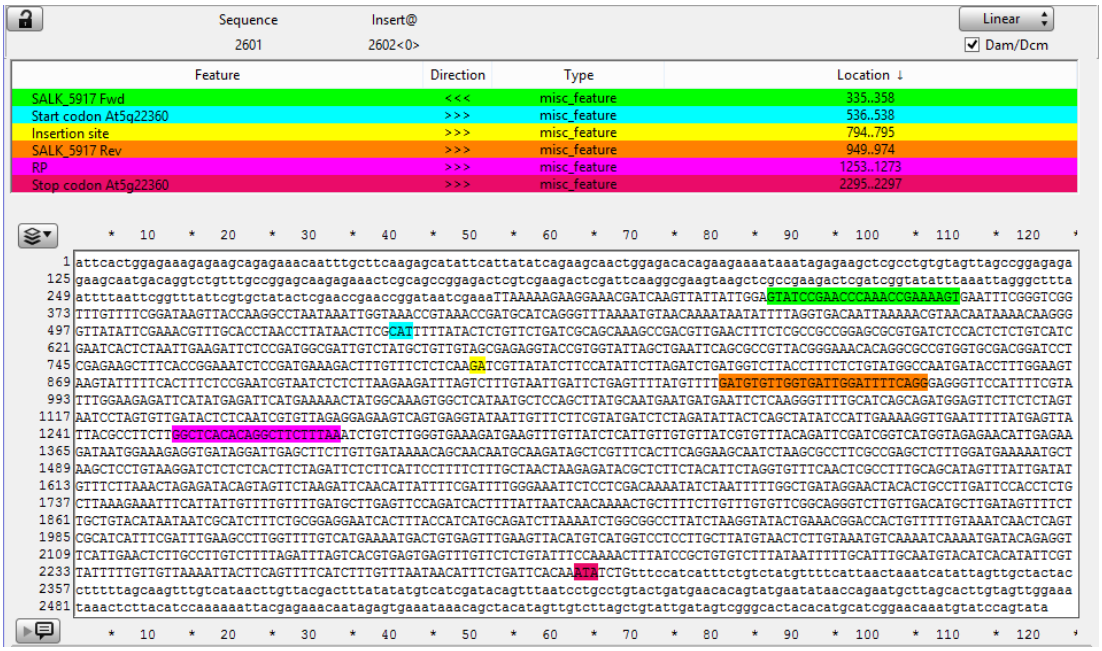

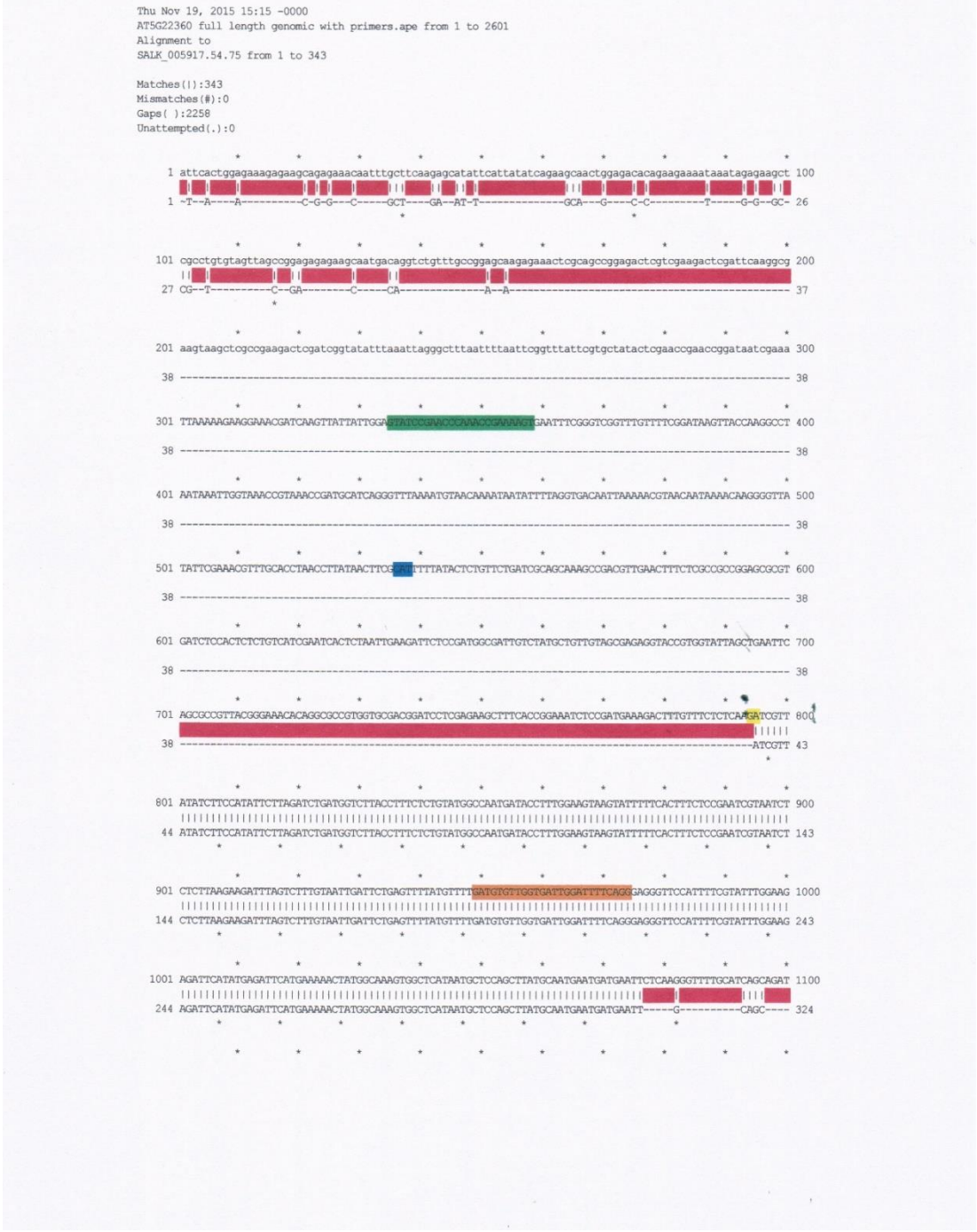
Thu Nov 19, 2015 15:15 -0000
AT5G22360 full length genomic with primers.ape from 1 to 2601
Alignment to
SALK_005917.54.75 from 1 to 343
Matches(|):343
Mismatches(#):0
Gaps( ):2258
Unattempted(.):0

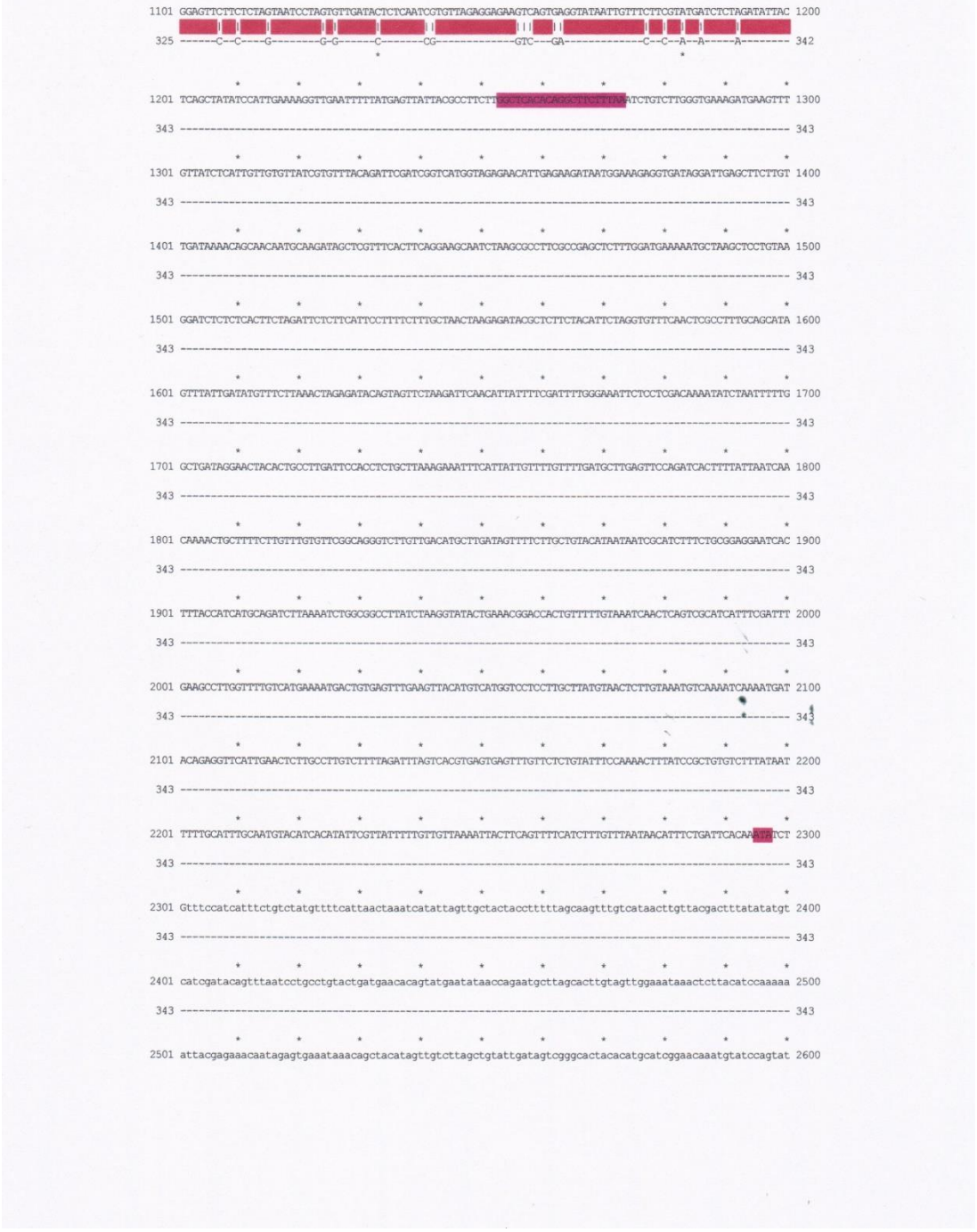

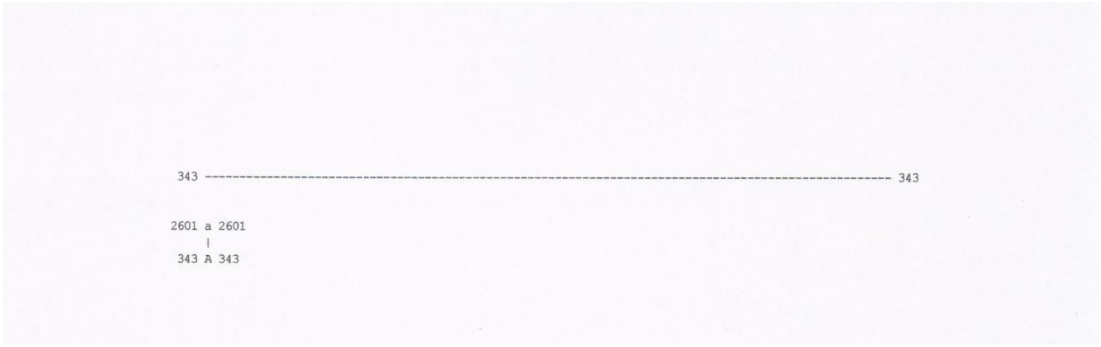
343
343
2601 a 2601
343 A 343

6.3 Appendix 3

PCR Gels

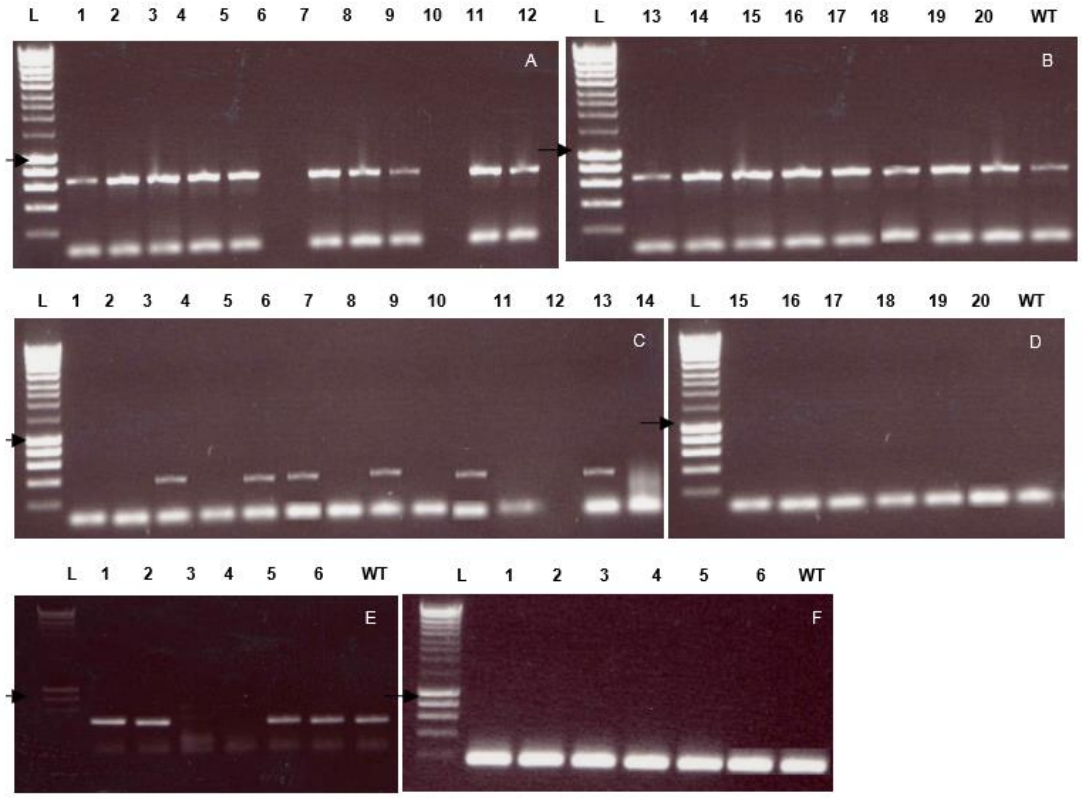

Taken from Kumari PhD thesis., 2011.

PCR Results of SALK_005917 (Arrow head= 1000bp)

A and B: PCR results of 20 seedlings with 360 (+1955) Forward and 360 (-2568) Reverse primers (product size= 642bp), Plant numbers 6 and 10 not giving bands

C and D: PCR results of 20 seedlings with 360 (-2566) Reverse and LBa1 primers (product size= 500bp), Plant numbers 3, 5,6, 8, 10 and 13 giving bands

E: Plant numbers 3, 5,6, 8, 10 and 13 -RT-PCR with 360 (+1955) Forward and 360 (-2568) Reverse primers

Lane 1- Plant number 3

Lane 2-Plant number 5

Lane 3-Plant number 6

Lane 4-Plant number 10

Lane 5-Plant number 5

Lane 6-Plant number 13

F: Plant numbers 3, 5,6, 8, 10 and 13 PCR with ACTIN2 primers (product size=180bp)

PLANT NO	PCR RESULTS			GENOTYPE
	FOR+REV	FOR+LBa1	RT-PCR	
1	†	—		Wild type
2	†	—		Wild type
3	†	—		Heterozygous
4	†	—		Wild type
5	—	†		Heterozygous
6	†	—	—	**Homozygous**
7	—	†		Wild type
8	†	†		Heterozygous
9	†	—		Wild type
10	†	†	—	**Homozygous**
11	†	—		Wild type
12	†	—		Wild type
13	†	†		Heterozygous
14	†	—		Wild type
15	†	†		Wild type
16	†	†		Wild type
17	†	—		Wild type
18	†	—		Wild type
19	†	†		Wild type
20	†	—		Wild type

PCR results, genotyping SALK_5917, taken from Kumari PhD thesis., 2011.

6.4 Appendix 4

Primary Root Length Assay

Primary Root Length/ mm			
	Col-0	Dom Neg	SALK_5917
	60.111	16.313	16.685
	58.232	15.231	13.189
	57.8	14.274	20.326
	62.767	13.825	5.517
	64.782	15.471	11.88
	61.572	18.041	5.294
	59.319	16.982	13.601
	57.436	21.02	16.977
	64.833	16.655	13.567
	60.111	16.478	18.915
	62.767	13.071	17.218
	59.319	16.084	20.779
	72.63	14.274	21.076
	73.556	15.832	20.413
	70.046	14.299	17.343
	71.754	16.309	19.142
	72.986	18.184	19.972
	70.834	17.57	19.747
Average	64.49194	16.10628	16.202278
Std Dev	5.864537	1.898614	4.8508132

Std Error	1.382285	0.447508	1.1433476

6.5 Appendix 5

Lateral Root Assay

Col-0:

Col-0 Lateral Root Assay				
	# Laterals	Lateral Density (root/cm)	Mean interbranch distance (cm)	Avg lateral length (cm)
	20	4.15	0.24	
	16	4.23	0.24	
	19	3.93	0.25	
	17	3.36	0.3	
	16	3.72	0.27	
	16	3.68	0.27	
	21	3.86	0.26	
	19	3.77	0.27	0.34
	23	4.4	0.23	
	20	4.15	0.24	
	17	3.75	0.27	
	18	3.73	0.27	
	14	3.71	0.27	
	18	3.13	0.32	
	9	2.34	0.43	
	12	3.07	0.33	

	15	2.78	0.36	
	9	3.02	0.33	0.28
	17	5.19	0.19	
	16	4.96	0.2	
	14	3.44	0.29	
	23	4.99	0.2	
	14	4.42	0.23	
	24	5.43	0.18	
	11	5.22	0.19	
	18	4.46	0.22	0.49
AVERAGE	16.769231	3.957307692	0.263461538	0.37
STD DEV	3.942666	0.786809038	0.05768482	0.108166538
STD ERROR	0.7732204	0.154305948	0.011312924	0.06244998

Col-0		
	Surface area (cm^2)	Volume (cm^3)
	0.35	0.0016
	0.41	0.002
	0.36	0.0016
	0.38	0.0018
	0.28	0.0011
	0.34	0.0016
	0.3	0.0014

	0.36	0.0015
	0.32	0.0013
	0.25	0.001
	0.35	0.0015
	0.32	0.0013
	0.32	0.0016
AVERAGE	0.333846154	0.001484615
STD DEV	0.042335655	0.000270327
STD ERROR	0.011741798	7.49753E-05

Dominant Negative:

Dom Neg Lateral Root Assay				
	# Laterals	Lateral Density (root/cm)	Mean interbranch distance (cm)	Avg lateral length (cm)
	5	2.55	0.39	
	11	5.28	0.25	
	9	5.81	0.3	
	6	7.8	0.14	
	8	2.6	0.41	
	3	2.76	0.36	
	9	4.37	0.25	
	12	5.67	0.18	0.27
	10	3.04	0.33	

	7	4.66	0.27	
	12	5.03	0.2	
	0	0	0	
	5	16.18	0.08	0.38
	9	4.64	0.22	
	10	3.32	0.39	0.51
AVERAGE	7.733333	4.914	0.251333333	0.386666667
STD DEV	3.411465	3.615363645	0.100112574	0.120138809
STD ERROR	0.880837	0.933482879	0.026756211	0.069362173

Dom Neg		
	Surface area (cm^2)	Volume (cm^3)
	0.18	0.000629
	0.25	0.000976
	0.2	0.0012
	0.09	0.000327
	0.24	0.000845
	0.12	0.000392
	0.18	0.00067
	0.23	0.000992
	0.23	0.00078996
	0.19	0.000728
	0.23	0.000915

	0.1	0.000403
	0.14	0.00047
	0.21	0.000785
	0.24	0.000849
	0.21	0.000835
	0.28	0.001
	0.23	0.001
	0.15	0.000588
	0.19	0.000723
	0.22	0.000864
AVERAGE	0.195714286	0.000760998
STD DEV	0.050751495	0.00023001
STD ERROR	0.011074884	5.01923E-05

SALK_5917:

SALK_5917 Lateral Root Assay				
	# Laterals	Lateral Density (root/cm)	Mean interbranch distance (cm)	Avg lateral length (cm)
	8	3.5	0.29	
	7	2.66	0.38	0.19
	10	3.76	0.27	0.26
	7	4.78	0.21	0.46
	10	4.28	0.23	

	8	7.23	0.17	0.3
AVERAGE	8.333333	4.368333333	0.258333333	0.3025
STD DEV	1.36626	1.575365566	0.073325757	0.114418821
STD ERROR	0.557773	0.643140299	0.029935115	0.057209411

SALK_5917		
	Surface area (cm^2)	Volume (cm^3)
	0.22	0.000782
	0.28	0.0011
	0.25	0.000926
	0.2	0.000732
	0.27	0.0012
	0.18	0.00068
	0.27	0.000988
	0.29	0.0012
	0.23	0.000847
	0.25	0.0009502
	0.1	0.000493
AVERAGE	0.230909091	0.000899836
STD DEV	0.055218574	0.000221347
STD ERROR	0.016649026	6.67387E-05

6.6 Appendix 6

Gravitropism Assay

Col-0:

Col-0					
	Angle at time interval				
	2h	4h	6h	8h	24h
	142	134.16	127.68	129.75	117.57
	133.58	109.87	106.97	107.49	99.98
	137.36	123.84	118.57	119.18	109.53
	142.46	143.94	134.31	118.61	105.08
	154.46	127.5	116.08	107.8	89.02
	151.77	131.78	134.46	127.2	105.91
	139.12	128.55	106.43	106.2	107.47
	139.81	135.88	128.24	133.07	134.65
	125.17	124.87	114.08	131.7	92.88
	142.16	112.52	108.75	101.32	91.9
	144.46	126.54	123.81	115.16	102.65
	151.42	115.85	111.77	123.94	96.89
	132.82	135.83	124.94	126.11	98.44
	154.59	150.85	144.77	139.57	125.02
	150.95	140.67	139.67	122.56	86.44
	180	158.01	157.52	158.2	135.72
	145.53	133.94	112.94	100.06	91.75
	168.02	147.09	131.56	132.14	112.67

	144.38	121.9	114.08	103.66	105.02
	156.5	141.95	142.99	135	116.85
	148.48	118.5	112.73	101.52	84.71
	171.67	120.28	104.73	91.76	96.75
	155.17	146.31	136.04	131.88	118.69
	164.05	138.31	139.64	137.15	130.92
	180	132.3	115.94	122.83	109.94
	165.47	124.33	104.06	100.53	103.41
	140.36	128.9	128.6	126.57	92.63
	150.19	131.59	123.94	125.02	102.42
	149.04	126.42	129.77	127.6	117.08
	145.19	128.91	116.99	103.26	91.39
	156.51	125.81	120.73	111.92	104.99
	143.13	148.8	135.53	130.59	100.41
AVERAGE	150.1819	131.75	124.01	120.2922	105.5869
STD DEV	12.92999	11.38484	13.26695	14.81759	13.57013
STD ERROR	2.285722	2.012574	2.345288	2.619405	2.398883
FULL SERIES STD DEV	19.65502				
FULL SERIES STD ERROR	1.553866				

Dominant Negative:

Dom Neg					
	Angle at time interval (°)				
	2h	4h	6h	8h	24h
	180	180	170.16	163.41	152.59
	180	153.92	140.08	137.73	113.48
	157.9	144.05	148.27	151.22	136.89
	152.67	123.31	132.59	132.22	117.33
	149.7	137.46	137.78	131.94	119.74
	144.62	152.95	135.9	140.74	140.06
	165.92	195.8	169.35	136.66	180
	173.21	92.73	180	180	180
	186.83	175.32	135.46	133.04	124.71
	172.87	140.6	133.6	135	213.69
	149.24	126.21	98.5	130.08	139.61
	153.43	148.8	123.27	109.02	234.68
	149.3	155.47	141.74	136.31	138.92
	167.32	135.35	137.76	137.82	56.89
	142.36	120.91			116.57
	199.61	185.71			65.12
	148.39	135.24			87.66
	149.98	133.39			
AVERAGE	162.4083	146.5122	141.7471	139.6564	136.3494
STD DEV	16.50978	25.60354	20.65303	16.55896	46.90528

STD ERROR	3.891392	6.034812	5.519754	4.425568	11.3762
FULL SERIES STD DEV	29.01279				
FULL SERIES STD ERROR	3.223643				

SALK_5917:

SALK_5917					
Angle at time interval (^{0})					
	2h	4h	6h	8h	24h
	153.9	139.52	128.51	141.84	105.93
	169	146.48	140.44	139.84	123.83
	160.64	147.87	139.92	134.56	127.86
	214.02	206.95	152.05	144.46	112.43
	210.96	137.69	152.93	142.59	135.39
	104.86	100.69	94.83	101.24	293.96
	135.94	128.86	142.87	140.67	140.92
	270	270	270	105.45	108.83
	162.88	132.99	104.87	91.43	233.43
	147.94	88.67	88.32	80.03	64.38
	152.78	150.43	116.57	97.13	112.23
	133.77	125.05	123.99	112.53	90.4
	136.99	101.27	111.32	108.43	203.75
	180	180	155.77	140.19	146.35

	167.42	176.99	160.89	149.17	171.11
	169.7	168.39	123.78	123.23	145.21
	117.41	106.33	90	97.13	132.71
	174.81	140.6	108.92	104.93	158.06
	132.41	114.44	124.27	126.39	115.35
	126.2	120.96	114.94	103.2	93.63
	180	168.02	155.96	126.61	90.84
	180	138.86	152.82	159.69	121.5
	154.54	138.81	114.31	112.63	269.51
	137.6	135.75	122.08	123.75	94.65
	141.12	140.41	85.1	66.5	48.76
	180	132.88	107.38	94.6	217.47
	161.25	160.02	134.12	103.57	227.55
	152.89	146.01	133.37	115.97	287.58
AVERAGE	161.0368	144.4621	130.3689	117.42	149.0579
STD DEV	32.98284	35.66183	35.05292	22.72655	65.54749
STD ERROR	6.233171	6.739452	6.624379	4.294915	12.38731
FULL SERIES STD DEV	43.15972				
FULL SERIES STD ERROR	3.647662				